TECHNICAL REPORT N-70-14

DISTANT PLAIN EVENTS 6 AND 1A PROJECT 3.02A, EARTH MOTION AND STRESS MEASUREMENTS

by

D. W. Murrell

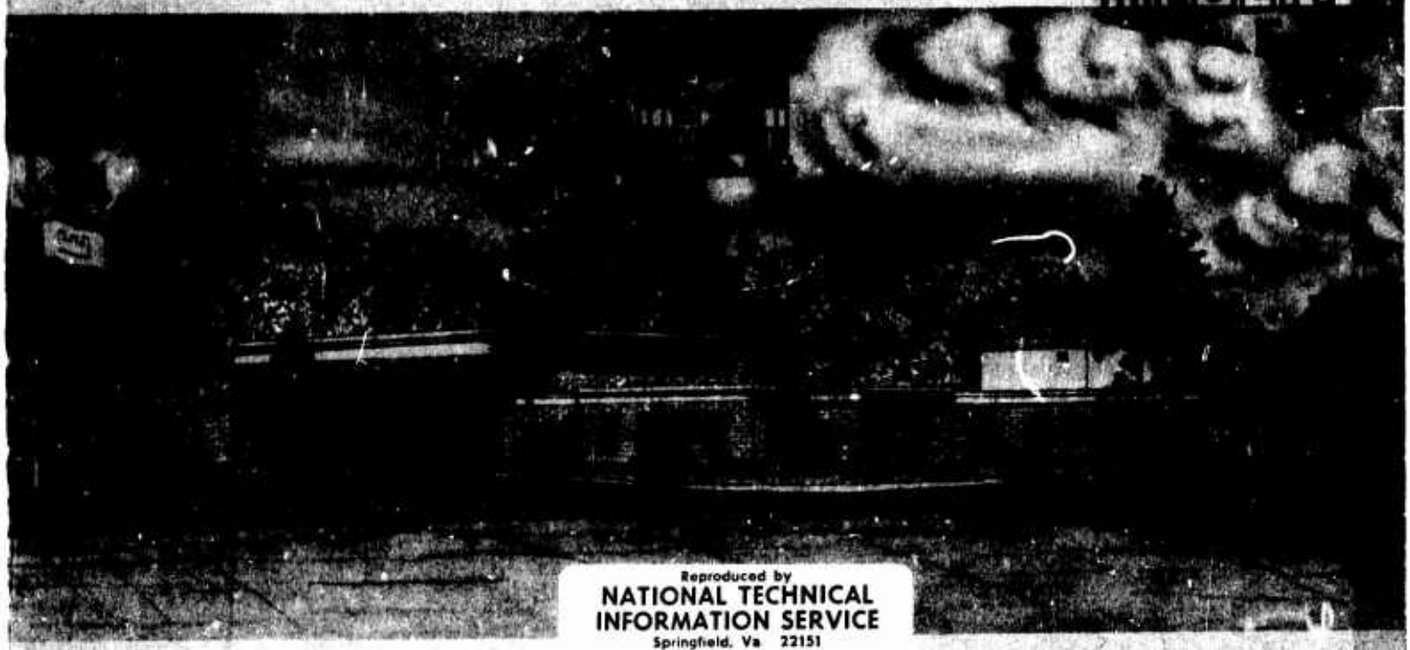

September 1970

Sponsored by Defense Atomic Support Agency

Conducted by U. S. Army Engineer Waterways Experiment Station, Vicksburg, Mississippi

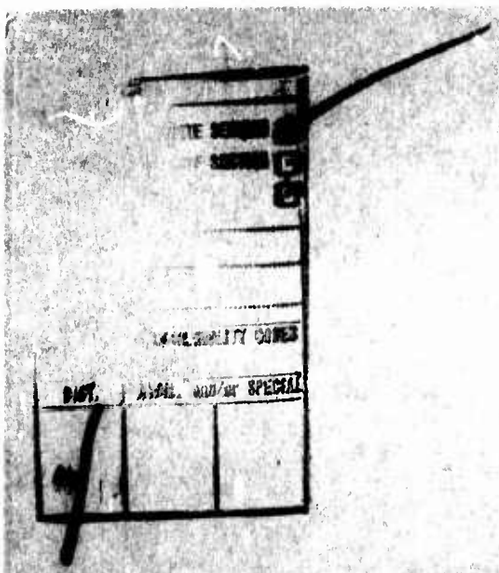

Destroy this report when no longer needed. Do not return it to the originator.

The findings in this report are not to be construed as an official Department of the Army position unless so designated by other authorized documents.

TECHNICAL REPORT N-70-14

DISTANT PLAIN EVENTS 6 AND 1A PROJECT 3.02A, EARTH MOTION AND STRESS MEASUREMENTS

by

D. W. Murrell

September 1970

Sponsored by Defense Atomic Support Agency

Conducted by U. S. Army Engineer Waterways Experiment Station, Vicksburg, Mississippi

ARMY-MRC VICKSBURG, MISS.

THE CONTENTS OF THIS REPORT ARE NOT TO BE USED FOR ADVERTISING, PUBLICATION, OR PROMOTIONAL PURPOSES. CITATION OF TRADE NAMES DOES NOT CONSTITUTE AN OFFICIAL ENDORSEMENT OR APPROVAL OF THE USE OF SUCH COMMERCIAL PRODUCTS.

ABSTRACT

The objectives of this study were to measure and analyze the earth motions produced by Events 6 and 1A of Operation Distant Plain. Event 6 was 100 tons of TNT stacked in a sphere, tangent to the ground surface. Event 1A was 20 tons of TNT also stacked in a sphere, but detonated on a tower at a height of burst of 29.5 feet.

Acceleration, particle velocity, and soil stress gages were installed for both events in order to measure the ground motion. For Event 6, these gages were placed in the region of 2,000- to 10-psi overpressure (49 to 680 feet from ground zero) and at depths of 1.5 to 30 feet. For Event 1A, gages were placed between the expected 10,000- and 500-psi overpressure levels (directly beneath the tower to 80 feet away) and at depths of 1.5 to 10 feet. Time histories obtained by this instrumentation are included in Appendixes A (Event 6) and B (Event 1A).

For Event 6, ground shock arrival times indicated development of outrunning ground motion at about the 30-psi level. Shock propagation velocities were calculated to be 1,100 ft/sec for the soil layer above the water table and 5,500 ft/sec below it.

Vertical particle accelerations for both events were correlated with overpressure. The ratio of acceleration to overpressure for the 1.5-foot depth was about 0.4 g/psi at the 1,000-psi level, and

increased to 1.0 at the 20-psi level. At depths of 5 and 10 feet, accelerations averaged 20 and 7.5 percent of the shallow data, respectively.

Vertical particle velocities at the 1.5-foot depth were also correlated on the basis of overpressure; the ratio of velocity to overpressure varied from 0.03 ft/sec/psi at 1,600 psi to 0.08 ft/sec/psi at 10 psi. Velocities attenuated less sharply with depth than did accelerations. Velocities at the 5-foot depth were about 40 percent of those at 1.5 feet, while those from the 10-foot depth were about 30 percent of those at 1.5 feet.

Horizontal velocities were dominated by the cratering-induced motion. These motions attenuated as the -2.7 power of distance.

Vertical stresses attenuated more rapidly than did the velocities, with stresses at the 5-foot depth averaging 25 percent of those at the 1.5-foot depth. Horizontal stresses measured below the water table behaved similar to free-water measurements, attenuating as the -1.15 power of distance, versus -1.13 power for water. Calculations of shear stress were made for three locations on each shot. Peak values ranged from 40 to 70 psi.

PREFACE

This report describes an experiment conducted by the U. S. Army Engineer Waterways Experiment Station (WES) as a part of Operation Distant Plain, Events 6 and 1A. This study was sponsored by the Defense Atomic Support Agency (DASA).

The work was conducted by personnel of the Nuclear Weapons Effects Division under the direction of Mr. G. L. Arbuthnot, Jr., Division Chief, Mr. L. F. Ingram, Chief, Physical Sciences Branch, and Mr. J. D. Day, Chief, Blast and Shock Section. Project personnel were Messrs. D. W. Murrell, Project Officer and author of this report, M. A. Vispi, Field Operations Officer, and C. M. Wright, all of the Blast and Shock Section, and Messrs. L. T. Watson, J. L. Pickens, and C. E. Tompkins of the WES Instrumentation Branch.

The author acknowledges the able assistance of the WES drill crew in drilling instrument holes and placing gages. The drill crew operated under the direction of Mr. A. L. Mathews, Chief, Exploration Section, Soils Division, and the immediate field supervision of Mr. J. L. Gatz.

COL John R. Oswalt, Jr., CE, COL Levi A. Brown, CE, and COL Ernest D. Peixotto, CE, were Directors of WES during this experiment and the preparation of this report. Messrs. J. B. Tiffany and F. R. Brown were Technical Directors.

CONTENTS

CONVERSION FACTORS, BRITISH TO METRIC UNITS OF MEASUREMENT

British units of measurement used in this report can be converted to metric units as follows.

Multiply	By	To Obtain
inches	2.54	centimeters
feet	0.3048	meters
tons (2,000 pounds)	907.185	kilograms
pounds per square inch	0.070307	kilograms per square centimeter
pounds per cubic foot	16.0185	kilograms per cubic meter
feet per second	30.48	centimeters per second

CHAPTER 1

INTRODUCTION

1.1 OBJECTIVES

The objectives of Project 3.02a of the Distant Plain Series were to measure earth motions and stresses on Events 6 and 1A and to analyze and correlate the results with those obtained on other pertinent detonations such as Snow Ball, Flat Top II and III, and Distant Plain 2A and 3. Cratering-induced ground motions were of special interest on Event 6, a 100-ton[1] spherical TNT detonation with the charge placed tangent to the ground surface. Event 1A, a 20-ton spherical TNT detonation with a height of burst of 29.5 feet, provided an opportunity to study airblast-induced ground motions at predicted overpressure levels up to 10,000 psi without significant crater-induced motions.

1.2 BACKGROUND

Events 6 and 1A of Operation Distant Plain, conducted at the Defence Research Establishment, Suffield (DRES), Alberta, Canada, during July and August 1967, were the culmination of the Distant Plain Series begun in July 1966.

---

[1] A table of factors for converting British units of measurement to metric units is presented on page 10.

Event 6, a 100-ton TNT detonation, used a tangent-sphere charge configuration to simulate as closely as possible the crater and airblast characteristics of a nuclear weapon surface burst. Briefly, this design was expected to produce a smaller, shallower crater than would a hemispherical (e.g. Snow Ball) or half-buried spherical (e.g. Flat Top and Distant Plain 3 and 5) charge. An excellent opportunity thus existed to obtain measurements of airblast-induced ground motions and stresses at air overpressure levels significantly higher than those associated with previous measurements. At the same time, this test allowed assessment of crater-induced motions which, within a few crater radii of the charge, can equal or exceed the airblast-induced motions. In regard to evaluating the response of buried strategic structures, these motions are very significant.

The Watching Hill Blast Range, with a water table and attendant seismic discontinuity at a depth of about 23 feet, presented a two-layered system for this experiment. The outrunning ground motion could then be easily documented and should correlate closely with data from Snow Ball, detonated at the same site.

Event 1A, a 20-ton TNT tower shot with the center of the spherical charge placed at a height of 29.5 feet, was designed to obtain experimental data on airblast and airblast-induced ground motions in the 300- to 10,000-psi overpressure region. Measurements of airblast-induced ground motions at these overpressures were needed

to extend the accumulation of ground motion data into this unexplored area.

1.3 GROUND MOTION AND STRESS PREDICTIONS

Estimates of ground motions and stresses for selecting proper gage ranges and making recording system gain settings for Event 6 were drawn from empirical data and empirically modified one-dimensional elastic equations. Predictions of soil stress were based on relative attenuations with depth observed on Operation Upshot-Knothole (Reference 1). Attenuation of vertical earth stress as a function of depth, at least to a depth of 10 feet, was determined to be

$$P = P_1\left(\frac{d}{d_1}\right)^{-0.37} \tag{1}$$

which describes the vertical stress P at a depth d in terms of stress P_1 at a depth d_1 (Reference 1). For the Distant Plain events, P_1 and d_1 were arbitrarily fixed to be the surface overpressure and 0.5 foot, respectively, thus allowing calculation of expected pressures at any desired depth.

Peak vertical particle velocities were calculated from the one-dimensional elastic equation relating stress and particle velocity

$$P = \rho C_p u \tag{2}$$

where P is the stress, ρ is the in situ density, C_p is the wave propagation velocity of the stress level of interest, and u is the particle velocity. Stresses used to calculate particle velocity were derived from Equation 1 above for the overpressure levels and depths of interest.

Estimates of peak vertical accelerations were made using peak velocities calculated from Equation 2 and estimated rise times for the velocity pulse. Assuming a parabolic velocity input, the peak acceleration becomes

$$A = \frac{2u}{T_r} \tag{3}$$

where T_r is the velocity rise time. Rise times for Equation 3 were computed as recommended by Reference 2

$$T_r = 0.001 + \frac{Z}{C_p} - \frac{Z}{C_s} \tag{4}$$

where Z is the depth below surface, C_p is the wave propagation velocity of the peak stress, and C_s is the seismic velocity, or pr ρ-agation velocity of very low stresses. Equation 4 then accounts for the observed increase of rise time with depth since $C_s > C_p$, which, in turn, produces a more rapid attenuation with depth of acceleration than of velocity. This, too, is an empirically documented phenomenon.

Horizontal (radial) measurements of airblast-induced velocity and acceleration were estimated to be 20 and 67 percent of the

predicted vertical measurements in the superseismic and outrunning regions, respectively. These empirical factors were determined from measurements made on Operation Snow Ball (Reference 3) and Distant Plain Events 1 through 5 (Reference 4), all conducted at DRES. Horizontal stress and stress measured on an axis inclined 45 degrees to the horizontal were both predicted to be 67 percent of the vertical stress at all locations except below the water table, where all three parameters were assumed to be equal due to the saturated nature of the material.

Table 1.1 lists estimated peak values expected for all parameters to be measured for Event 6. These values were, in most cases, set up to be the upper bound of recording capability since prediction information contained in Reference 5, made available just before the shot, indicated lesser motions, particularly at higher pressures. Briefly, Reference 5 suggests that motion-to-overpressure ratios, predicted to be constant for a particular depth by Equations 1 and 2, actually decrease at higher pressures due to the more rapid rate of decay ($\partial P/\partial t$) of high pressures.

Estimated ground motions for Event 1A were calculated using the methods of Reference 5. Recording ranges were then selected to be as close as possible to the estimate. Soil stresses were calculated as for Event 6, i.e. using Equation 1. Predicted motions and stresses for Event 1A are listed in Table 1.2.

TABLE 1.1 ESTIMATED PEAK MOTIONS AND STRESSES, EVENT 6

Location	Horizontal Range	Gage Depth G	Acceleration		Velocity		Stress		
			Vertical AV	Horizontal AH	Vertical UV	Horizontal UH	Vertical PV	Horizontal PH	45 Degrees PS
	feet	feet	g's	g's	ft/sec	ft/sec	psi	psi	psi
61012	49	5	760	152	79	16	850	--	--
61014	49	17	--	--	--	--	540	--	--
61015	49	30	--	--	--	--	--	445	--
61021	60	1.5	2,180	435	92	18	1,000	--	--
61022	60	5	570	115	59	12	640	425	425
61024	60	17	--	--	--	--	410	410	410
61025	60	30	--	--	--	--	--	334	--
61031	80	1.5	1,450	290	62	12	670	--	--
61032	80	5	380	74	40	8	430	275	275
61034	80	17	--	--	--	--	270	270	270
61035	80	30	--	--	--	--	220	220	220
61041	98	1.5	1,090	218	46	9.2	500	--	--
61042	98	5	285	57	30	6	320	215	215
61044	98	17	--	--	--	--	200	200	200
61045	98	30	--	--	--	--	--	170	--
61051	140	1.5	581	116	25	5	270	--	--
61052	140	5	152	30	16	3.2	170	115	115
61054	140	17	--	--	--	--	110	110	110
61055	140	30	--	--	--	--	90	90	90
61061	162	1.5	436	87	19	4	200	--	--
61062	162	5	114	23	12	2.4	130	90	90
61064	162	17	--	--	--	--	80	80	--
61065	162	30	--	--	--	--	--	70	--
61071	325	1.5	73	--	3.1	2.0	--	--	--
61073	325	10	8.0	--	1.5	1.0	--	--	--
61081	400	1.5	4	--	1.9	1.2	--	--	--
61083	400	10	4.8	--	0.92	0.6	--	--	--
61091	480	1.5	29	--	1.2	0.8	--	--	--
61093	480	10	3.2	--	0.6	0.4	--	--	--
61101	680	1.5	14.5	--	0.6	0.4	--	--	--
61103	680	10	1.6	--	0.3	0.2	--	--	--

TABLE 1.2 ESTIMATED MOTIONS AND STRESSES, EVENT 1A

Location	Horizontal Range	Gage Depth G	Acceleration		Velocity		Stress		
			Vertical AV	Horizontal AH	Vertical UV	Horizontal UH	Vertical PV	Horizontal PH	45 Degrees PS
	feet	feet	g's	g's	ft/sec	ft/sec	psi	psi	psi
11011	0	1.5	--	--	--	--	7,500	--	--
11012	0	5	200	--	15	--	5,000	--	--
11013	0	10	50	--	5	--	3,000	--	--
11031	35	1.5	200	60	14	2.5	--	--	--
11033	35	10	50	8.5	3.7	0.6	--	--	--
11041	53	1.5	200	34	14.5	2.5	--	--	--
11042	53	5	85	14	6	1	640	425	425
11043	53	10	50	8	3.8	0.6	500	340	340
11061	80	1.5	200	34	15	2.5	--	--	--
11062	80	5	90	15	7	1.2	200	170	170
11063	80	10	50	8.2	4	0.7	140	90	90

CHAPTER 2

PROCEDURE

2.1 DESCRIPTION OF TEST SITE

Distant Plain Events 6 and 1A were detonated on the Watching Hill Blast Range of DRES. Over the area instrumented for this project, the ground surface was essentially flat with an elevation of approximately 2,164 feet above mean sea level. Geologically, the test site lies in the southern end of the Ross Depression, which has apparently once been covered by a large lake. The soils to a depth of 200 feet are lacustrine deposits consisting of fairly uniform beds of clays and silts with occasional sand lenses (Reference 6).

Detailed accounts of the soil survey and testing are given in References 7 and 8. Briefly, Project 3.10, Soil Sampling and Testing (References 7 and 8), reported the upper 5.5 feet of soil to be a tan, sandy, silty clay. From this point to a depth of about 30 feet, the soil was sandy silt. Below this depth to about 75 feet was a gray plastic clay. The upper 30 feet of soil (both layers) was about 40 percent air by volume, resulting in a high compressibility. For example, a dynamic uniaxial strain test on a sample taken from the upper 5 feet produced a 23 percent vertical strain at 4,000 psi. Upon unloading, the material recovered only about 2 percent of this strain (Reference 8).

2.2 INSTRUMENTATION LAYOUT

A total of 114 earth motion and stress gages were installed for Event 6 to obtain measurements of particle velocity (38 channels), acceleration (30 channels), and earth stress (46 channels). Ninety gages, including all the stress gages, were installed in the predicted 300- to 2,000-psi overpressure range to assess strong earth motions and stresses in the superseismic region, or region of first arrival of the airblast-induced shock. Eleven locations were instrumented for ground motion in this region, at depths of 1.5 and 5 feet. A single canister containing horizontal (radial) and vertical accelerometers and horizontal and vertical velocity gages was installed at each location. A total of 23 locations were instrumented for earth stress at depths of 1.5 to 30 feet. At each of eleven of these locations, three stress gages were installed, oriented so as to determine vertical stress (PV), horizontal stress (PH), and stress at an angle of 45 degrees with the horizontal (PS). By using the three gages oriented as described, it was possible to calculate the principal stresses, their directions, and the shear stress component. The total gage array for Event 6 is listed in Tables 2.1 and 2.2, and is depicted graphically in Figure 2.1.

For Event 1A, 51 gages were installed including 18 particle velocity gages, 18 accelerometers, and 15 soil stress gages. For this event, where assessment of airblast-induced motion was the objective,

all gages were installed in the relatively high overpressure region of 500 psi to an estimated 10,000 psi directly beneath the shot tower. The gage array for Event 1A is given in Tables 2.3 and 2.4, and in Figure 2.2.

2.3 INSTRUMENTATION

2.3.1 Gages and Calibration. All particle motion gages used on this project were commercially available units which have proved reliable in numerous field or laboratory soil motion experiments. The particle velocity gages were the Sparton Southwest, Inc., Model 601. This gage was developed under a Defense Atomic Support Agency contract by Stanford Research Institute and modified by Sandia Corporation. The Model 601 is a variable reluctance gage of the highly overdamped accelerometer design.

Two different types of accelerometers were used. Pace Model A18 variable reluctance gages were installed at expected acceleration levels of less than 200 g's, while Endevco Model 2261 semiconductor strain gage accelerometers were used at higher levels.

The soil stress gages were constructed by the Waterways Experiment Station (WES) using our own design. Basically, the gage is a dual diaphragm gage with two arms of a full semiconductor strain gage bridge bonded to each diaphragm. Reference 9 gives a detailed account of the development and testing of this gage.

All velocity gages were calibrated by using the free fall of the pendulum method. The variable reluctance accelerometers were statically calibrated on a rotary accelerator (spin table), while the strain gage models were dynamically calibrated with a dynamic shock calibrator of the dropping ball type. The soil stress gages were calibrated statically in a small pressure chamber.

The calibrations for all gages were reproduced just prior to shot time by shunting a resistor across one arm of the bridge circuit, producing a circuit imbalance of a known velocity equivalence.

2.3.2 Gage Canisters and Placement. All motion gages installed at a particular location were mounted in a single aluminum canister along with associated calibration and line-matching electronics. Figure 2.3 shows a typical canister with mounted gages. All canisters were potted with paraffin in order to (1) resist water leakage, and (2) damp high frequency vibrations. The final density of the assembled canister was 100 pcf, which provided a good match with the in situ soil. The stress gages were cast in soil-cement plugs consisting of native soil, about 3 percent portland cement, and about 10 percent water to enable compaction. For Event 1A, the motion gage canisters were recovered after Event 6 and reinstalled intact. The soil stress gages, however, were removed from their plugs, checked out, and recast before installation for Event 1A.

In all cases the instrument holes were backfilled with the same soil-cement mixture used for the stress gage plugs. This mixture, though perhaps slightly stiffer than the in situ soil, provided a good density match and is considered to be a significant improvement over dry sand or cement grout for matching alluvial soils.

Instrument cables were protected downhole by heavy-duty reinforced rubber hose, and in the main cable trench were fed into 3-inch-diameter plastic pipe. This method proved satisfactory since the few cables which broke broke well after significant motion peaks had occurred.

2.3.3 Recording System. Signal conditioning and recording equipment was housed in a wooden bunker located about 2,700 feet southwest of Event 6 ground zero (GZ).

The basic signal conditioning equipment for all variable reluctance gages was the CEC 113-B (System D), a 3-kHz carrier-demodulator amplifier. Outputs from this system were recorded on CEC 5-119 oscillographs. The strain-gage transducer outputs were fed into an operational amplifier system designed and constructed by WES, and were recorded on CEC VR-3300 FM magnetic tape recorders.

Calibration and recorder start signals were produced by a cam-type timing device which itself was triggered by the -30-second signal from DRES Control. The -2-second signal from Control was used as a safety valve, and was programmed to jump all recorders to operating

speed. The zero time pulse from Control was recorded directly on all oscillographs, and was superimposed on the 1-kHz timing channel on magnetic tape. Figure 2.4 shows the interior of the Project 3.02a instrument bunker.

TABLE 2.1 PARTICLE MOTION INSTRUMENTATION, EVENT 6

Station	Range	Predicted Airblast Overpressure	Gages[a] at Depths, in Feet, of		
			1.5	5	10
	feet	psi			
6101	49	2,000	--	X	--
6102	60	1,500	X	X	--
6103	80	1,000	X	X	--
6104	98	750	X	X	--
6105	140	400	X	X	--
6106	162	300	X	X	--
6107	325	50	Y	--	Y
6108	400	30	Y	--	Y
6109	480	20	Y	--	Y
6110	680	10	Y	--	Y

[a] X = vertical acceleration, vertical velocity, horizontal acceleration, horizontal velocity; Y = vertical acceleration, vertical velocity, horizontal velocity.

TABLE 2.2 EARTH STRESS INSTRUMENTATION, EVENT 6

Station	Range	Predicted Airblast Overpressure	Gages[a] at Depths, in Feet, of			
			1.5	5	17	30
	feet	psi				
6101	49	2,000	--	V	V	Y
6102	60	1,500	V	X	X	Y
6103	80	1,000	V	X	X	X
6104	98	750	V	X	X	Y
6105	140	400	V	X	X	X
6106	162	300	V	X	Z	Y

[a] V = vertical stress; X = vertical stress, horizontal stress, 45-degree (shear) stress; Y = horizontal stress; Z = vertical stress, horizontal stress.

TABLE 2.3 PARTICLE MOTION INSTRUMENTATION, EVENT 1A

Station	Range	Predicted Airblast Overpressure	Gages[a] at Depths, in Feet, of		
			1.5	5	10
	feet	psi			
1101	0	10,000	--	Y	Y
1103	35	3,000	X	--	X
1104	53	1,500	X	X	X
1106	80	500	X	X	X

[a] X = vertical acceleration, vertical velocity, horizontal acceleration, horizontal velocity; Y = vertical acceleration, vertical velocity.

TABLE 2.4 EARTH STRESS INSTRUMENTATION, EVENT 1A

Station	Range	Predicted Airblast Overpressure	Gages[a] at Depths, in Feet, of		
			1.5	5	10
	feet	psi			
1101	0	10,000	Y	Y	Y
1104	53	1,500	--	X	X
1106	80	500	--	X	X

[a] Y = vertical stress; X = 3-component stress (horizontal stress, vertical stress, 45-degree (shear) stress).

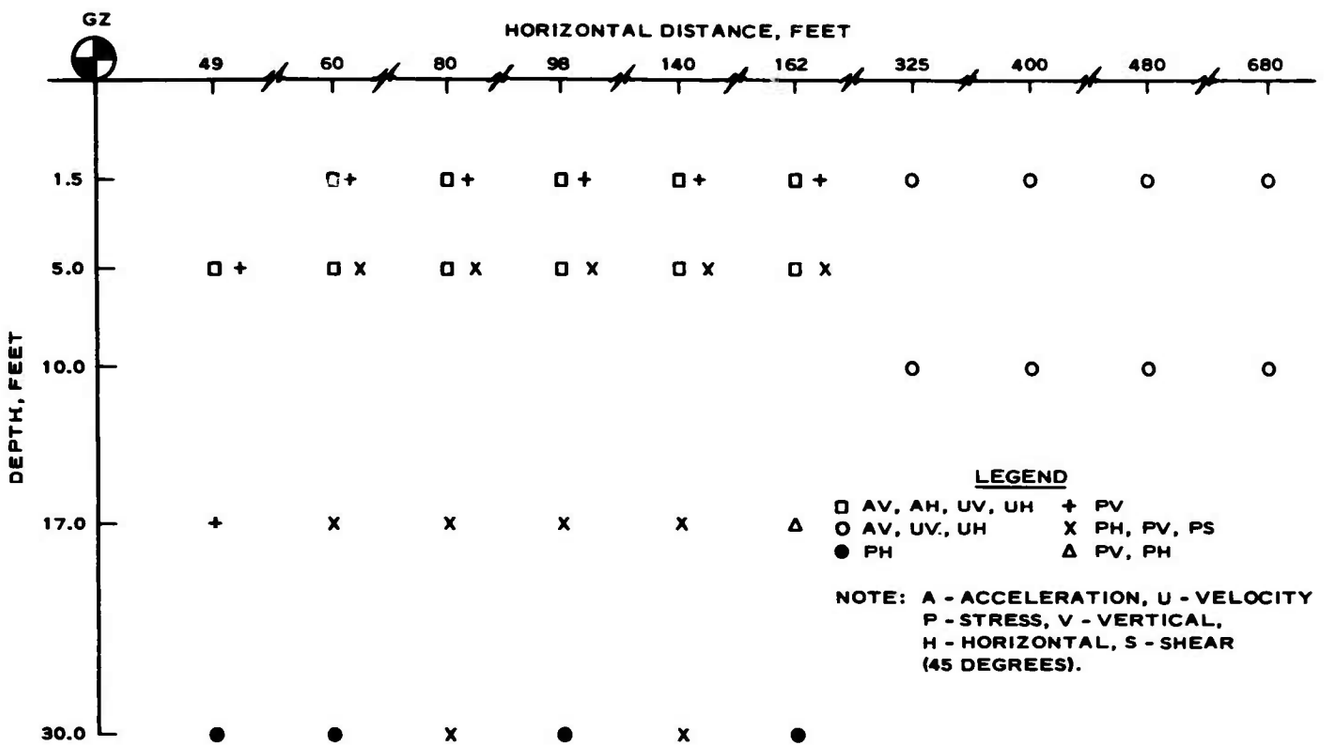

Figure 2.1 Instrumentation layout, Event 6.

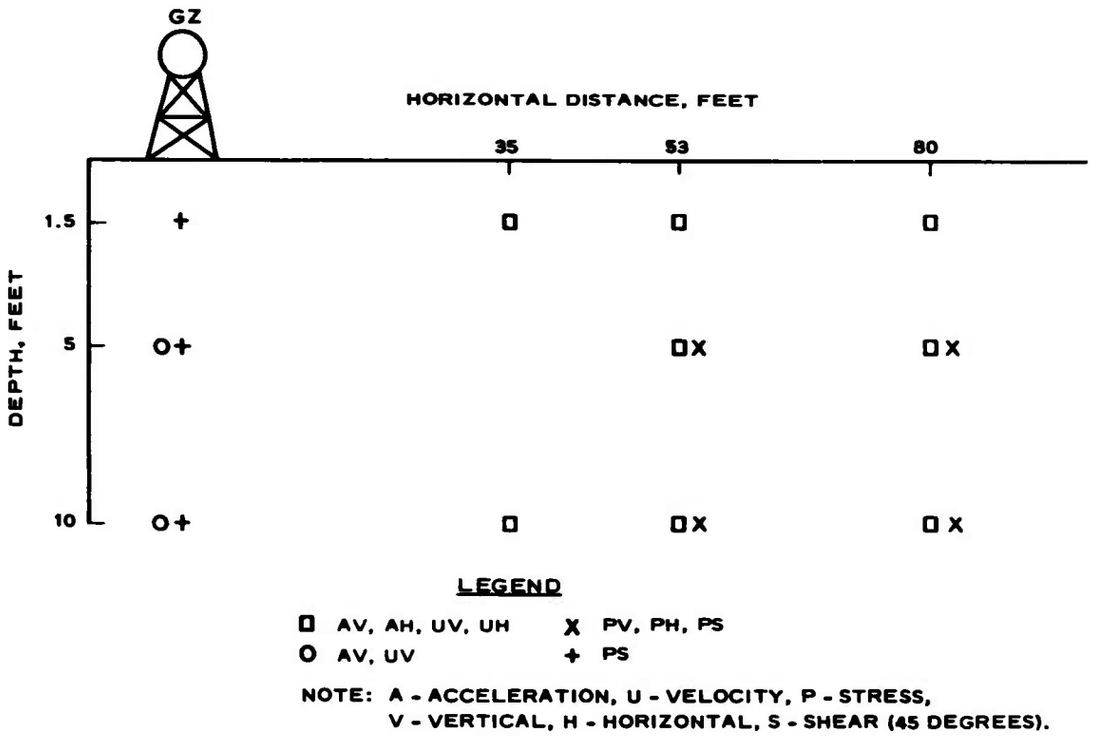

Figure 2.2 Instrumentation layout, Event 1A.

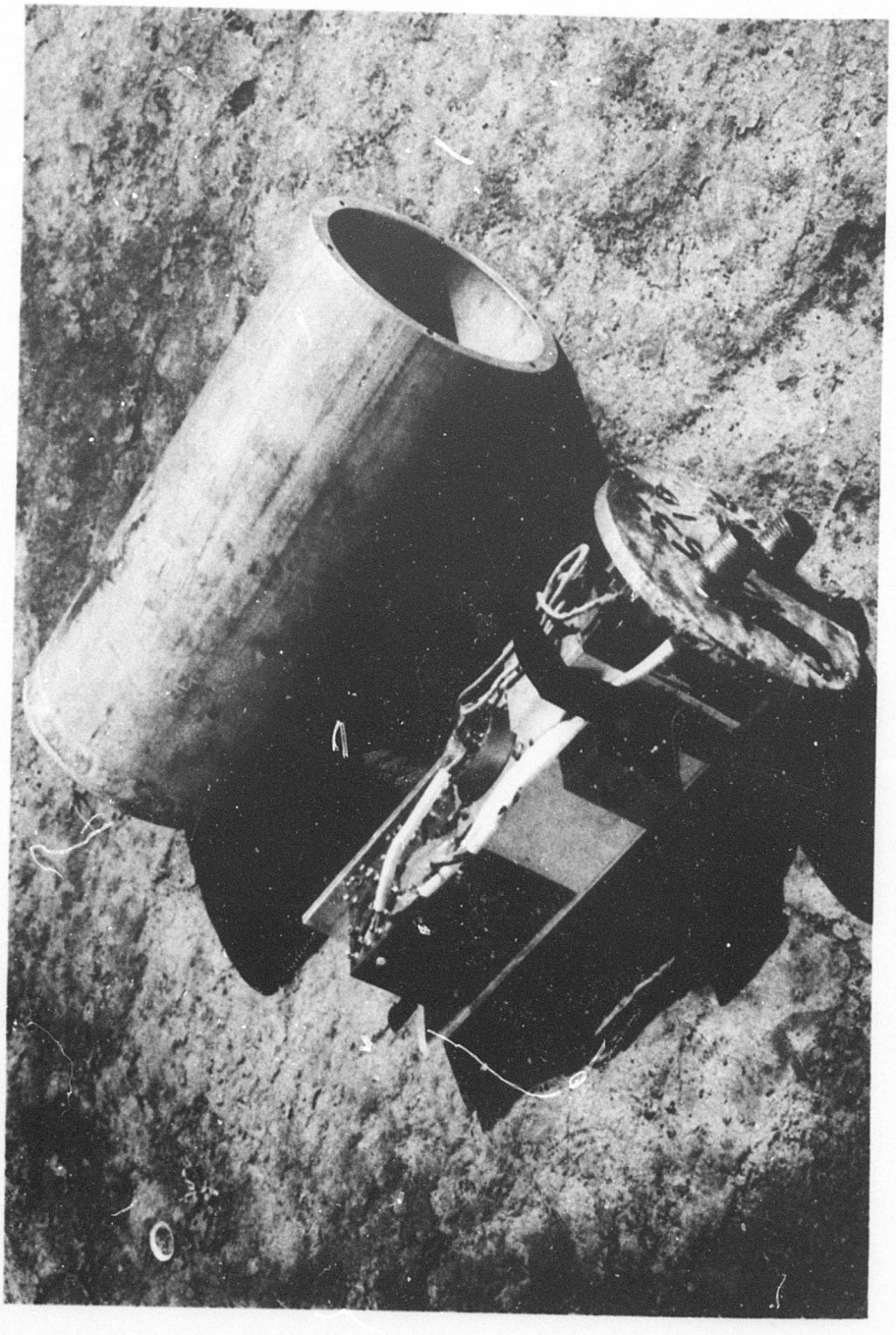

Figure 2.3 Motion gage canister.

Figure 2.4 Interior of instrument bunker.

CHAPTER 3

RESULTS AND DISCUSSION

3.1 DATA RECOVERY

The calibration and recording sequence initiating signal at -30 seconds was received and all equipment operated as programmed for both Events 6 and 1A. A good zero time pulse was recorded for both events.

Of the 114 gages installed for Event 6, 110 yielded good quality data. Two gages were inoperable at shot time, and two additional gages produced extremely noisy outputs and yielded no usable data. A summary of peak measured motions, first integrals of accelerations, and shock arrival times is presented in Table 3.1. Peak stress data are summarized in Table 3.2.

Fifty-one gages were installed for Event 1A, and all were operable at shot time and indicated shock arrival times. However, the four motion gages located beneath the tower yielded no useful peaks due to strong signals which overdrove the galvanometers and saturated the magnetic tape systems. The remaining 47 gages all produced good quality data. Table 3.3 presents peak measured and computed (integrals) motions obtained on Event 1A, and Table 3.4 lists the corresponding stress data.

Appendix A contains time histories of all motion and stress

records obtained for Event 6. Appendix B is a similar presentation of Event 1A data.

3.2 ARRIVAL TIMES, EVENT 6

Shock arrival times were established for all 110 successfully recorded gages on Event 6. For the most part, good agreement was noted for arrival times registered by the several gages located at a single point. In the case of motion gages, the vertically oriented accelerometer generally had the most rapid frequency response and indicated the earliest shock arrival, as would be expected. The latest arrivals were most often recorded by the horizontal velocity gages partially because of the slower response of velocity gages and, additionally, because of the relatively low initial motion. (This point will be discussed in more detail later.)

Shock propagation velocities were calculated from the measured arrival times and were found to average approximately 1,100 ft/sec for the near-surface layer and approximately 5,500 ft/sec for the saturated lower layer. Both of these values are in close agreement with results obtained on Operation Snow Ball (Reference 3) and by seismic surveys.

Figure 3.1 is a shock front profile for Event 6 constructed from airblast arrival time data (Reference 10), ground shock arrival times measured on this project, and the calculated propagation velocities.

Development of outrunning refracted energy can easily be seen on this plot. Directly induced energy, refracted along the higher velocity layer, is continuously fed back into the overburden as an upward-moving shock front. Figure 3.1 indicates that this upward-moving wave began to outrun the airblast-induced wave at the surface at a distance of about 400 feet, or at a pressure level of about 30 psi. The 30-psi level is very nearly the same point of outrunning noted for Snow Ball, detonated at the same site but of five times the yield of Event 6.

3.3 VERTICAL PARTICLE ACCELERATION

3.3.1 Event 6. Peak vertical particle accelerations for Event 6 are plotted versus horizontal range in Figure 3.2. Data from all three depths instrumented, i.e., 1.5, 5, and 10 feet, are shown, and attenuation of motion with both increasing depth and distance is apparent. In the superseismic region, at distances of less than 400 feet, however, there is some data scatter, and attenuation patterns are less pronounced. One point in particular (at a distance of 98 feet from GZ and a depth of 1.5 feet) appears high.

At both the 1.5- and 5-foot depths, a trend is noticeable toward a flattening of the curve at shorter ground ranges (or conversely, i.e. at larger distances, the curve steepens). This is what Reference 5 predicted would happen at high overpressures and lends support

to the proposed decrease of motion-to-overpressure ratios with increasing overpressure.

Data presented in Figure 3.2 from locations in the outrunning region are airblast-induced downward peaks in order to maintain consistency for correlation purposes. In this region, the airblast-induced motion arrived later than refracted energy but clearly dominated that from the outrunning wave at the 1.5-foot depth, being an order of magnitude or so higher. At the 10-foot depth, however, the upward pulse from the refracted wave and the airblast-induced motions were roughly equal in magnitude.

3.3.2 Event 1A. Figure 3.3 is a plot of peak downward acceleration versus horizontal distance for Event 1A. A rapid attenuation of acceleration is apparent with both depth and distance. A quite rapid attenuation with depth, somewhat more rapid than noted on Event 6, can be seen between the 1.5- and 5-foot depths, although insufficient data points are available to establish a firm trend.

Figure 3.4 shows time histories of the three vertical accelerations at 1.5-, 5-, and 10-foot depths at a distance of 53 feet. The sharp downward spike, characteristic of airblast-induced motion, is seen at all three depths and is followed by an upward rebound. This rebound was consistently about 40 to 50 percent of the downward peak magnitude, and was very nearly the same as for Event 6, indicating a lack of effect of shot geometry or yield on this phenomenon. The

airblast-induced pulses demonstrate clearly the pulse widening and lengthening rise times at increasing depths which is generally associated with the passage of a sharp disturbance through dissipative materials. The rebound pulse is also noted to increase in width with increasing depth.

3.3.3 Discussion and Correlation. In general, vertical particle accelerations appeared to be somewhat higher at equivalent overpressures for Event 1A than for Event 6. Figure 3.5 is a plot of the ratio of acceleration to overpressure (g's/psi) versus overpressure for the 1.5-foot depth. Included in this plot for comparison purposes are data from Distant Plain Event 3 (Reference 4) and Flat Top Events II and III (data at a nominal 1-foot depth, Reference 11). These three events were geometrically identical, i.e. 20-ton half-buried spheres of TNT. Distant Plain Event 3 was detonated at DRES, Drowning Ford Site, and the Flat Top shots were fired at the Nevada Test Site (NTS). From Figure 3.5, it is obvious that a good correlation exists among these several detonations to the extent that charge weight (a factor of five between Distant Plain Event 6 and the others) and location (DRES versus NTS) have no apparent effect. As mentioned above, the data from Event 1A were somewhat higher at equivalent overpressures than for Event 6, and fall clearly above the body of the points in this figure. This may be explained by the fact that rather disturbed airblast waveforms were noted for Event 1A,

including secondary shocks and a somewhat flattened waveform as opposed to classical peaks (Reference 12).

The trend toward lesser motion/overpressure ratios at higher pressures predicted by Reference 5 is evident in Figure 3.5. A straight line fit to the data points indicates a decay of this ratio from about 1 g/psi at 20 psi to about 0.4 g/psi at 1,000 psi. There is admittedly a lot of scatter in the data, but none of the detonations, except Event 1A, produced data uniformly high or low with respect to the average, and a $\pm$30 percent variation would include most of the data points.

Figure 3.6 is a plot of accelerations normalized to the 1.5-foot depth versus depth. This plot shows the relative attenuation with depth below the 1.5-foot depth for Distant Plain Events 6, 1A, and 3. There is somewhat more data scatter at the 5-foot depth than at the 10-foot depth, contrary to what might be expected. Again, difference in yield was not a significant contribution. From this plot, accelerations at 10-foot depths are seen to drop off to about 0.075 $\pm$ 20 percent of those measured at 1.5-foot depths, while those at the 5-foot depths ran about 0.20 $\pm$ 50 percent of the shallower data. For Operation Snow Ball, no instrumentation was installed at the 1.5-foot depth. However, accelerations measured at a depth of 15 feet averaged 26 percent of those at 5 feet. An extrapolation of Figure 3.6 data to the 15-foot depth would indicate that 26 percent is a

reasonable figure for attenuation from 5 to 15 feet. Thus a quite rapid attenuation of acceleration in the DRES alluvium (above the water table) is seen to exist. This can be attributed to the very high compressibility and hysteretic behavior of the upper layer of soil, which, as stated previously, was about 40 percent air by volume.

3.4 HORIZONTAL ACCELERATION

Peak outward horizontal (radial) accelerations are plotted versus distance for Events 6 and 1A in Figures 3.7 and 3.8, respectively. A rapid attenuation with both increasing distance and depth is apparent for data from both events, although the Event 6 data (Figure 3.7) show some scatter and the attenuation patterns are less well defined.

The peak horizontal accelerations (AH) for both events were considerably less than corresponding vertical accelerations (AV) at all pressure levels and depths instrumented. The ratio of AH to AV ranged from 0.1 to 0.3, indicating the predominantly downward direction of the airblast-induced ground shock, at least at these relatively high pressure levels (>300 psi).

3.5 VERTICAL PARTICLE VELOCITY

3.5.1 Event 6. Figure 3.9 presents peak vertical particle velocities from Event 6 versus horizontal distance for all three depths

instrumented. As with the accelerations, rapid attenuation with both distance and depth is noted, with the flattening effect at closer distances again apparent. The curve decay between the superseismic region and the outrunning region is quite steep, in fact, is steeper than the acceleration decay. This would seem to point out that airblast-induced particle velocities are affected to some extent by the phenomenon of outrunning itself. That the effect, whatever its cause, is real is evidenced by the fact that the groups of data points are consistent in themselves.

An interesting aspect of this plot is the seemingly large motion measured at the 98-foot distance and 1.5-foot depth, exactly what was noted in Figure 3.2, the acceleration-distance plot. This reinforces the credibility of the data. At the same time, however, the measurement at a depth of 5 feet was the least of all the superseismic measurements at that depth. This would suggest a local anomaly at the 1.5-foot depth and 98-foot distance, possibly arising from inconsistent or particularly soft backfill in the upper 1.5 feet.

3.5.2 Event 1A. Figure 3.10 shows peak vertical velocities versus distance measured on Event 1A. A quite consistent pattern can be seen, with the flattening effect again prominent at both 1.5- and 10-foot depths.

The peak velocities are somewhat higher than were the

measurements at similar pressure levels on Event 6. This, too, is consistent with the acceleration data.

3.5.3 Discussion and Correlation. On past events, vertical particle velocity data have been more easily correlatable, and consequently more accurately predicted, than acceleration data. For the same five experiments discussed in Section 3.3.3 (Distant Plain 6, 1A, and 3, Flat Top II and III), however, this does not appear to be the case.

Figure 3.11 is a correlation based on the particle velocity to overpressure ratio. More scatter is shown here than was noted for the acceleration data, with Distant Plain Event 6 data points contributing heavily to this. It was stated in Section 3.5.1, however, that there was a very rapid decay of particle velocity in the outrunning region, and this shows up strikingly in the four Event 6 data points in the lower right-hand corner of Figure 3.11. Neglecting these four points, a more consistent relationship stands out, with the majority of the points falling within ± 40 percent of an average curve. As expected, the ratio increases with decreasing overpressure, from about 0.03 ft/sec/psi at 1,600 psi to 0.08 ft/sec/psi at 10 psi, roughly the same rate of increase as the acceleration data. This, in turn, would imply a constant relation between acceleration and velocity over the region discussed, i.e. 10 psi to about 1,600 psi, which can be expressed as follows: a(in g's) = 13u (in ft/sec).

The scatter in velocity data is again encountered when an attempt is made to correlate depth attenuation, as in Figure 3.12. Here only a very general attenuation with depth is noted, with considerable overlapping of the data from various depths. Nevertheless, useful information can be gained from this plot if the lack of precision is kept in mind when attaching significance to the decay characteristics. At a depth of 5 feet, the velocities appear to be roughly 0.4 $\pm$ 50 percent of those at 1.5-foot depths, and at 10-foot depths are about 0.3 $\pm$ 50 percent of those at 1.5-foot depths. The Flat Top III data are, with one exception, quite consistent in averaging a ratio of 0.14 for the 17-foot depth instrumented on that shot. These rates of attenuation are all less than noted for accelerations, which can be attributed to the dependence of peak acceleration not only on the peak velocity, but also on the velocity rise time, which increases with distance traveled by the shock wave.

3.6 HORIZONTAL PARTICLE VELOCITIES

Horizontal (radial) velocity, probably more than any other parameter, shows distinctly the arrival of two separate disturbances for the crater-producing detonations: the airblast-induced and direct- or cratering-induced motions. Figure 3.13 shows a selection of horizontal velocity gage records from the 5-foot depth and at distances of 49, 60, and 140 feet for Event 6. The initial arrival of

the airblast-induced motion is clearly seen on each of these time histories. It is followed by a crater-induced pulse of both greater magnitude and significantly longer duration. The time period between arrivals steadily increases with distance, since in this region (>300 psi) the airblast wave is traveling several times as fast as the directly transmitted energy.

Airblast-induced horizontal velocities have generally been difficult to correlate since well-defined attenuation patterns often do not exist due to data scatter. Figures 3.14 and 3.15 plot airblast-induced horizontal velocity versus distance for Events 6 and 1A, respectively, and in both cases this axiom holds true. Both events exhibit broad patterns of attenuation with depth and distance. However, the fivefold scatter of the data would make any straight line fit extremely tenuous at best.

Figure 3.16 is a plot of cratering-induced horizontal velocity versus distance for Event 6. Regular decay is noted to exist, in contrast to the airblast-induced motion, and there is relatively small data scatter. The rate of attenuation with distance is as the -2.7 power of distance, a reasonable number for energy transmission through alluvial soil. Motions at 1.5- and 5-foot depths are not significantly different, pointing out the primarily outward direction of motion of this pulse.

3.7 DISPLACEMENT

Tables 3.5 and 3.6 list peak transient displacements calculated from particle velocity measurements for Events 6 and 1A, respectively. For Event 6, both peak upward and downward vertical displacements are listed, while for Event 1A, where no cratering-induced motion existed, only downward vertical displacements are listed.

From Table 3.5 it can be seen that the upward (cratering-induced) displacements greatly exceed the downward (airblast-induced) displacements at the smaller distances. This is caused by the very much longer duration of the cratering-induced velocity. Cratering-induced velocity attenuates more rapidly, however, such that its advantage in duration is diminished, and at the greater distances the upward and downward displacements become roughly equal.

Figures 3.17 and 3.18 are plots of upward and outward cratering-induced displacements, respectively. Rapid attenuation of displacement is evident in both cases, with the vertical component decreasing as the -3.7 power of distance and the horizontal as the -2.4 power.

The airblast-induced displacements for Event 1A (Table 3.6) show the sharp decrease with depth dictated by a highly compressible medium. With the exception of the horizontal displacement at Location 11041, which appears unreasonably low, both components of displacement at the 1.5-foot depth were three to six times greater than corresponding displacements at the 10-foot depth.

A comparison of vertical downward displacements at locations of similar overpressure shows that displacements for the two events were at least similar. For example, displacements at Locations 61061 and 61062, Event 6, where the overpressure was 280 psi, were 0.31 and 0.10 foot, respectively; at Locations 11061 and 11062, Event 1A, where the overpressure was 310 psi, displacements were 0.20 and 0.11 foot.

3.8 SOIL STRESS MEASUREMENTS

3.8.1 Event 6. Figure 3.19 is a plot of peak vertical stress versus distance for Event 6. The data points plotted for the 1.5-foot depths are consistent in themselves in defining a rather slow rate of attenuation with distance. Inasmuch as all these points are in the superseismic region, the attenuation rate would seem to be consistent with the flattening noticed for particle velocities (Figure 3.9) and accelerations (Figure 3.2) in the same region.

Vertical stresses measured at the 5- and 17-foot depths exhibit a great deal more scatter than do stresses at the shallower locations. In particular, the data from both depths at the 140-foot distance are significantly higher than the body of data and contribute heavily to an anomalous decay pattern. Neglecting these two points as being atypical, depth attenuations were calculated for comparison with particle velocity data. Peak stresses at the 5-foot depth averaged 0.25 $\pm$ 50 percent of those at 1.5-foot depths, which is a more

rapid decay with depth than the 0.4 ± 50 percent noted for velocities.

Figure 3.20 is a plot of peak horizontal stresses measured at the 30-foot depth. Figure 3.1 indicates the primary disturbance at this depth to be a horizontally moving direct-induced wave. Since the soil medium below a depth of about 22 feet is a saturated material of low compressibility and low shear strength (approximately 10 psi, Reference 8), the rate of stress attenuation could be expected to approximate that in free water, i.e., attenuation as the -1.13 power of distance. This is in fact the case in Figure 3.20, since the five points measured over a horizontal distance of 49 to 162 feet define an attenuation as the -1.15 power of distance with only a small amount of scatter present.

3.8.2 Event 1A. Soil stress measurements for Event 1A (Table 3.4) were limited to three locations under the shot tower and four additional locations; for this reason no graphic display of attenuation with depth or distance would be pertinent. The only measurement of stress at the 1.5-foot depth was beneath the shot tower, and the peak was 4,960 psi. Peaks of 951 and 276 psi were measured at the 5- and 10-foot depths, respectively (Figure 3.21). The ratio of stress at 5-foot depth to that at 1.5-foot depth was 0.19, which is in reasonable agreement with ratios calculated for Event 6 data.

3.8.3 Three-Component Stress, Events 6 and 1A. Three components of stress were successfully measured at eight of the eleven

locations where arrays were installed for Event 6, and at all four locations for Event 1A. Not all of these measurements proved useful for the calculation of shear stress, however, primarily due to tensile stress indications on the horizontally oriented gage. Calculations of shear stress and principal stresses were accomplished for three arrays on each event, however; Figures 3.22 through 3.27 are time histories of the calculated shear and principal stresses for these locations.

The first two plots for Event 6 (Figures 3.22 and 3.23) are from the 140-foot range and 17-foot depth and the 162-foot range and 5-foot depth, respectively. Data from both of these points show a single major pulse of shear stress on the order of 60 psi. In both cases the peak major principal stress is higher than the measured vertical stress (24 and 60 percent higher, respectively) and the minor principal stress is very low, often negative. The third plot for Event 6 (Figure 3.24) is from a point below the water table, 80-foot range and 30-foot depth. The shear stress from this location rises sharply to a peak of -40 psi, then after several rather sharp oscillations, oscillates with a longer period about a -25-psi mean. The major and minor principal stresses are noted to have a very similar waveform, and a nearly constant difference ($\sigma_1 - \sigma_3$) of 50 psi. This implies a Mohr envelope with a ϕ of 0 , which is consistent with

soils test data (Reference 8) from samples from below the water table.

Figures 3.25, 3.26, and 3.27 present shear and principal stress calculations for three locations from Event 1A. The first two plots (Figures 3.25 and 3.26) are for the 5- and 10-foot depths at a distance of 53 feet from GZ. The major principal stress is somewhat lower at the 10-foot depth than at the 5-foot depth, as expected, and in both cases the major principal stress is within 20 percent of the measured vertical stress. The peak shear stresses for the 5 and 10-foot depths were 40 and 50 psi, respectively, which is reasonably close to that determined for the two points for Event 6 (approximately 60 psi).

Figure 3.27 presents the data from the 80-foot range and 5-foot depth for Event 1A. The major principal stress calculation again showed very close agreement with the measured vertical stress (350 psi calculated versus 317 psi measured). The peak shear stress was 100 psi, making both shear and major principal stresses considerably higher than was found at the same depth but closer to GZ (Figure 3.25). The waveform at the closer stations (53-foot range), however, is somewhat disturbed, and resembles more closely that measured below the water table on Event 6 (Figure 3.24). A local anomaly, perhaps arising from a disturbed airblast wave, is thus suggested at the 53-foot range.

TABLE 3.1 MOTION DATA SUMMARY, EVENT 6

Location	Gage Type and Orientation[a]	Horizontal Range	Depth	Time of Arrival	Airblast-Induced Acceleration	Particle Velocity	
						Airblast Induced	Cratering Induced
		feet	feet	msec	g's	ft/sec	ft/sec
61012	AV	49	5	5.9	115	18.3	12.4
	UV	--	--	7.1	--	13.3	12.6
	AH	--	--	8.7	39	5.1	26.0
	UH	--	--	8.2	--	2.9	17.3
61021	AV	60	1.5	5.1	326	25.3	19.4
	UV	--	--	5.3	--	25.9	19.8
	AH	--	--	5.4	63.4	2.20	16.2
	UH	--	--	4.9	--	1.62	11.2
61022	AV	60	5	8.6	59.6	9.5	10.1
	UV	--	--	No record	--	--	--
	AH	--	--	8.1	33.0	1.30	12.4
	UH	--	--	11.0	--	1.23	11.6
61031	AV	80	1.5	6.9	283	23.2	--
	UV	--	--	7.5	--	23.2	11.0
	AH	--	--	6.9	84.6	2.74	7.49
	UH	--	--	7.0	--	2.81	5.55
61032	AV	80	5	8.5	92.3	10.3	7.70
	UV	--	--	10.9	--	9.0	6.86
	AH	--	--	10.5	7.3	0.3	5.80
	UH	--	--	10.3	--	0.5	6.15
61041	AV	98	1.5	8.7	544	24.3	8.6
	UV	--	--	8.8	--	31.3	5.4
	AH	--	--	9.0	53.6	1.90	2.60
	UH	--	--	9.8	--	1.24	3.63
61042	AV	98	5	11.0	67.7	10.0	6.3
	UV	--	--	13.3	--	6.34	3.61
	AH	--	--	12.8	7.42	0.32	4.8
	UH	--	--	15.9	--	0.38	2.38
61051	AV	140	1.5	15.2	229	25.8	3.2
	UV	--	--	15.4	--	19.0	1.8
	AH	--	--	16.2	43	2.40	--
	UH	--	--	16.1	--	1.97	2.0
61052	AV	140	5	16.7	43.4	6.00	5.10
	UV	--	--	18.0	--	8.38	1.81
	AH	--	--	18.6	5.82	0.40	1.78
	UH	--	--	18.8	--	0.44	1.73
61061	AV	162	1.5	18.6	191	20.0	--
	UV	--	--	19.0	--	17.3	2.7
	AH	--	--	19.0	29.8	1.95	1.2
	UH	--	--	21.3	--	0.80	1.35
61062	AV	162	5	21.9	62.3	11.4	--
	UV	--	--	24.6	--	8.3	1.67
	AH	--	--	22.2	7.81	1.0	--
	UH	--	--	22.8	--	0.59	1.40
61071	AV	325	1.5	70.8	57.8	[b]	[c]
	UV	--	--	71.5	--	1.00	--
	UH	--	--	72.8	--	0.18	--
61073	AV	325	10	77.2	4.77	--	--
	UV	--	--	80.0	--	0.55	--
	UH	--	--	77.9	--	0.36	--
61081	AV	400	1.5	101	31.7	--	--
	UV	--	--	101	--	0.72	--
	UH	--	--	101	--	0.26	--
61083	AV	400	10	95.8	2.25	--	--
	UV	--	--	95.0	--	0.15	--
	UH	--	--	96.0	--	0.22	--
61091	AV	480	1.5	115.0	31.9	--	--
	UV	--	--	118.0	--	0.50	--
	UH	--	--	121.0	--	0.40	--
61093	AV	480	10	108.0	2.60	--	--
	UV	--	--	112.0	--	0.14	--
	UH	--	--	111.0	--	0.32	--
61101	AV	680	1.5	155.0	9.53	--	--
	UV	--	--	155.0	--	0.38	--
	UH	--	--	160.0	--	0.19	--
61103	AV	680	10	147	1.85	--	--
	UV	--	--	146	--	0.14	--
	UH	--	--	148	--	0.16	--

[a] A = acceleration, U = velocity, V = vertical, H = horizontal.
[b] Accelerometer records at this range and beyond had too much baseline shift to produce reliable integrals.
[c] Direct cratering-induced motions were insignificant beyond this point.

TABLE 3.2 STRESS DATA SUMMARY, EVENT 6

Location	Gage Type and Orientation[a]	Horizontal Range	Depth	Time of Arrival	Peak Stress
		feet	feet	msec	psi
61012	PV	49	5	No record	--
61014	PV	49	17	20.0	537
61015	PH	49	30	17.4	492
61021	PV	60	1.5	5.2	463
61022	PV	60	5	7.5	200
	PH	--	--	7.8	149
	PS	--	--	7.5	123
61024	PV	60	17	20.8	117
	PH	--	--	24.2	67
	PS	--	--	24.7	325
61025	PH	60	30	19.0	420
61031	PV	80	1.5	7.3	495
61032	PV	80	5	10.2	76
	PH	--	--	10.1	23
	PS	--	--	10.0	177
61034	PV	80	17	No record	--
	PH	--	--	18	280
	PS	--	--	17.8	119
61035	PV	80	30	23.4	216
	PH	--	--	23.3	274
	PS	--	--	23.3	276
61041	PV	98	1.5	9.2	388
61042	PV	98	5	12.7	97
	PH	--	--	12.5	28
	PS	--	--	12.6	166
61044	PV	98	17	22.5	34
	PH	--	--	20.5	78
	PS	--	--	22.6	52
61045	PH	98	30	26.9	263
61051	PV	140	1.5	19.5	431
61052	PV	140	5	20.0	314
	PH	--	--	19.3	204
	PS	--	--	No record	--
61054	PV	140	17	30.8	149
	PH	--	--	29.4	66
	PS	--	--	30.7	33
61055	PV	140	30	33.7	177
	PH	--	--	No record	--
	PS	--	--	34.2	53
61061	PV	162	1.5	19.4	417
61062	PV	162	5	21.6	85
	PH	--	--	21.7	58
	PS	--	--	21.4	17
61064	PV	162	17	30.4	78
	PH	--	--	33.3	117
61065	PH	162	30	37.1	129

[a] P = stress, V = vertical, H = horizontal, S = shear (45 degrees).

TABLE 3.3 MOTION DATA SUMMARY, EVENT 1A

Location	Gage Type and Orientation[a]	Horizontal Range	Depth	Time of Arrival	Acceleration	Velocity
		feet	feet	msec	g's	ft/sec
11012	AV	0	5	6.2	No peak recorded	
	UV	--	--	6.6	No peak recorded	
11013	AV	0	10	12.8	No peak recorded	
	UV	--	--	11.0	No peak recorded	
11031	AV	35	1.5	5.3	731	38.1
	UV	--	--	6.8	--	43.4
	AH	--	--	5.9	104	8.37
	UH	--	--	7.5	--	4.2
11033	AV	35	10	13.1	58.5	11.25
	UV	--	--	13.5	--	6.52
	AH	--	--	12.6	18.9	2.56
	UH	--	--	10.0	--	1.96
11041	AV	53	1.5	8.0	682	38.0
	UV	--	--	8.8	--	36.1
	AH	--	--	8.0	103	4.3
	UH	--	--	8.6	--	2.6
11042	AV	53	5	11.7	64.5	10.5
	UV	--	--	12.9	--	11.1
	AH	--	--	13.8	21.5	1.47
	UH	--	--	14.2	--	1.85
11043	AV	53	10	13.0	44.2	9.4
	UV	--	--	15.1	--	6.27
	AH	--	--	17.0	11.5	1.40
	UH	--	--	15.2	--	1.96
11061	AV	80	1.5	12.7	293	19.8
	UV	--	--	13.6	--	14.3
	AH	--	--	11.0	60.2	2.0
	UH	--	--	13.4	--	1.73
11062	AV	80	5	15.7	46.1	7.4
	UV	--	--	17.6	--	6.41
	AH	--	--	16.5	4.4	1.60
	UH	--	--	17.0	--	0.74
11063	AV	80	10	21.5	24.7	4.88
	UV	--	--	22.4	--	3.66
	AH	--	--	21.1	3.24	0.63
	UH	--	--	22.8	--	0.58

[a] A = acceleration, U = velocity, V = vertical, H = horizontal.

TABLE 3.4 STRESS DATA SUMMARY, EVENT 1A

Location	Gage Type and Orientation[a]	Horizontal Range	Depth	Time of Arrival	Peak Stress
		feet	feet	msec	psi
11011	PV	0	1.5	4.4	4,960
11012	PV	0	5	7.4	951
11013	PV	0	10	11.8	276
11042	PV	53	5	11.2	164
	PH	--	--	10.6	79.4
	PS	--	--	9.1	121
11043	PV	53	10	13.4	108
	PH	--	--	14.9	77
	PS	--	--	15.0	116
11062	PV	80	5	13.8	317
	PH	--	--	13.8	55.3
	PS	--	--	13.8	107
11063	PV	80	10	16.6	46
	PH	--	--	17.1	12.5
	PS	--	--	16.0	75

[a] P = stress, V = vertical, H = horizontal, S = shear (45 degrees).

TABLE 3.5 PEAK TRANSIENT DISPLACEMENTS, EVENT 6

Location	Range	Depth	Peak Displacement		
			Downward	Upward	Outward
	feet	feet	feet	feet	feet
61012	49	5.0	0.17	5.1	6.5
61021	60	1.5	0.3	5.2	3.2
61022	60	5.0	--	--	6.0
61031	80	1.5	0.17	1.56	1.52
61032	80	5.0	0.08	1.80	1.70
61041	98	1.5	0.32	0.18	1.40
61042	98	5.0	0.08	0.65	0.80
61051	140	1.5	0.31	--	0.68
61052	140	5.0	0.15	0.17	0.82
61061	162	1.5	0.31	--	0.36
61062	162	5.0	0.10	--	0.38

TABLE 3.6 PEAK TRANSIENT DISPLACEMENTS, EVENT 1A

Location	Range	Depth	Peak Displacement	
			Downward	Outward
	feet	feet	feet	feet
11031	35	1.5	0.56	0.19
11033	35	10	0.13	0.085
11041	53	1.5	0.50	0.040
11042	53	5	0.20	0.15
11043	53	10	0.13	0.15
11061	80	1.5	0.20	0.27
11062	80	5	0.11	0.09
11063	80	10	0.06	0.045

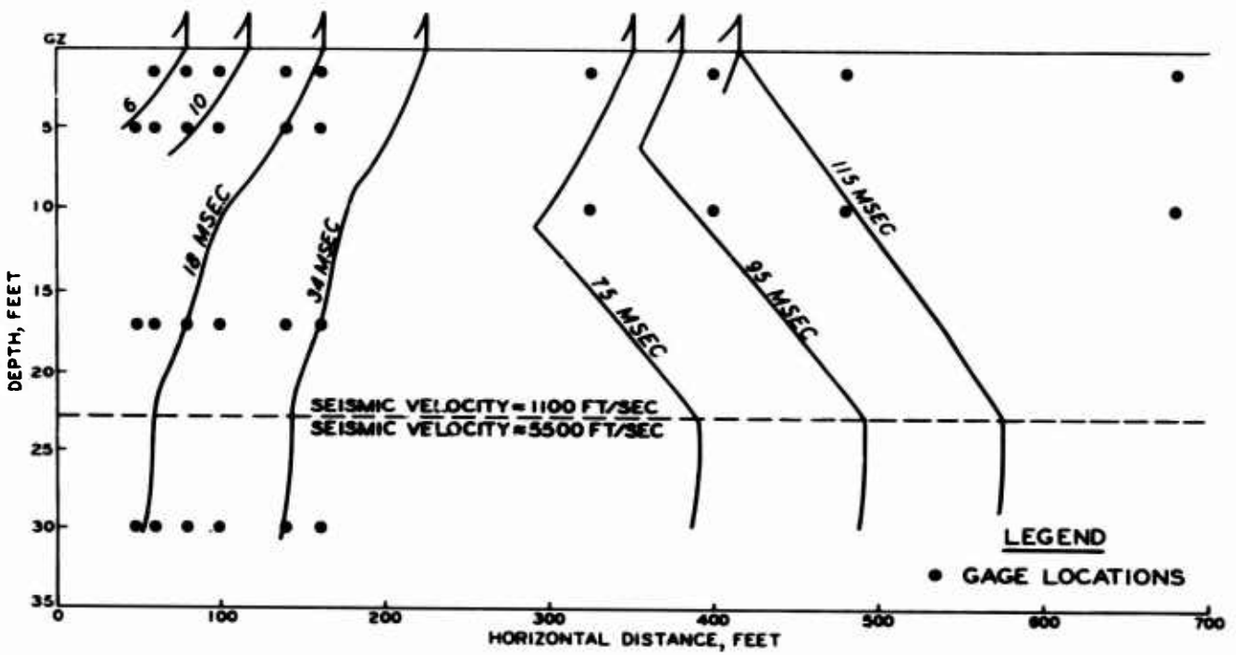

Figure 3.1 Shock front profile, Event 6.

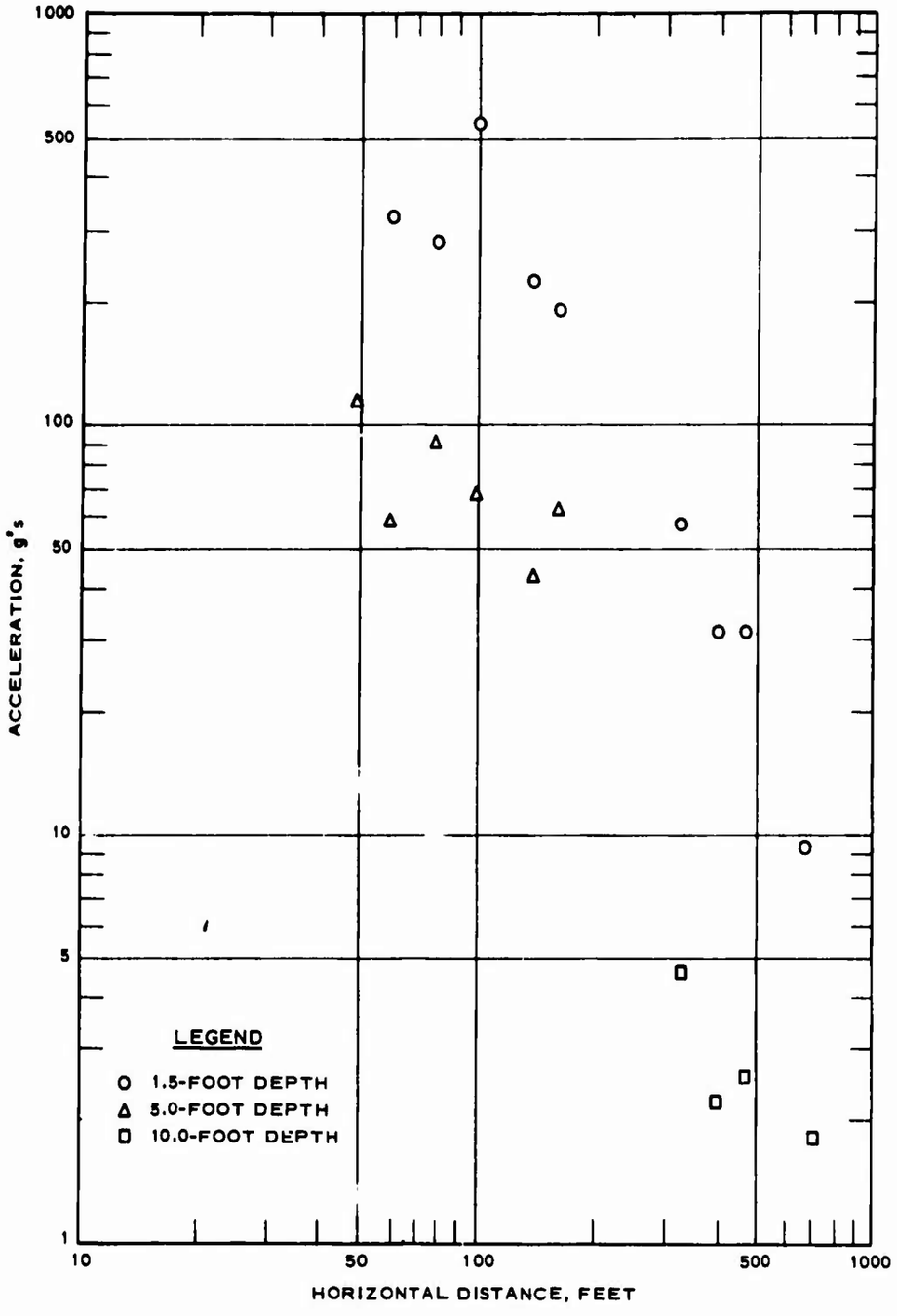

Figure 3.2 Peak vertical downward acceleration versus horizontal distance, Event 6.

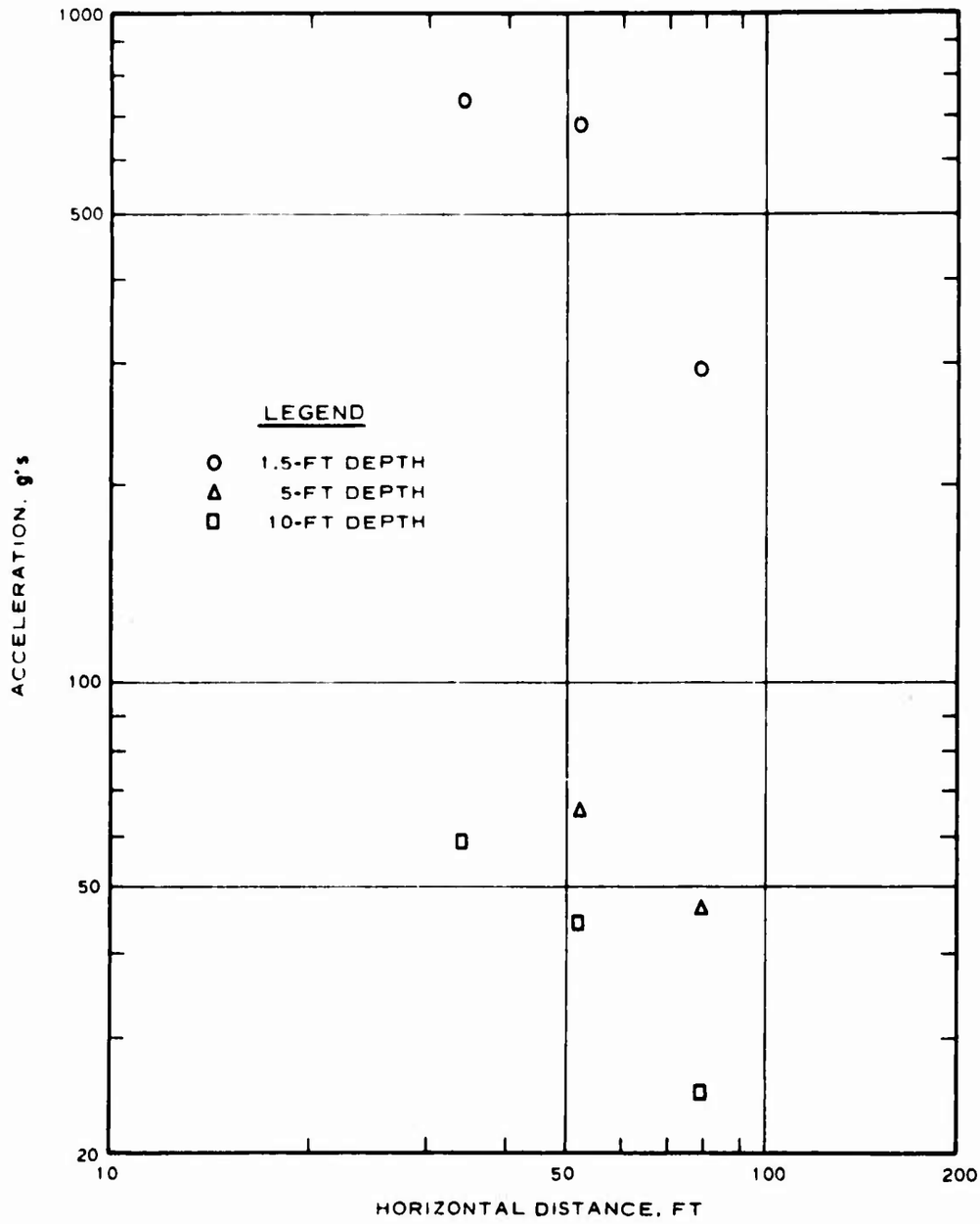

Figure 3.3 Peak vertical downward acceleration versus horizontal distance, Event 1A.

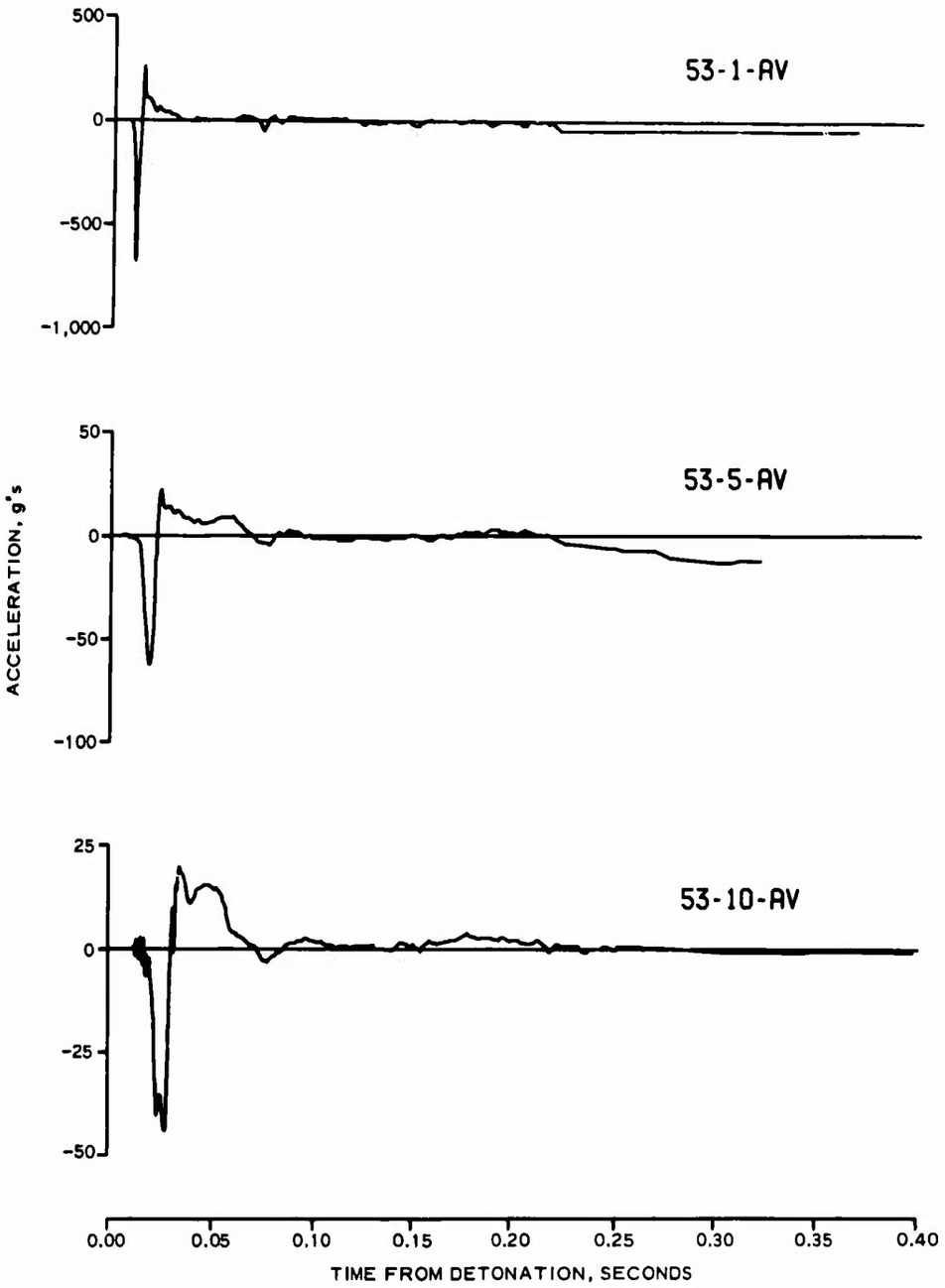

Figure 3.4 Time histories of vertical acceleration, 53-foot horizontal distance, Event 1A.

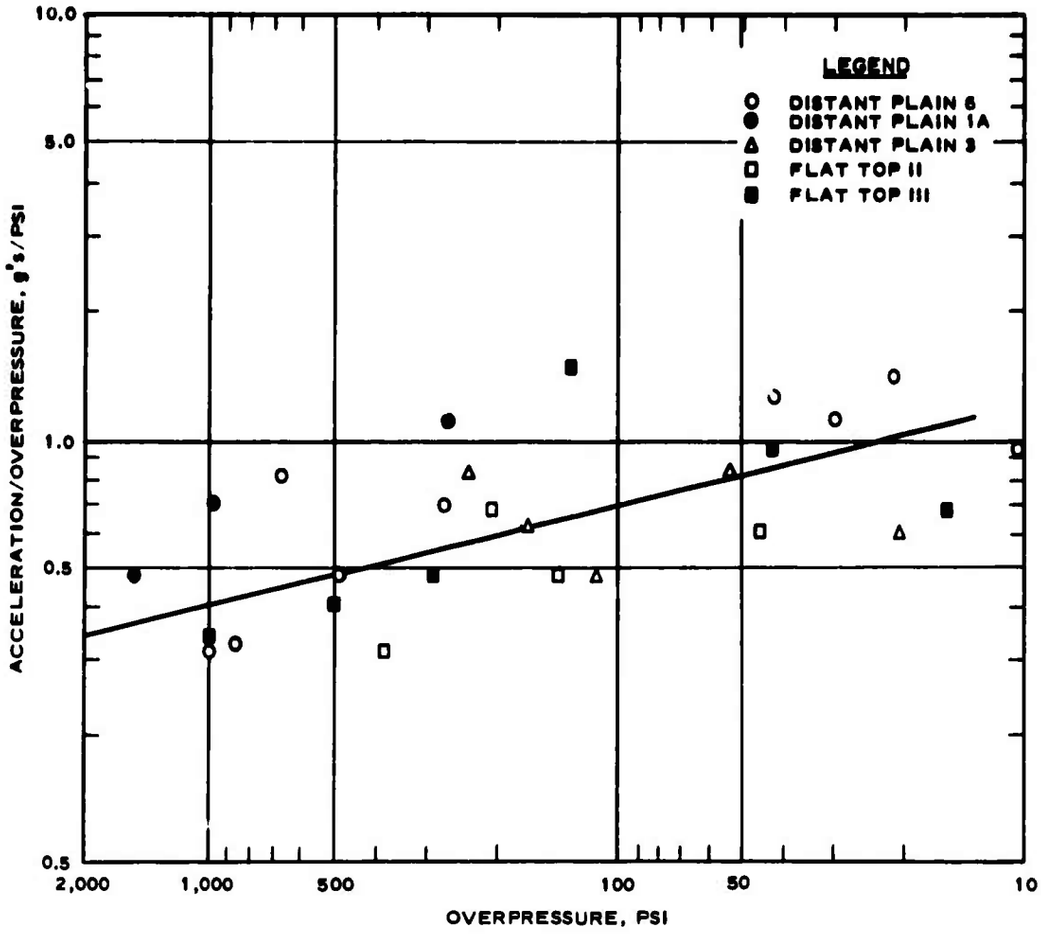

Figure 3.5 Correlation of vertical accelerations, 1.5-foot depth.

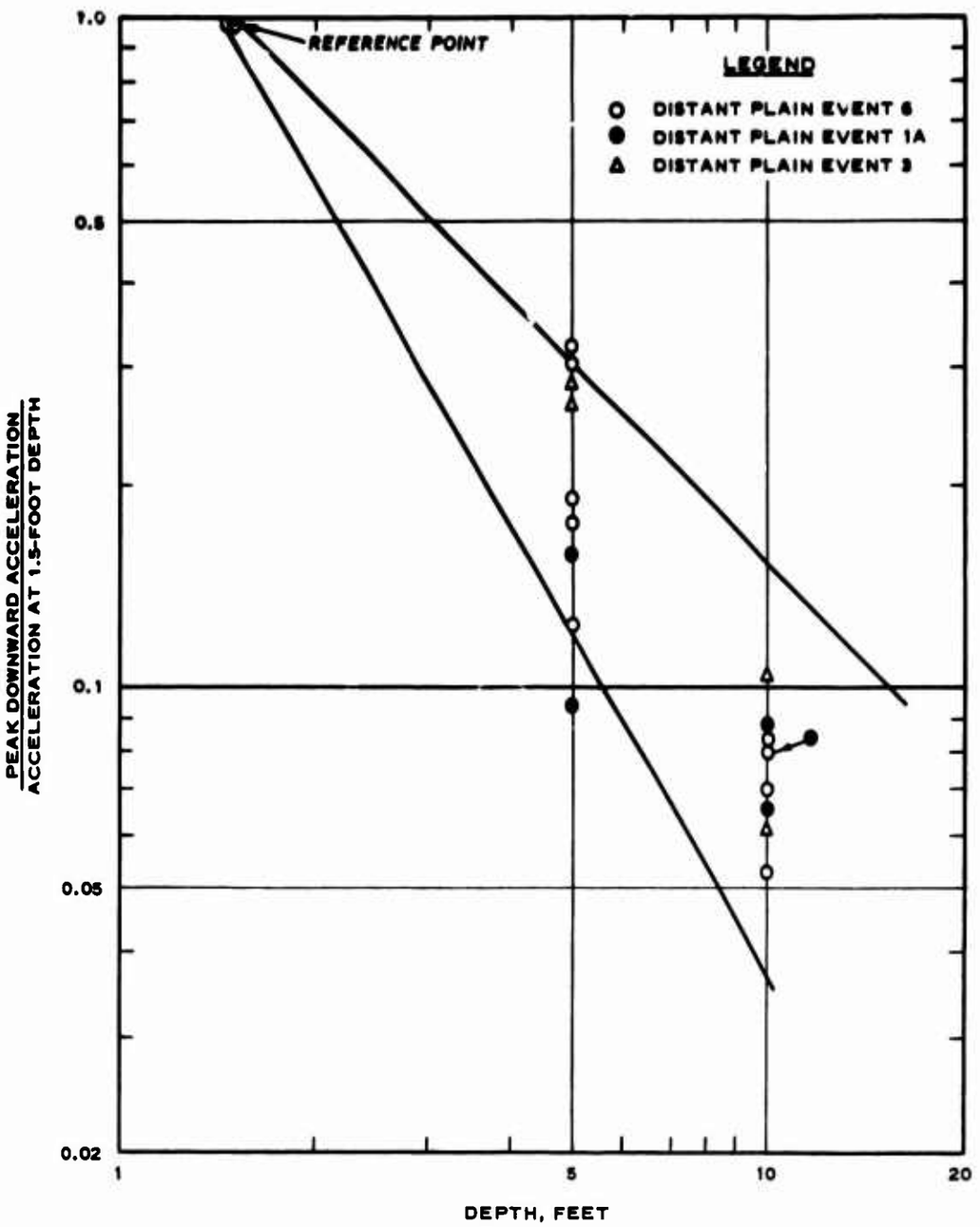

Figure 3.6 Vertical acceleration attenuation with depth.

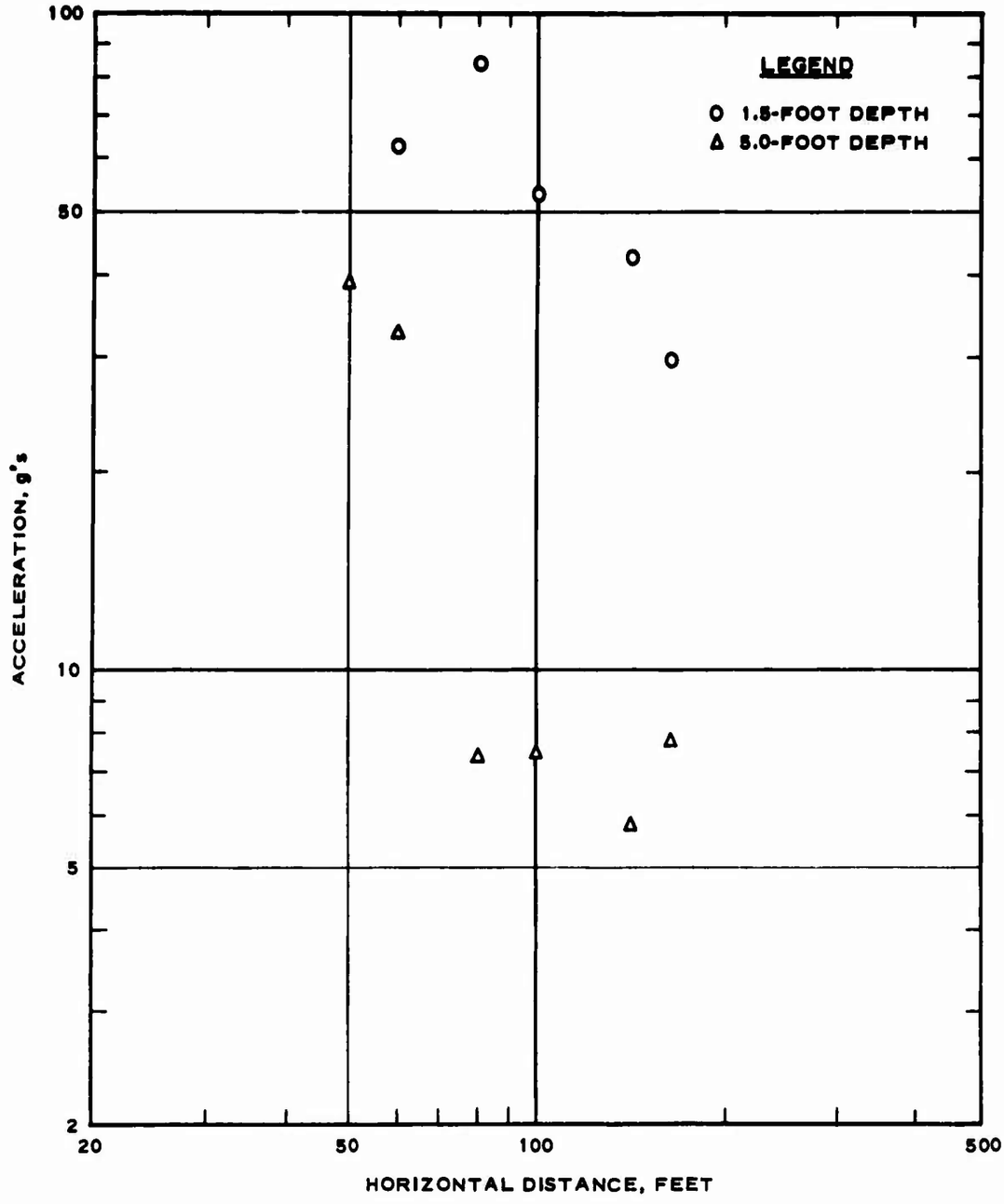

Figure 3.7 Peak outward horizontal acceleration versus distance, Event 6.

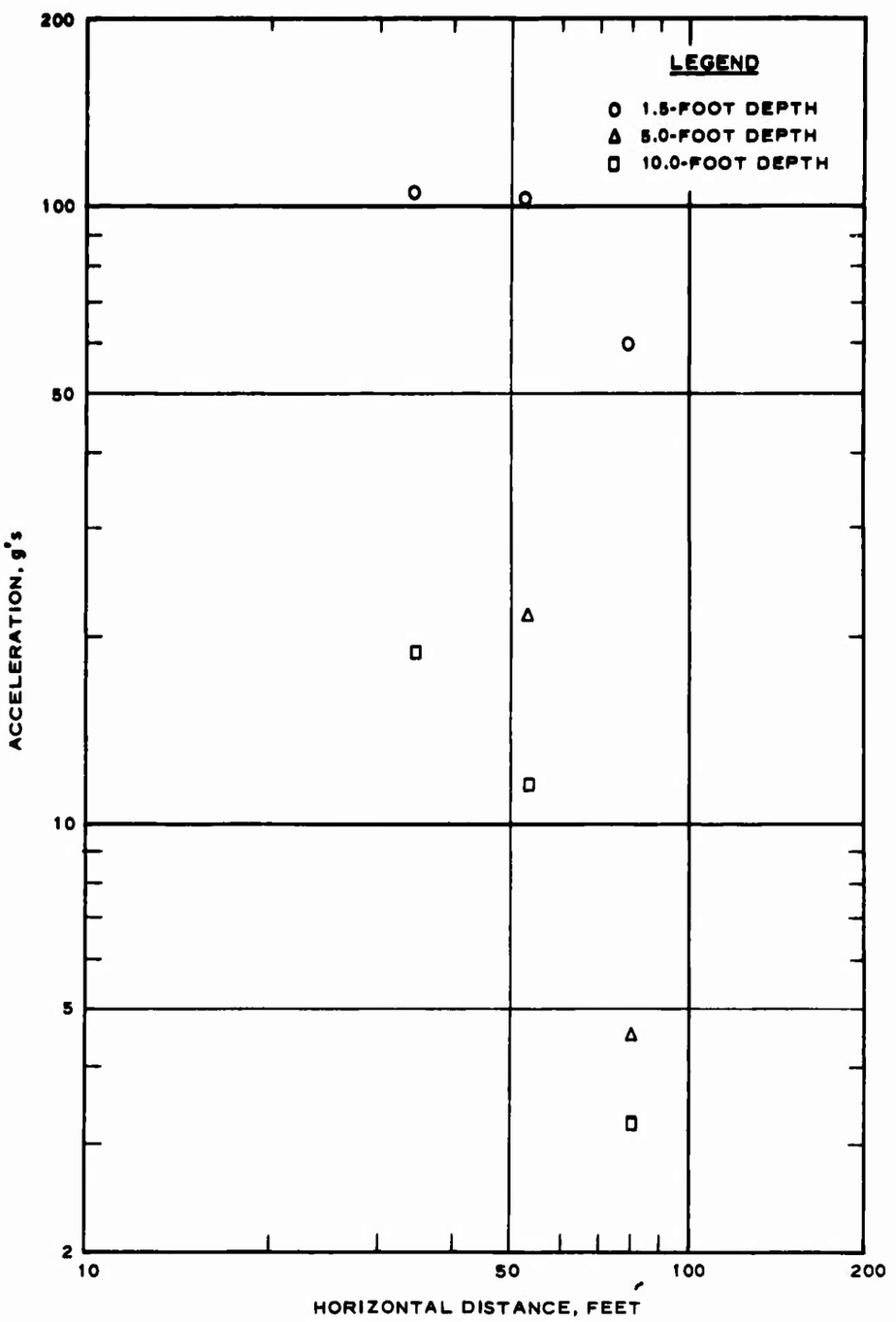

Figure 3.8 Peak outward horizontal acceleration versus distance, Event 1A.

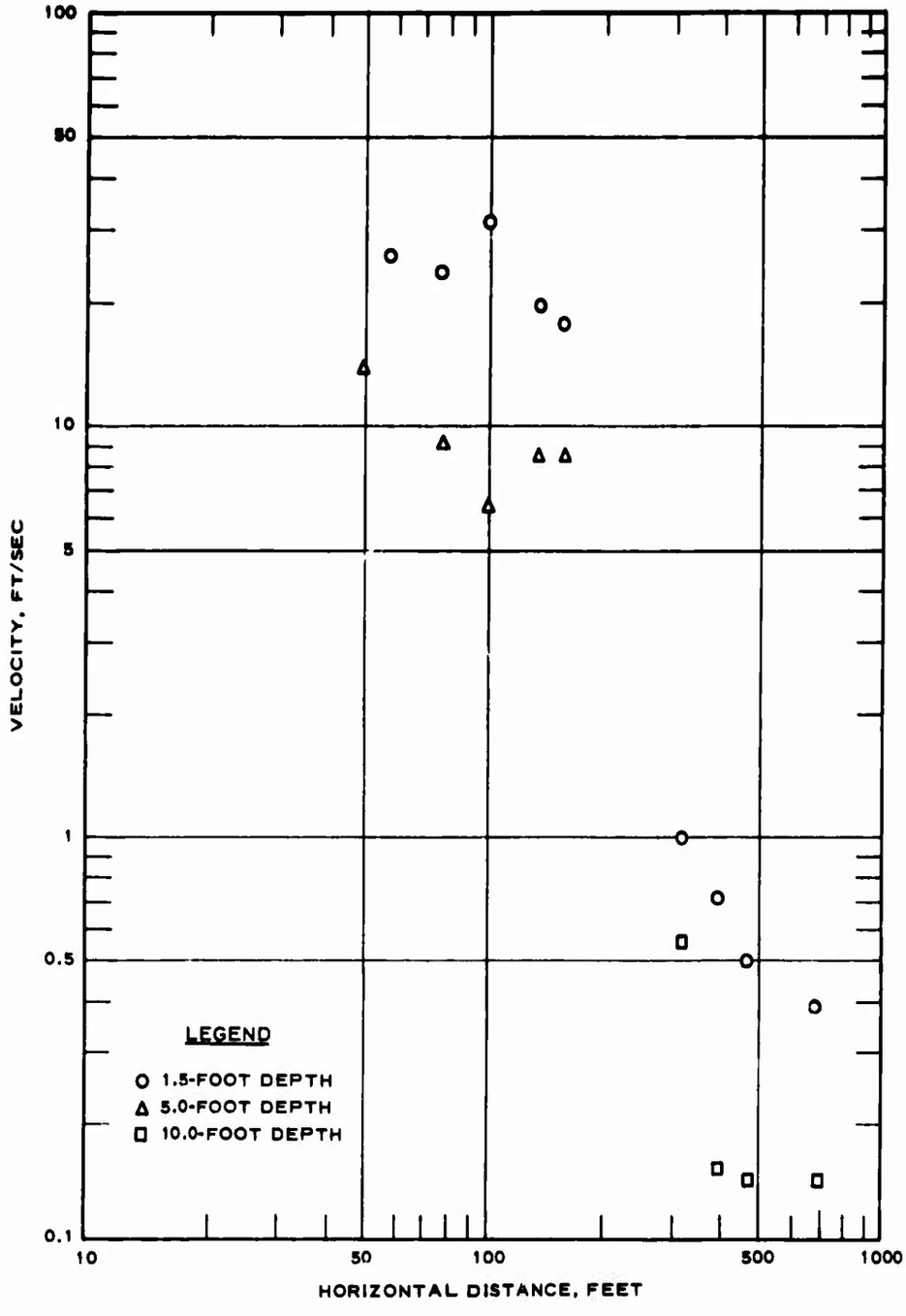

Figure 3.9 Peak vertical downward particle velocity versus distance, Event 6.

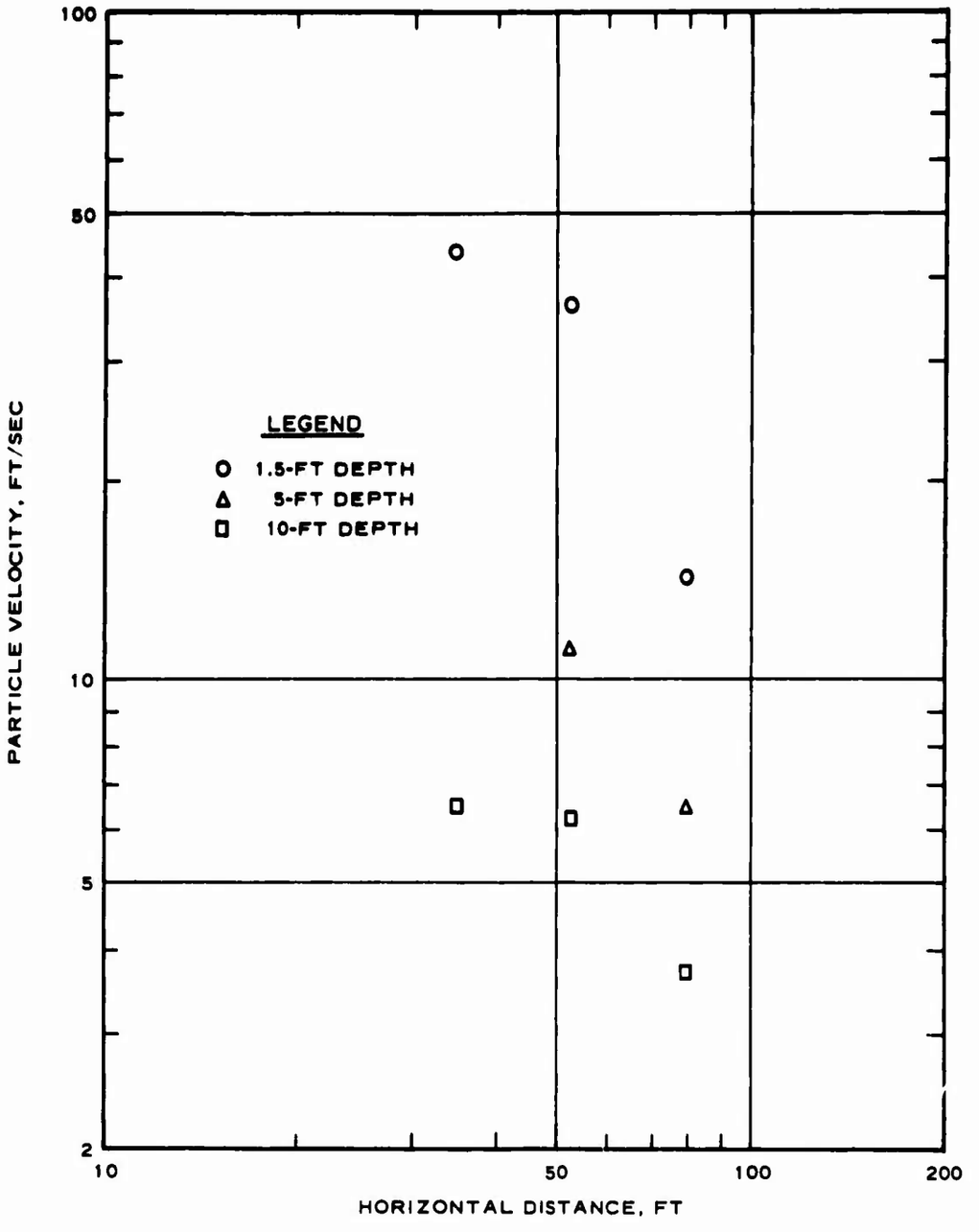

Figure 3.10 Peak vertical downward particle velocity versus distance, Event 1A.

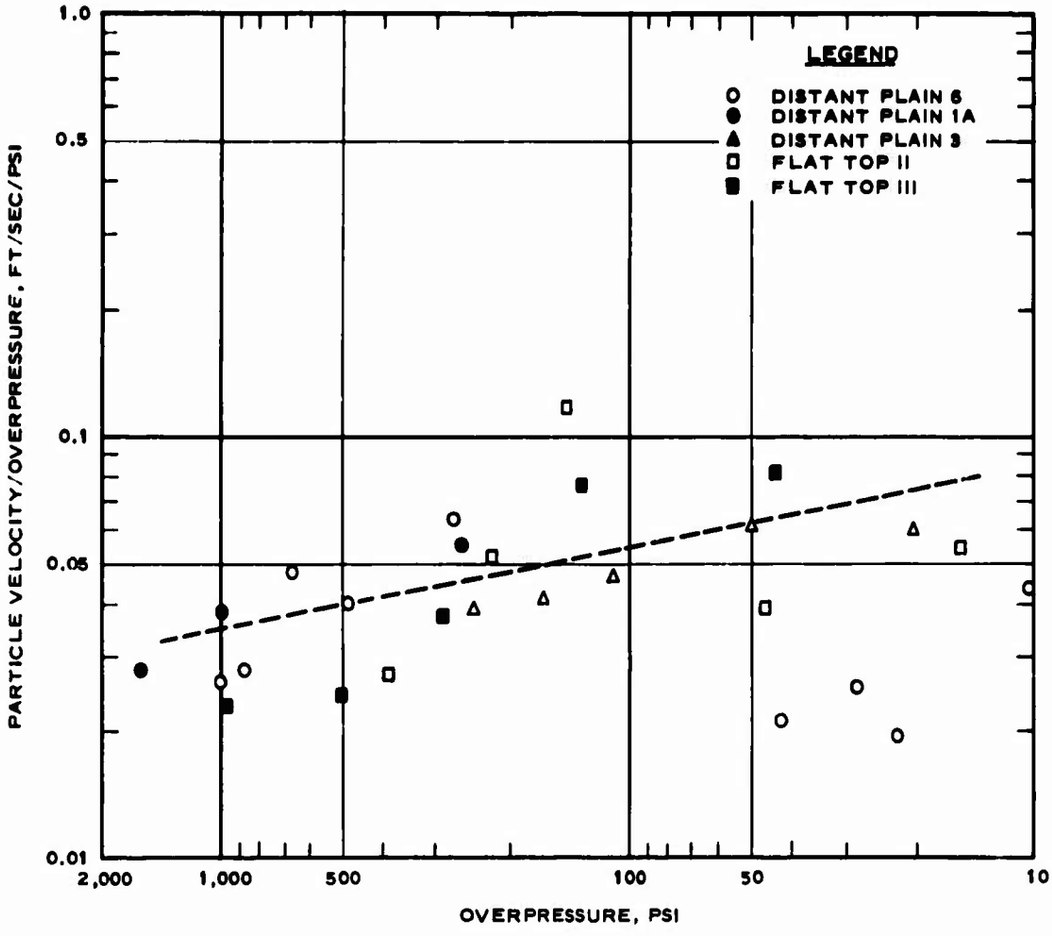

Figure 3.11 Velocity/overpressure ratio versus overpressure, 1.5-foot depth.

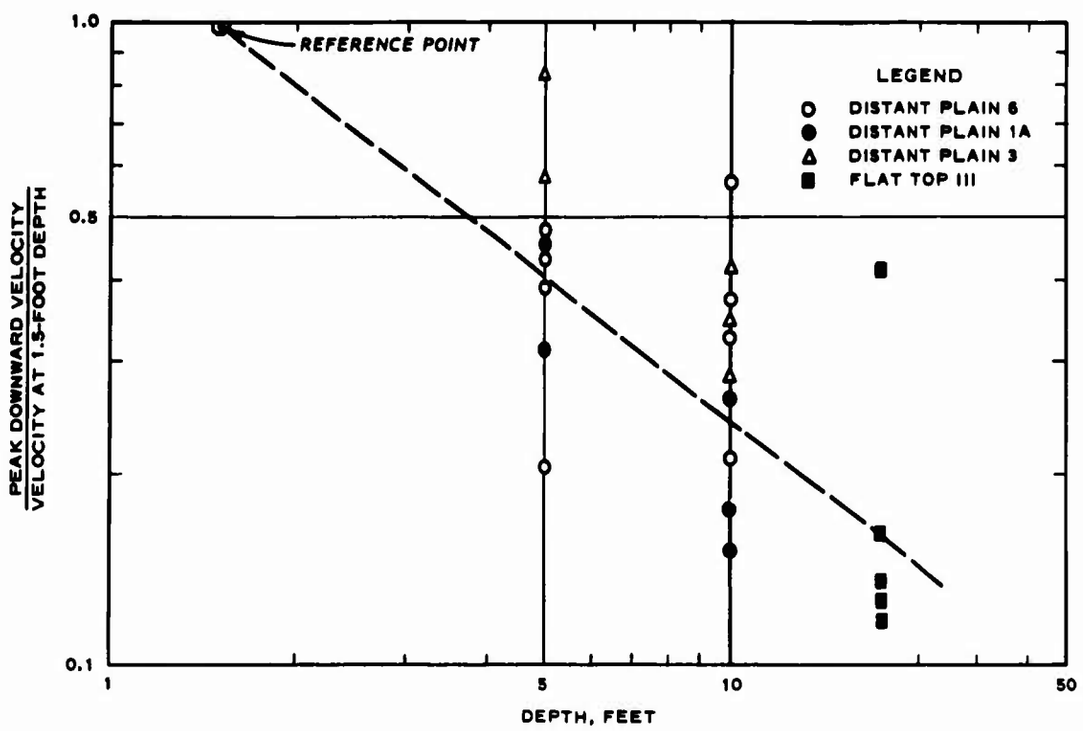

Figure 3.12 Vertical particle velocity attenuation with depth.

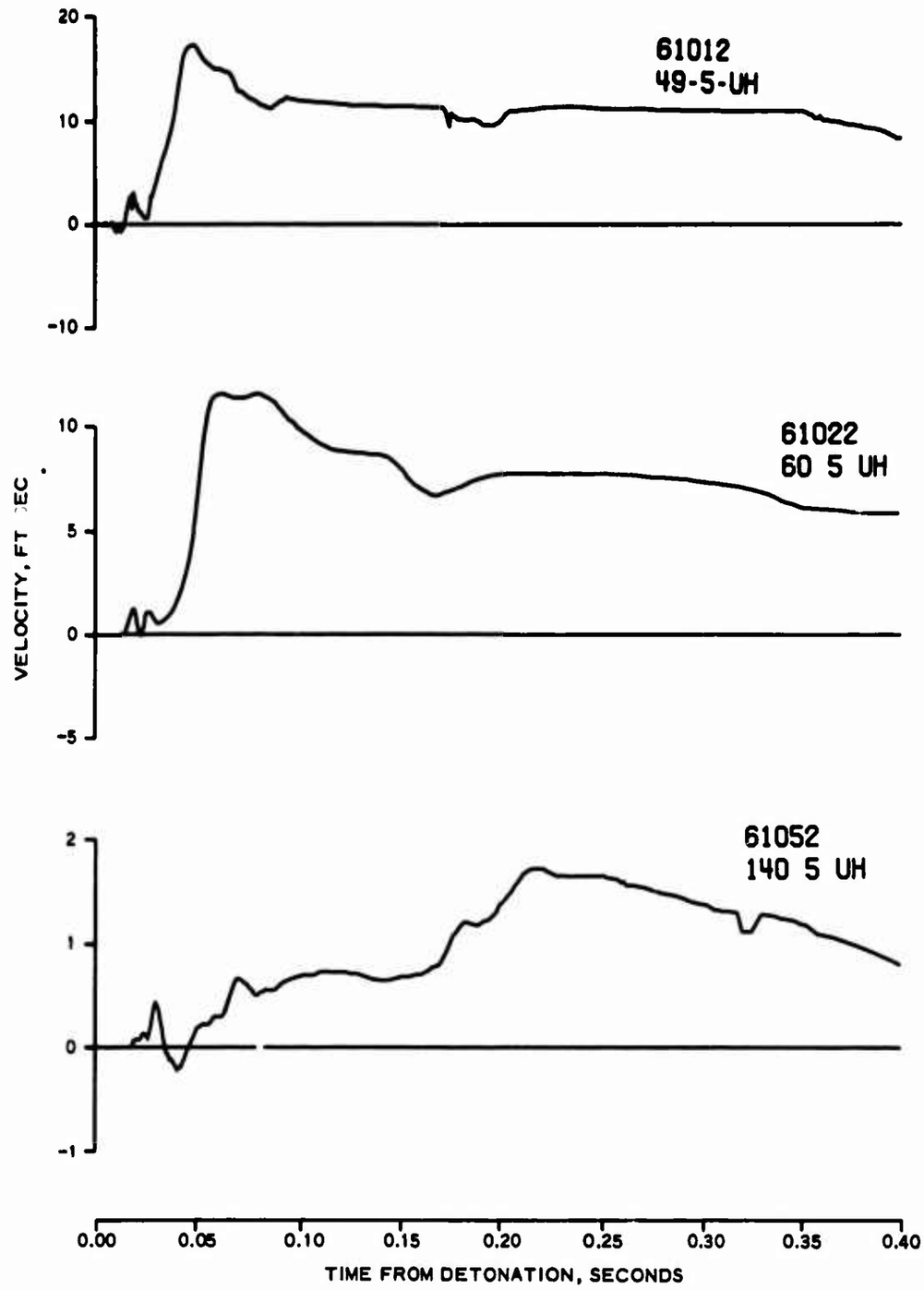

Figure 3.13 Time histories of selected horizontal velocities, Event 6.

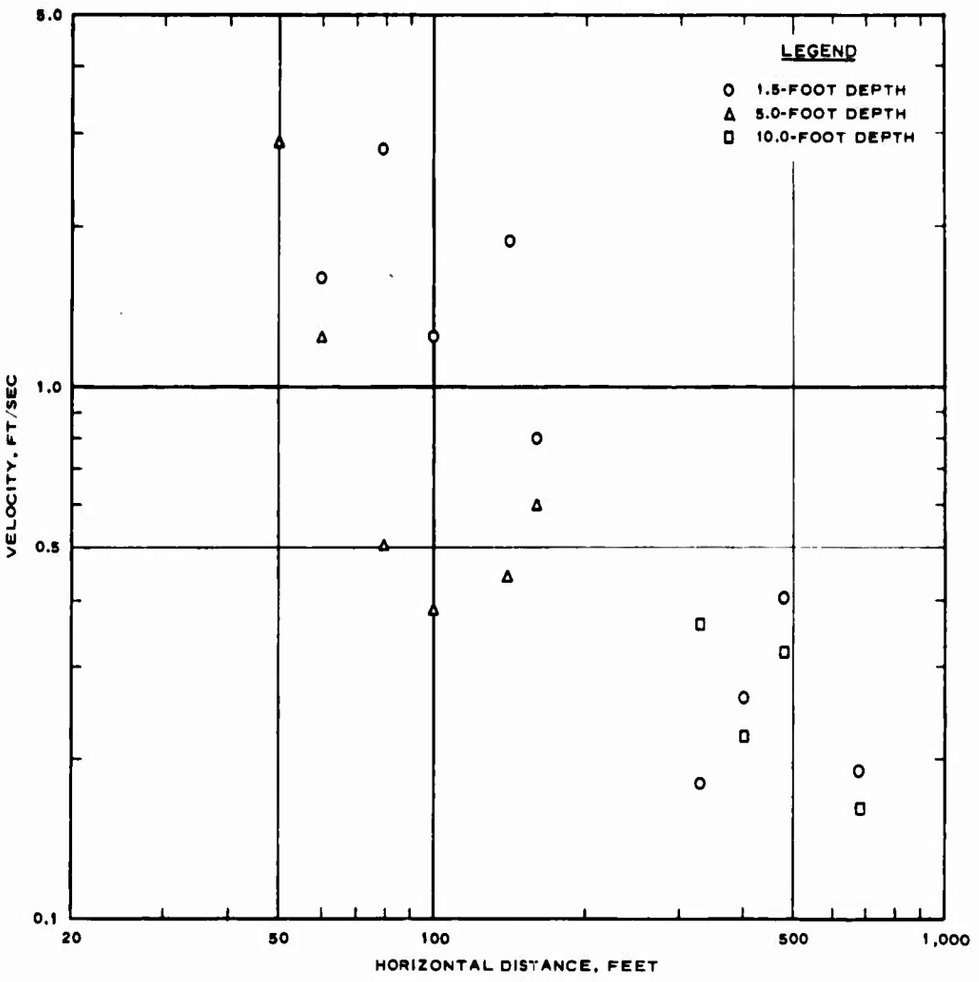

Figure 3.14 Peak outward airblast-induced particle velocities versus distance, Event 6.

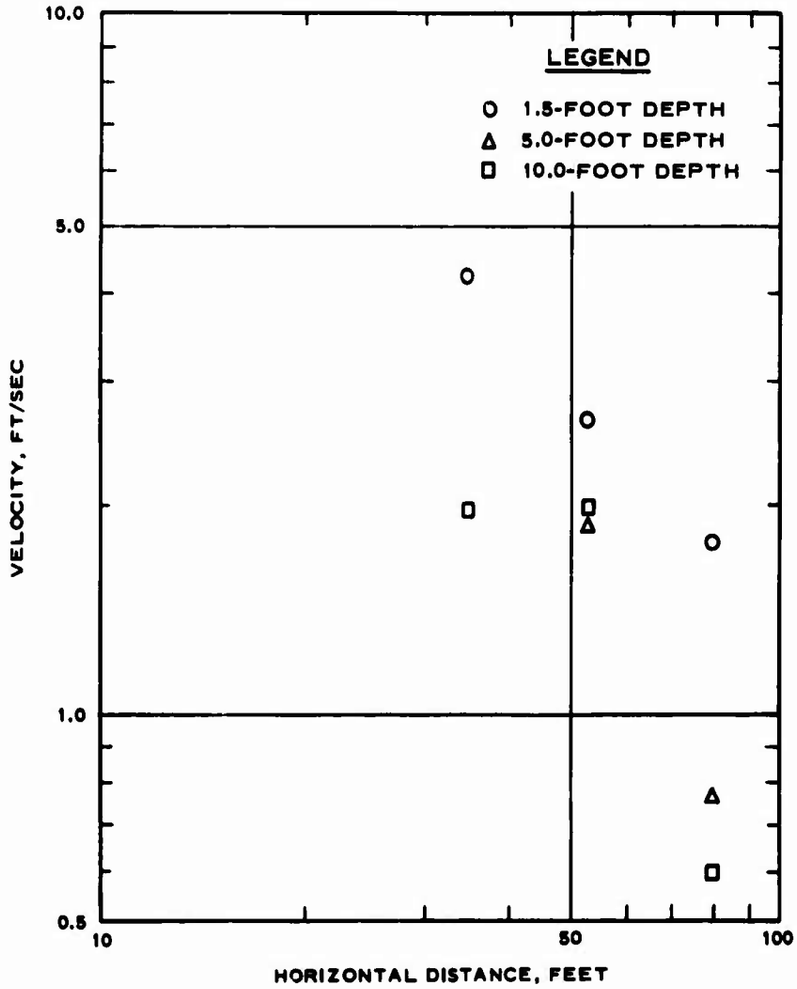

Figure 3.19 Peak outward airblast-induced particle velocities versus distance, Event 1A.

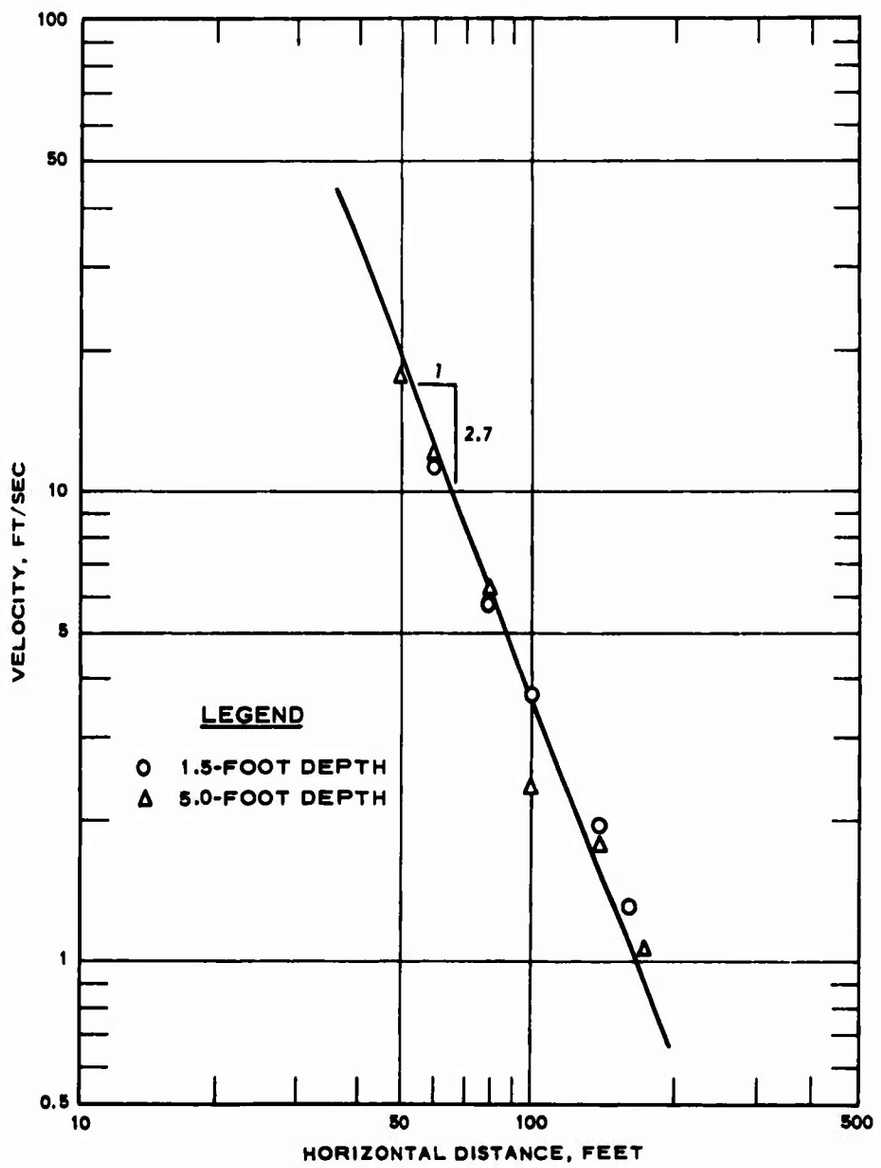

Figure 3.16 Peak outward cratering-induced particle velocity versus distance, Event 6.

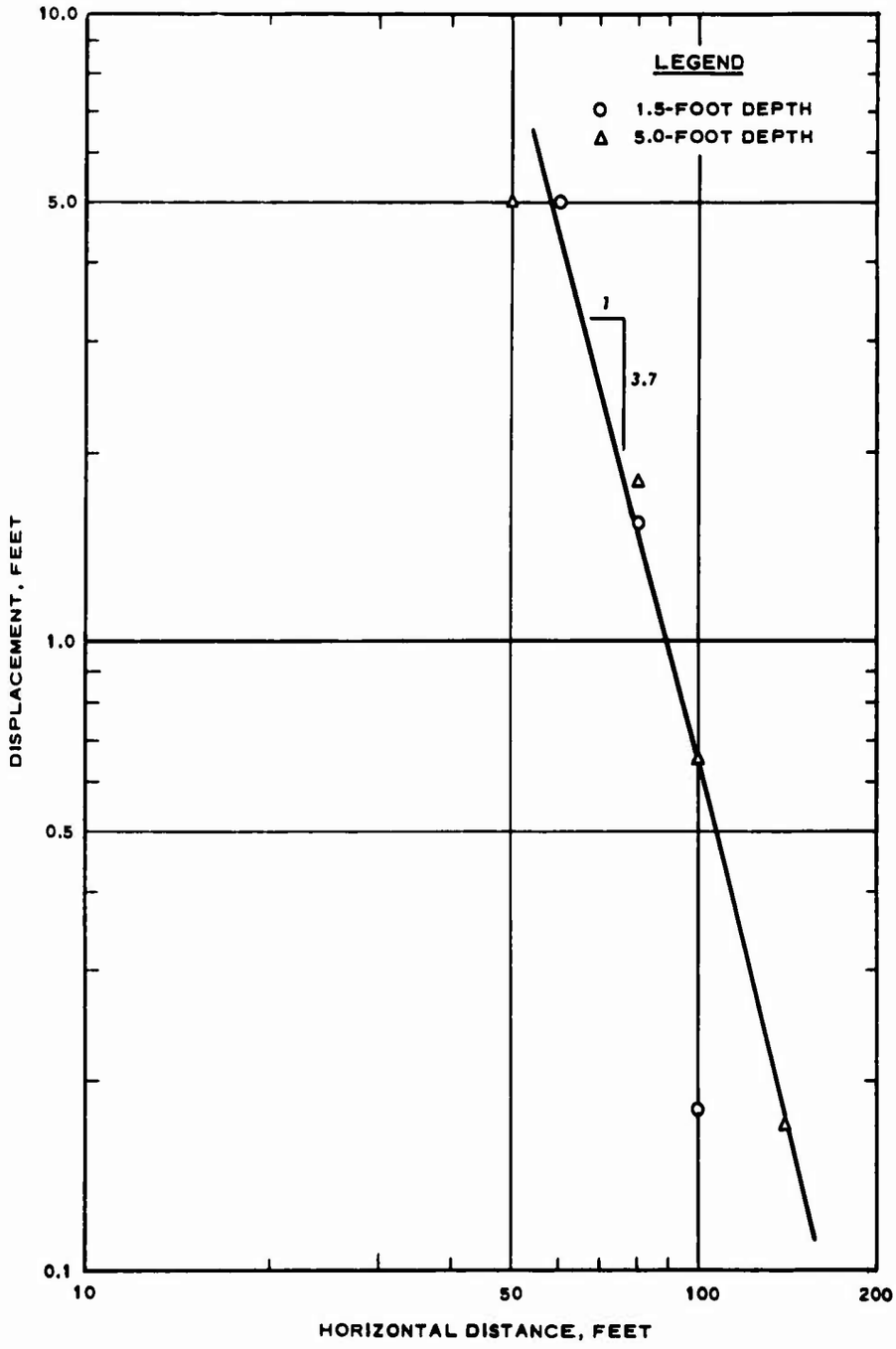

Figure 3.17 Peak upward transient displacement versus distance, Event 6.

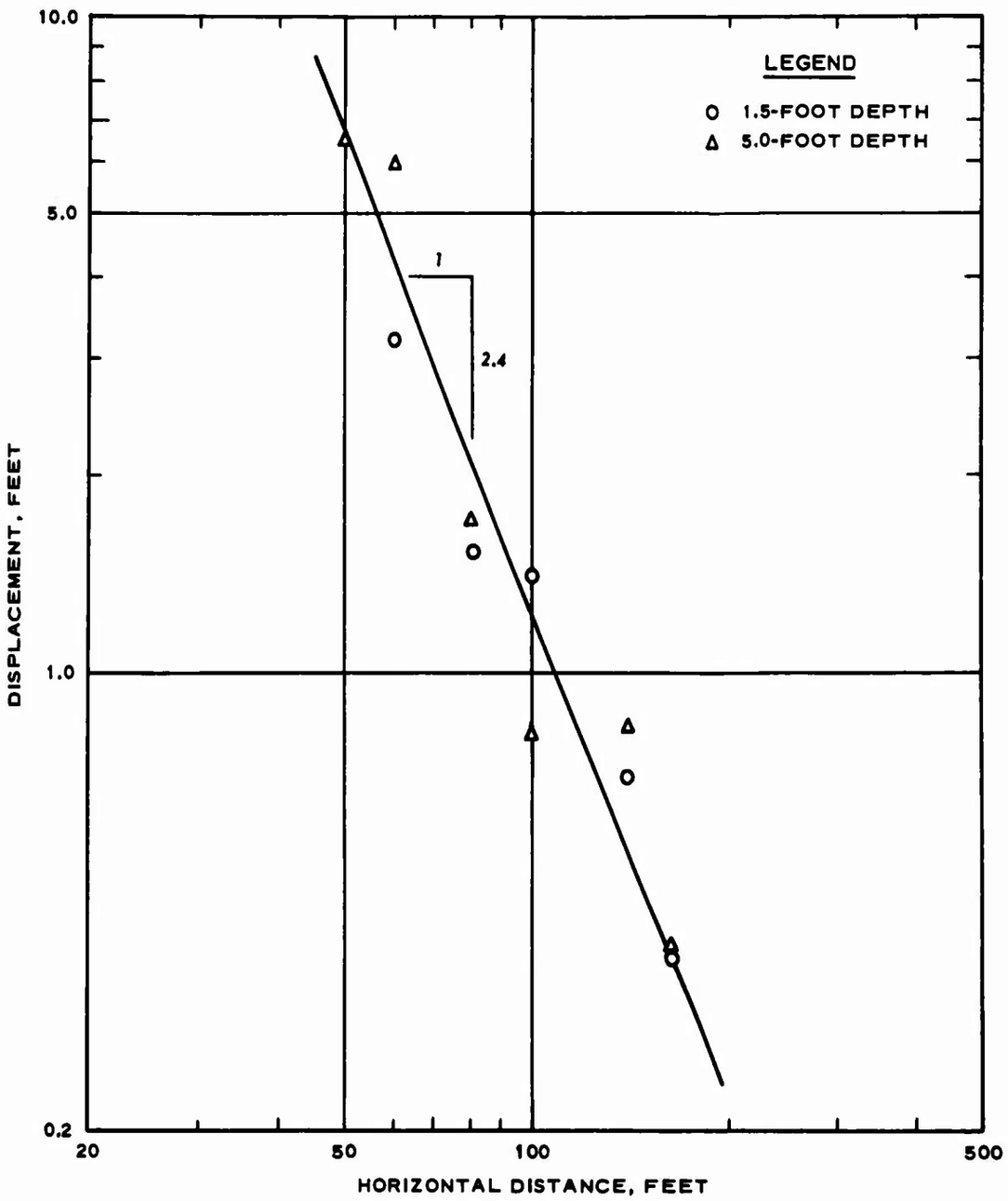

Figure 3.18 Peak outward transient displacement versus distance, Event 6.

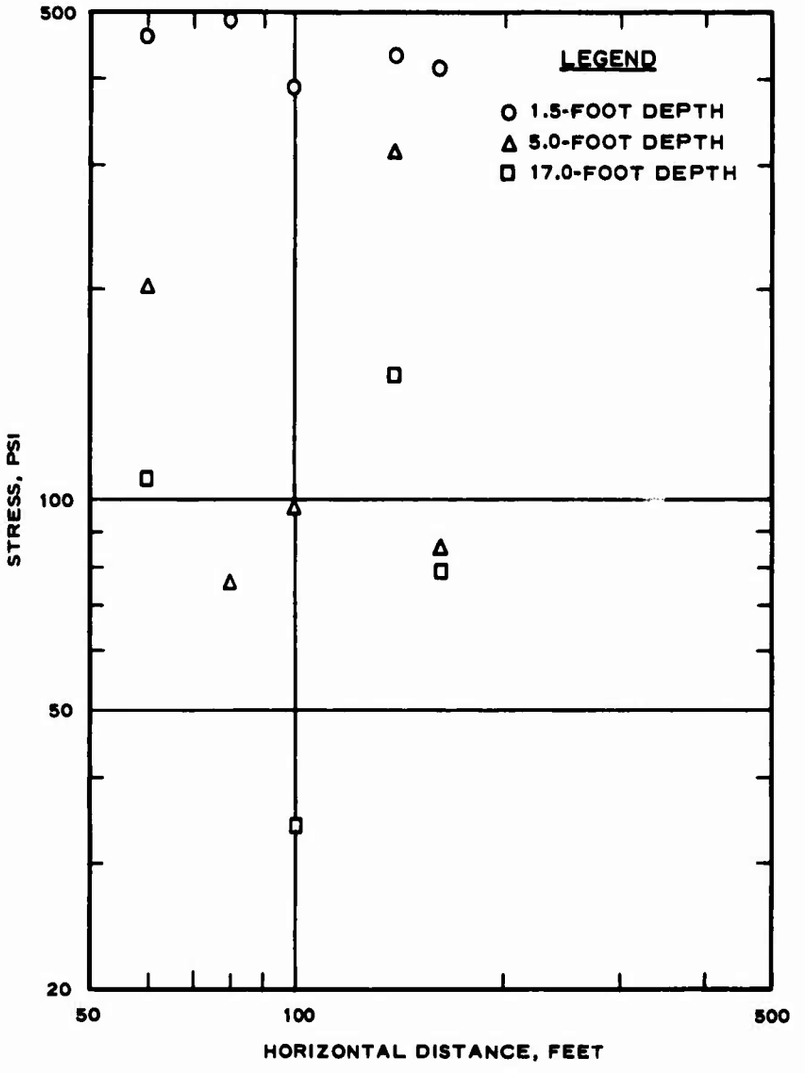

Figure 3.19 Peak vertical stress versus horizontal distance, Event 6.

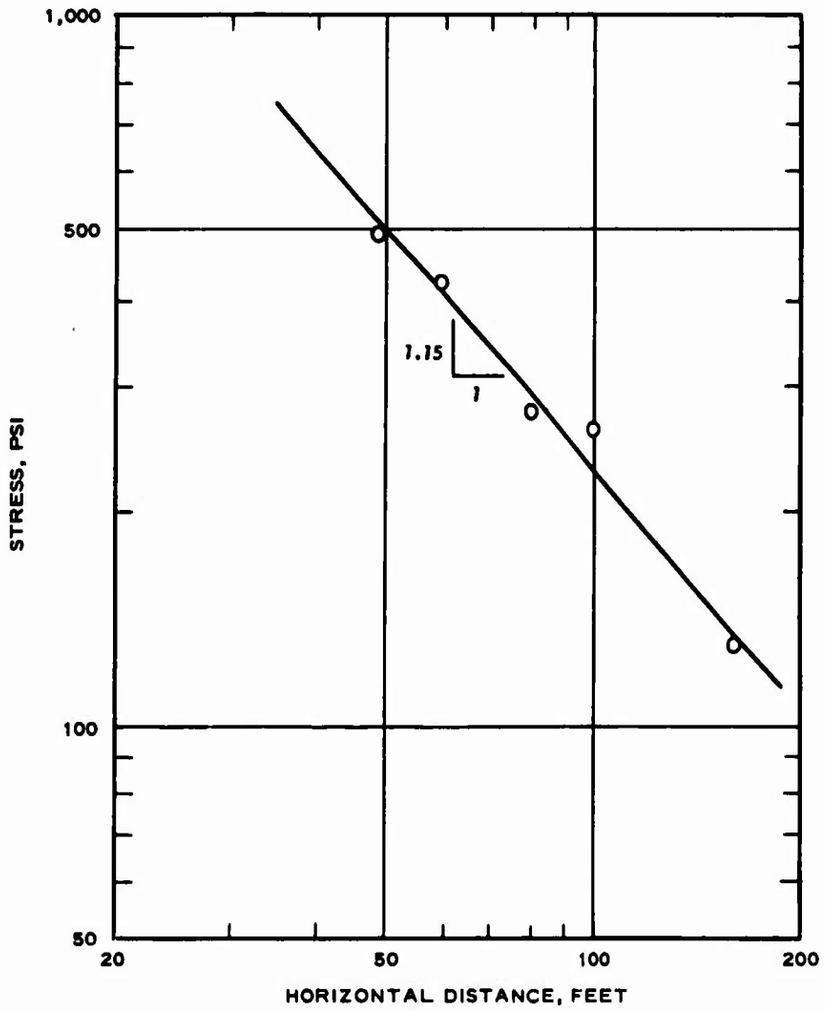

Figure 3.20 Peak horizontal stress versus horizontal distance, 30-foot depth, Event 6.

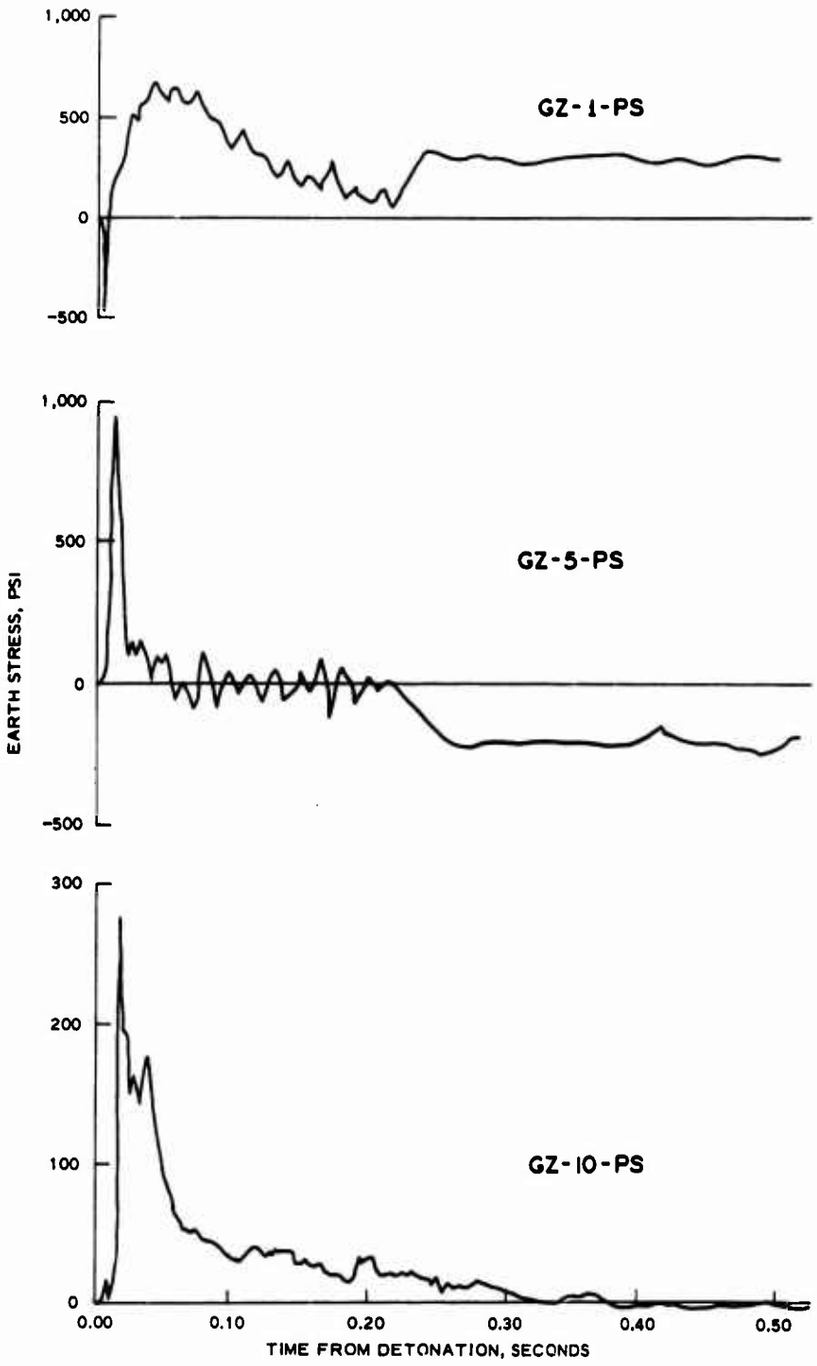

Figure 3.21 Stress-time histories, ground zero, Event 1A.

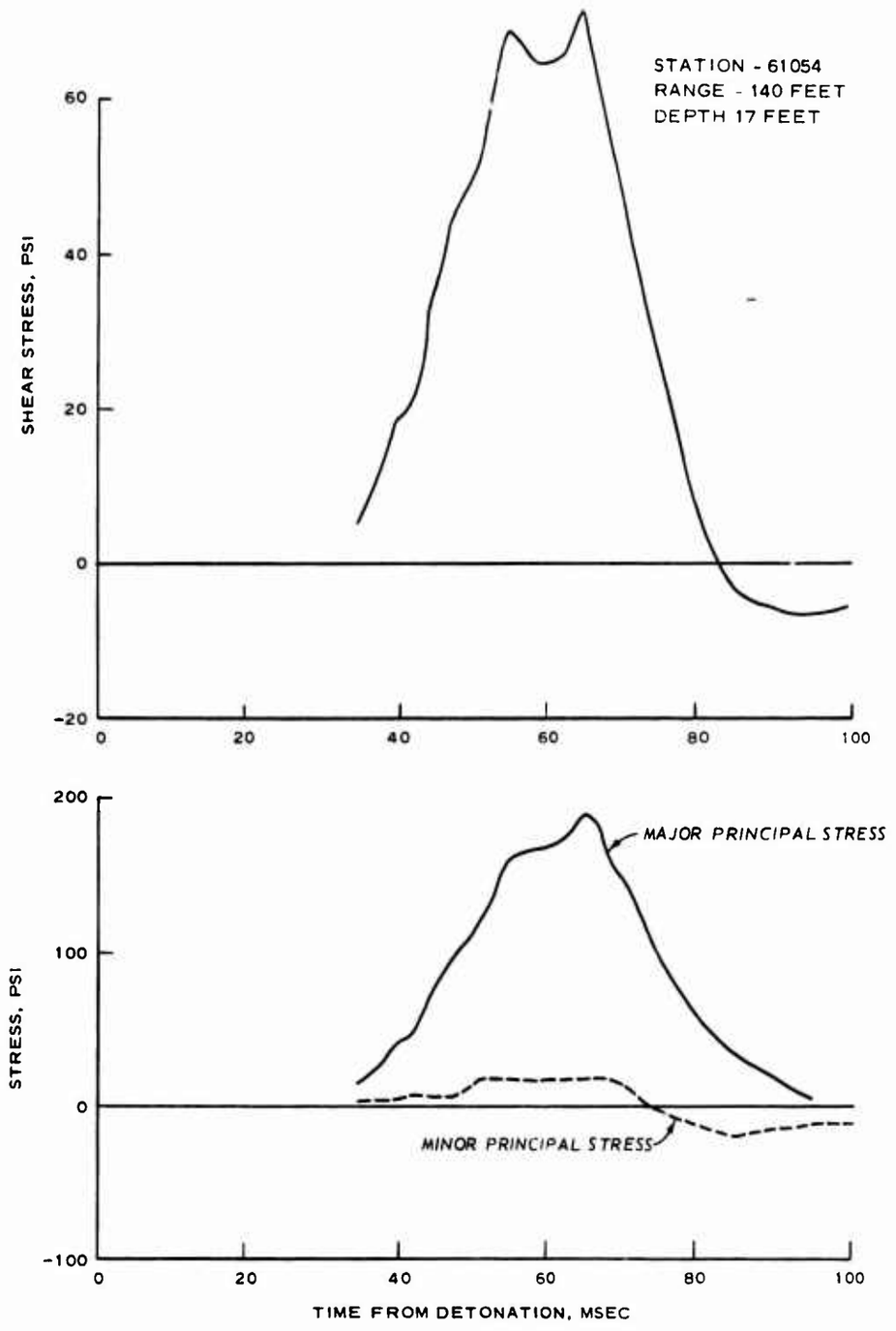

Figure 3.22 Shear and principal stress data, Location 61054, Event 6.

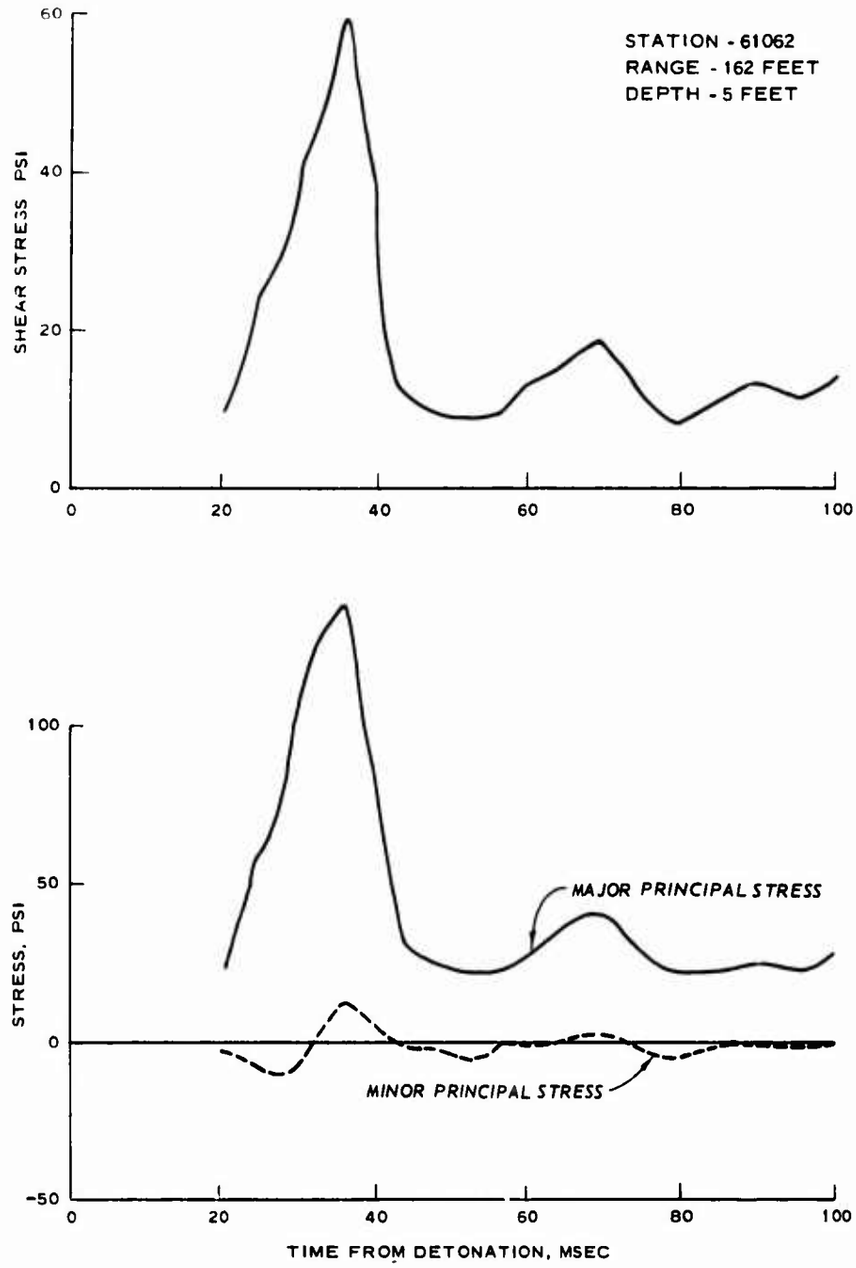

Figure 3.23 Shear and principal stress data, Location 61062, Event 6.

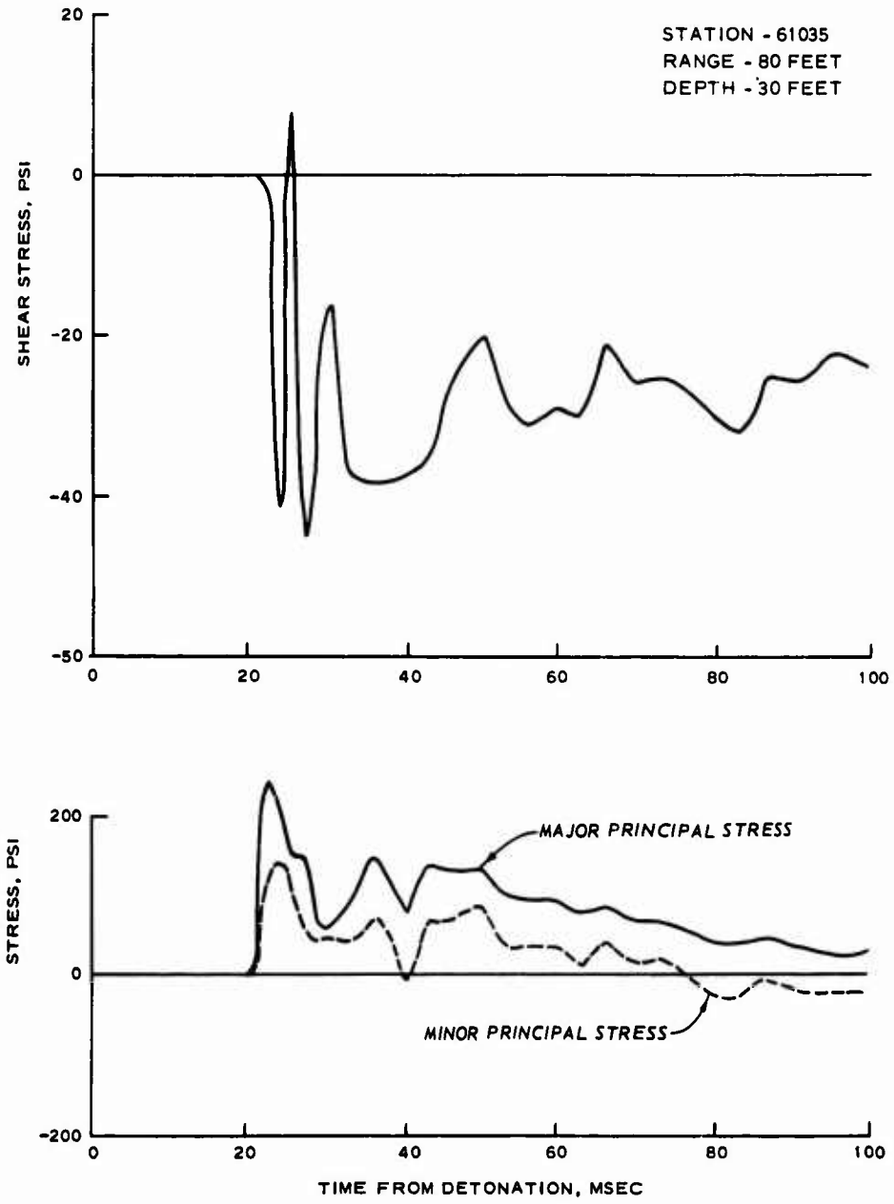

Figure 3.24 Shear and principal stress data, Location 61035, Event 6.

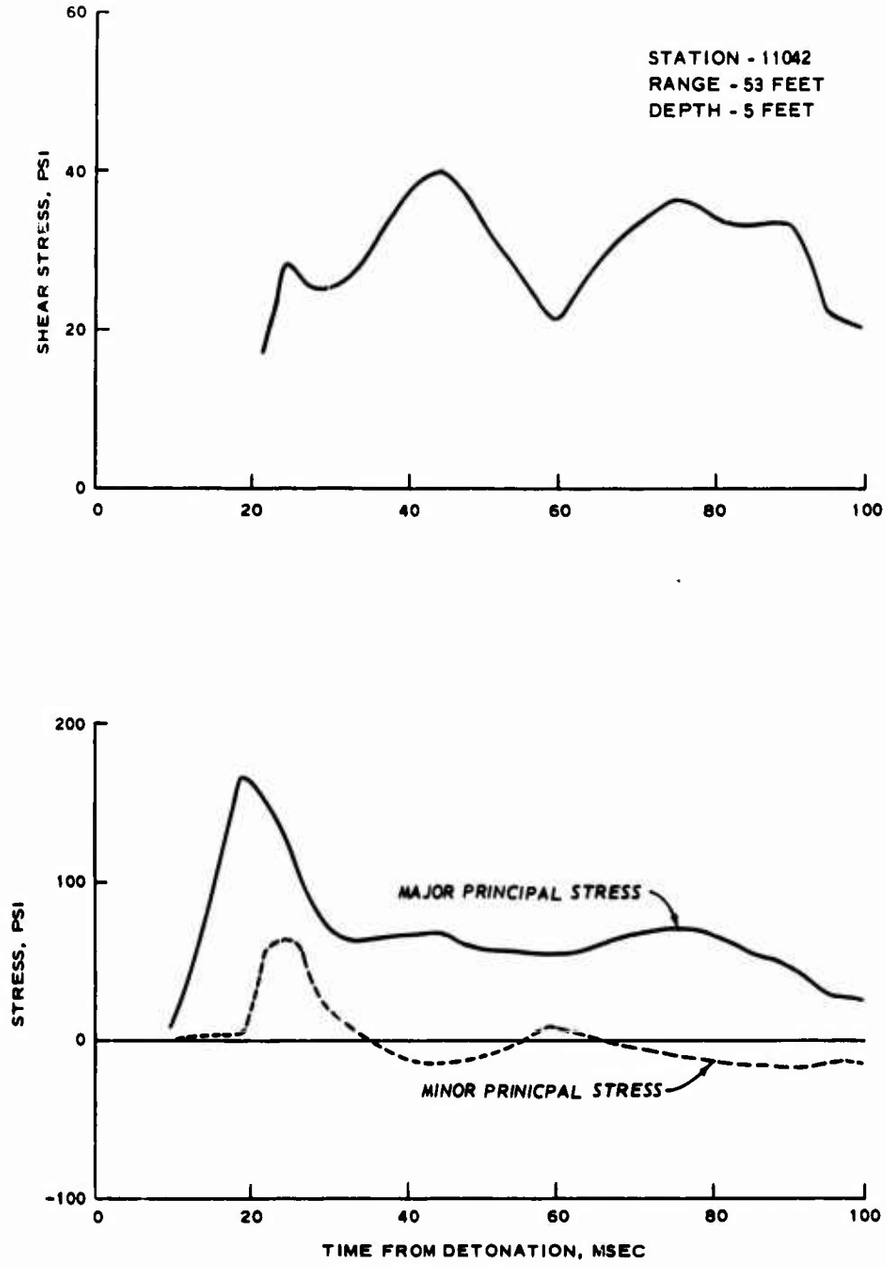

Figure 3.25 Shear and principal stress data, Location 11042, Event 1A.

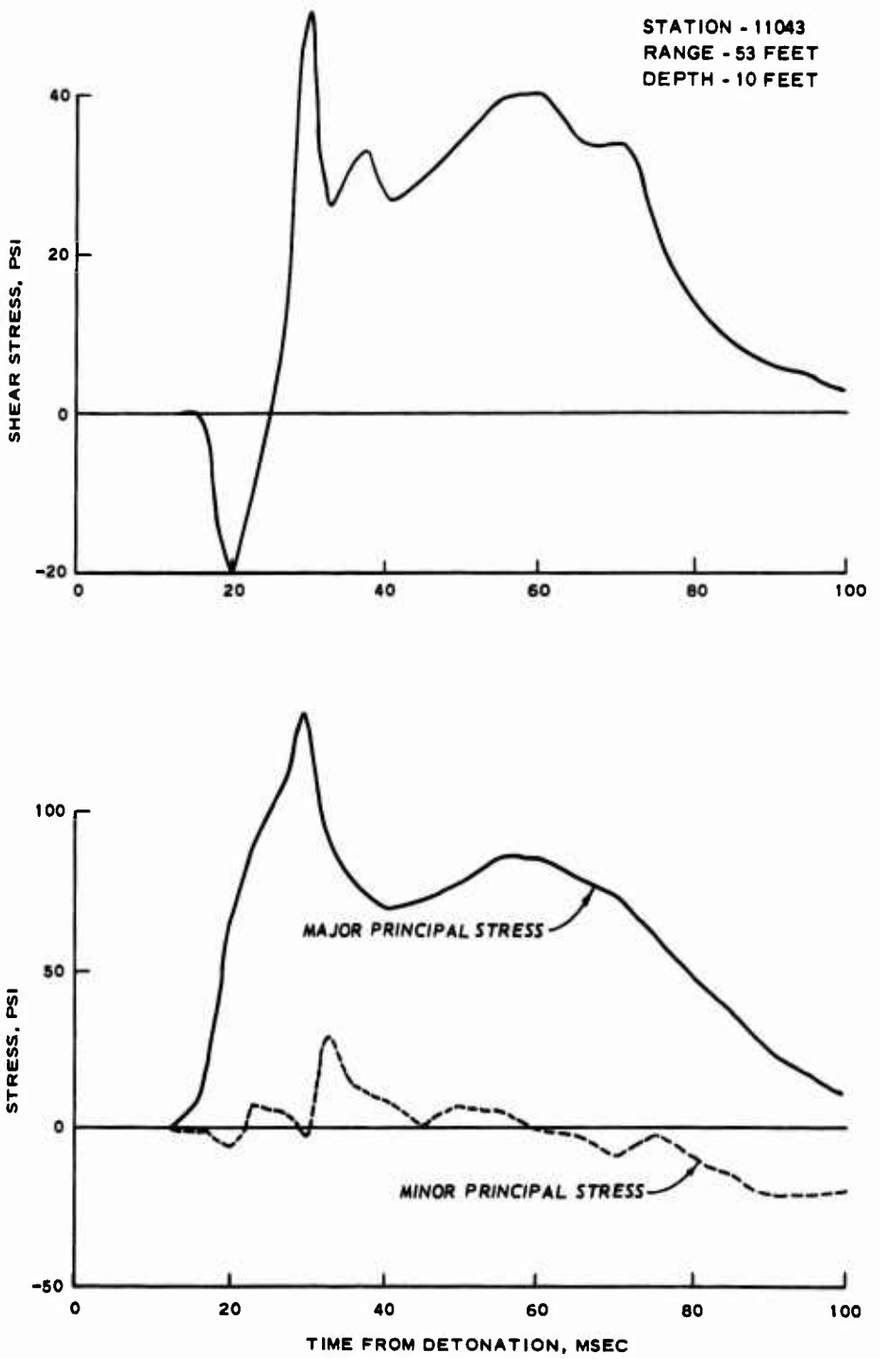

Figure 3.26 Shear and principal stress data, Location 11043, Event 1A.

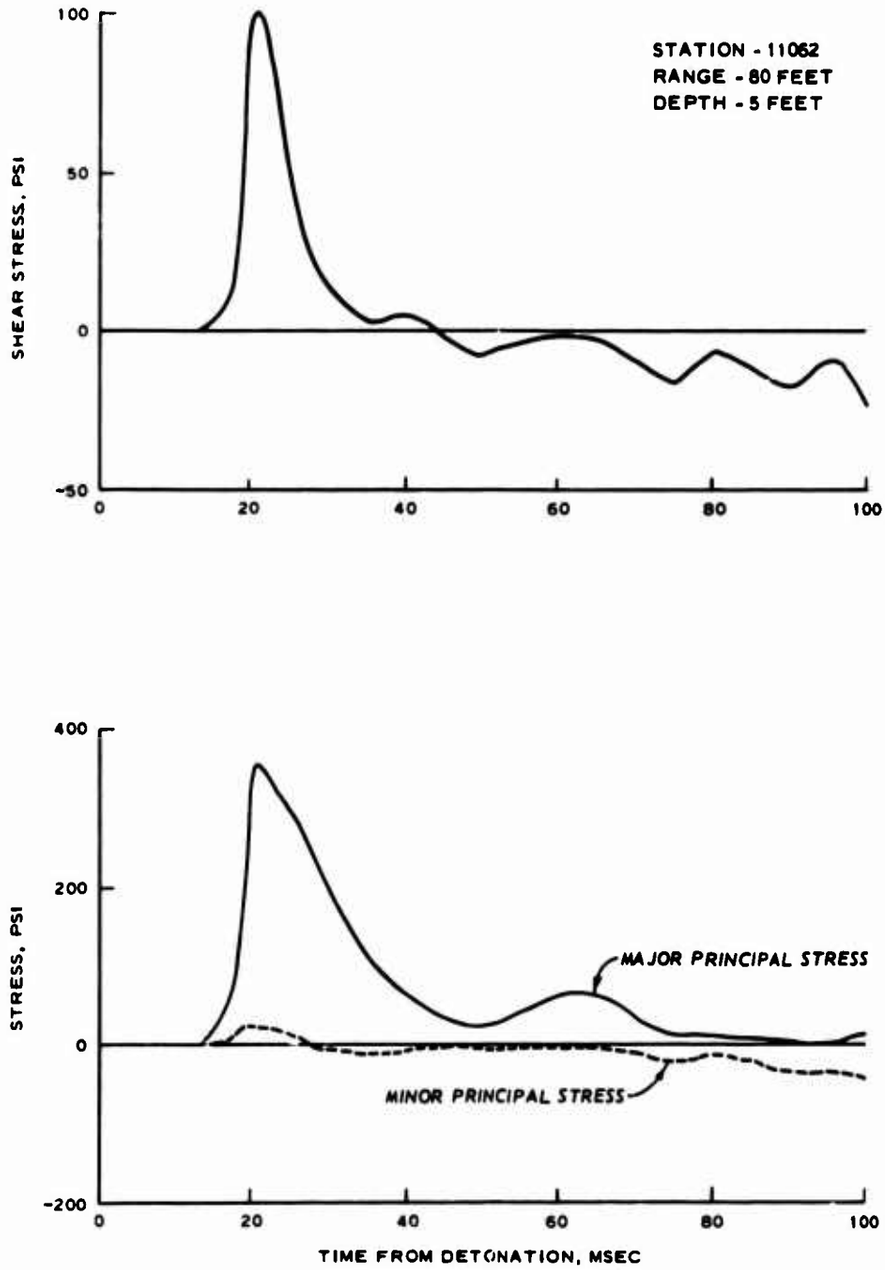

Figure 3.27 Shear and principal stress data, Location 11062, Event 1A.

CHAPTER 4

CONCLUSIONS

Overall instrument performance for Distant Plain Events 6 and 1A was excellent. Over 95 percent of the gages installed for the two events yielded good quality data of uniformly high signal-to-noise ratio.

Arrival times were obtained for all successfully recorded gages, and were used to calculate propagation velocities of both above- and below-water-table soil layers. These velocities were 1,100 and 5,500 ft/sec, respectively, and were both essentially the same as those determined on Operation Snow Ball and by seismic surveys. Arrival times also provided the first indication of outrunning ground motion, and were used to construct a shock front profile for Event 6 (Figure 3.1). From this profile it was determined that the outrunning ground motion, which had been refracted along the water table, arrived at the ground surface prior to the airblast at a distance of 400 feet from GZ, or at the 30-psi level. This was nearly the same pressure level as was found for Snow Ball and indicates that yield plays a minor part in the pressure level associated with outrunning, at least for the Watching Hill test site.

Peak vertical accelerations attenuated sharply with both increasing range and depth. The ratio of acceleration to overpressure

for the 1.5-foot depth was found to increase from about 0.4 g/psi at 1,000 psi to about 1 g/psi at 20 psi for Event 6 data, and correlated very well with data from the Distant Plain Event 3 and Flat Top Events II and III. Event 1A data were consistently above the norm for this correlation, but were within the data scatter. Disturbed airblast waveforms probably account for the deviation.

Peak vertical accelerations at the 5-foot depth were attenuated to 20 percent of those at the 1.5-foot depth, and those at the 10-foot depth averaged 7.5 percent of the shallower data. These figures were in good agreement with Distant Plain Event 3 data.

The two correlation curves (Figures 3.5 and 3.6) would thus provide predictions of acceleration with relatively high confidence, at least for the range of yields encountered (20 to 100 tons).

Peak vertical particle velocities also attenuated sharply with both increasing distance and depth, although the effect was less pronounced than for accelerations.

Ratios of vertical particle velocity to overpressure for the 1.5-foot depth also increased with decreasing overpressure, and varied from about 0.03 ft/sec/psi at 1,600 psi to about 0.08 ft/sec/psi at 10 psi.

Peak vertical velocities at the 5-foot depth were found to average 40 percent of those at the 1.5-foot depth, while velocities at a depth of 10 feet averaged 30 percent of the 1.5-foot data.

Horizontal particle velocities for Event 6 were dominated by the cratering-induced pulse which attenuated in a regular manner as the -2.7 power of distances. These velocities varied from 17.3 ft/sec at Location 61012 to 1.35 ft/sec at Location 16061. In contrast, particle velocities induced by passage of the airblast were 2.9 ft/sec and 0.80 ft/sec for the same two locations.

Displacements calculated for Event 6 were also dominated by the cratering-induced pulse. This disturbance caused upward and outward particle motion of considerable magnitude. The upward and outward components of displacement at Location 16012, for example, were 5.1 and 6.5 feet, respectively. The vertical component decreased as the -3.7 power of horizontal distance, while the horizontal displacement attenuated as the -2.4 power.

Displacements for Event 1A were airblast-induced only and were consequently directed downward and outward. The vertical displacements were found to agree reasonably well with those calculated at similar pressure levels for Event 6.

Soil stresses measured on Event 6 at locations above the water table showed more scatter than did motion measurements, and attenuated with depth more rapidly. Measurements from below the water table, at a depth of 30 feet, attenuated as the -1.15 power of distance, a rate which approximates that of free water.

Calculations of principal stresses and shear stresses were

successfully made for three locations on each event. Peak major principal stresses were found to run somewhat higher than the measured vertical stresses, emphasizing the obliquity of the airblast-induced shock front. With one exception, Location 11062, all calculations of shear stress gave peak values of between 40 and 70 psi. Since these represent measurements for a variety of overpressures, this region of shear stress would appear to be an upper bound for the material.

APPENDIX A

EVENT 6 TIME HISTORIES

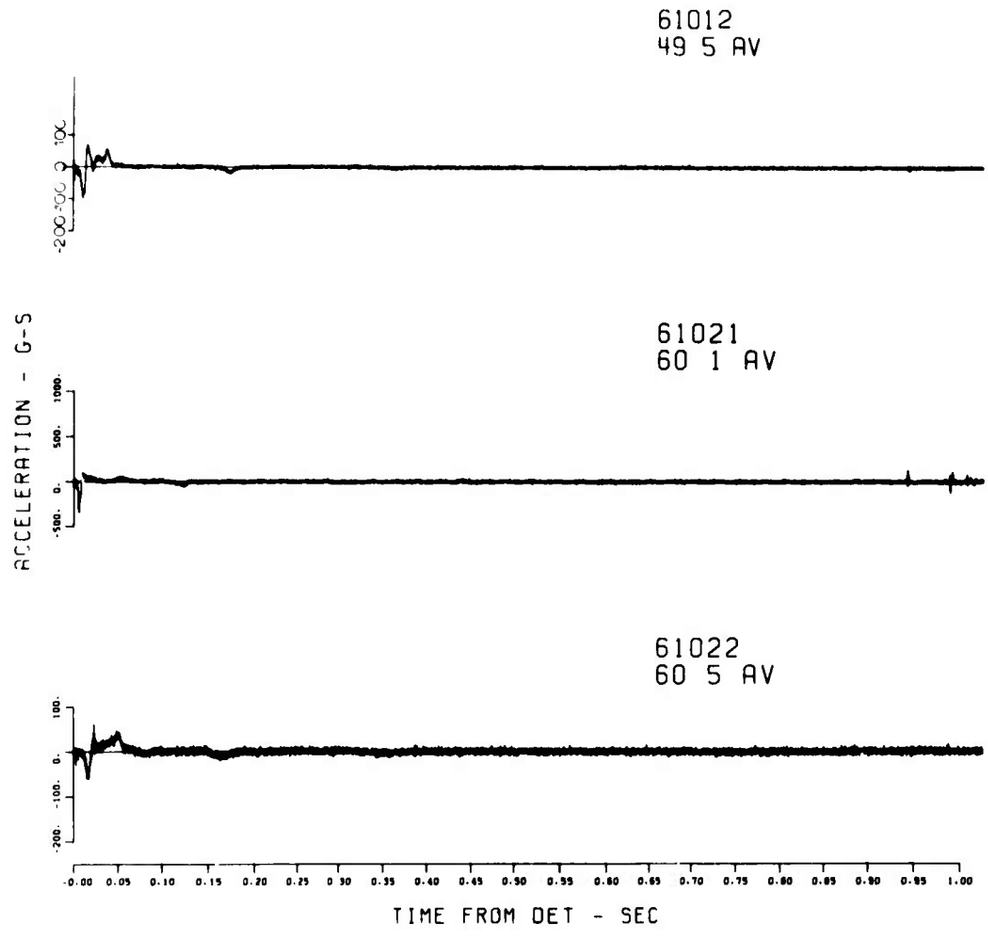
61012
49 5 AV
61021
60 1 AV
61022
60 5 AV
ACCELERATION - G-S
-500. 0. 500. 1000.
-200. -100. 0. 100.
-0.00 0.05 0.10 0.15 0.20 0.25 0.30 0.35 0.40 0.45 0.50 0.55 0.60 0.65 0.70 0.75 0.80 0.85 0.90 0.95 1.00
TIME FROM DET - SEC

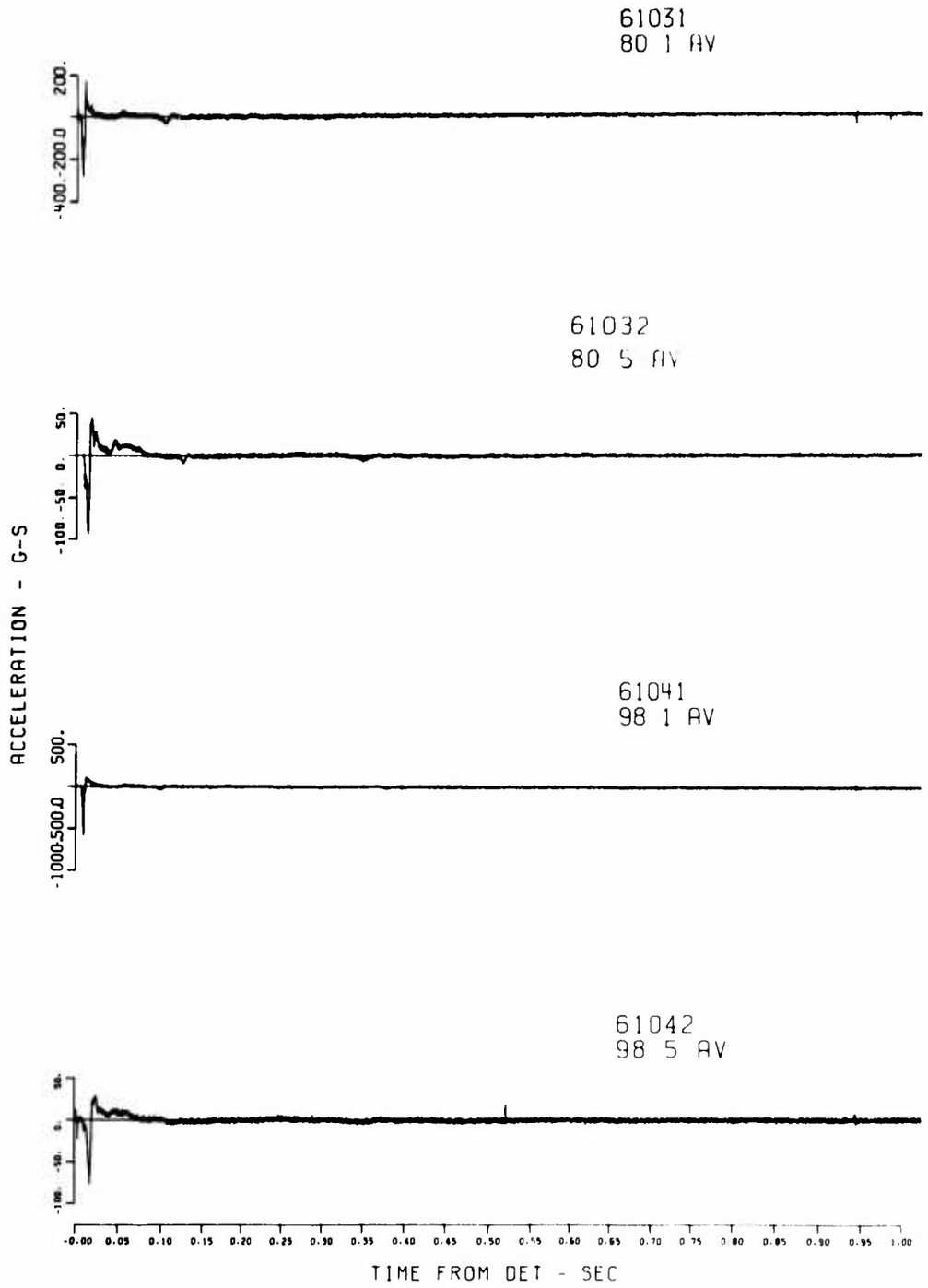
61031
80 1 AV
200.
-400. -200.0
61032
80 5 AV
50.
0.
-100. -50.
61041
98 1 AV
500.
-1000-500.0
61042
98 5 AV
-0.00 0.05 0.10 0.15 0.20 0.25 0.30 0.35 0.40 0.45 0.50 0.55 0.60 0.65 0.70 0.75 0.80 0.85 0.90 0.95 1.00
TIME FROM DET - SEC
ACCELERATION - G-S

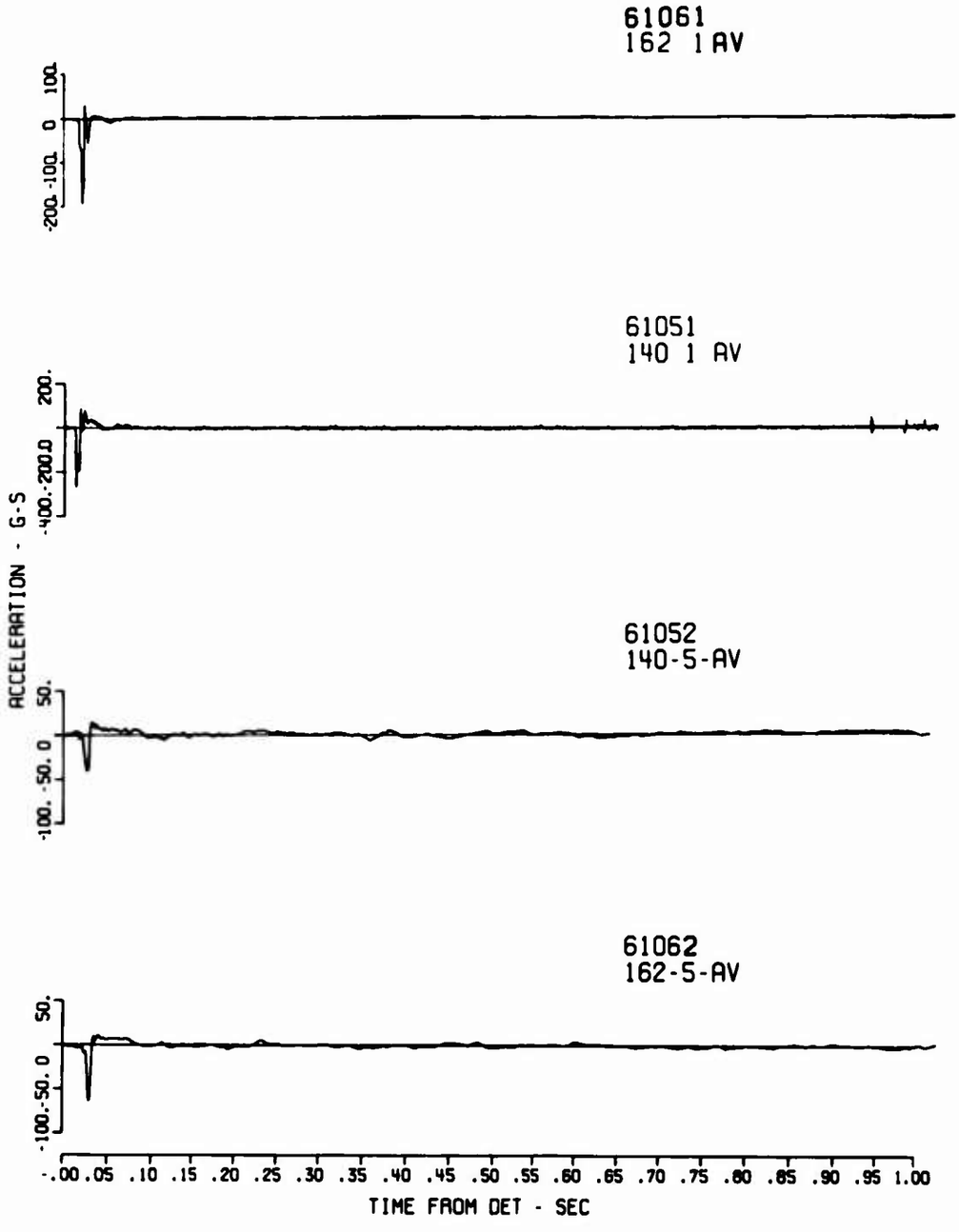
61061
162 1 AV
100.
0
-100.
-200.
61051
140 1 AV
200.
-200.0
-400.
61052
140-5-AV
50.
0
-50.
-100.
61062
162-5-AV
50.
0
-50.
-100.
ACCELERATION - G-S
-.00 .05 .10 .15 .20 .25 .30 .35 .40 .45 .50 .55 .60 .65 .70 .75 .80 .85 .90 .95 1.00
TIME FROM DET - SEC

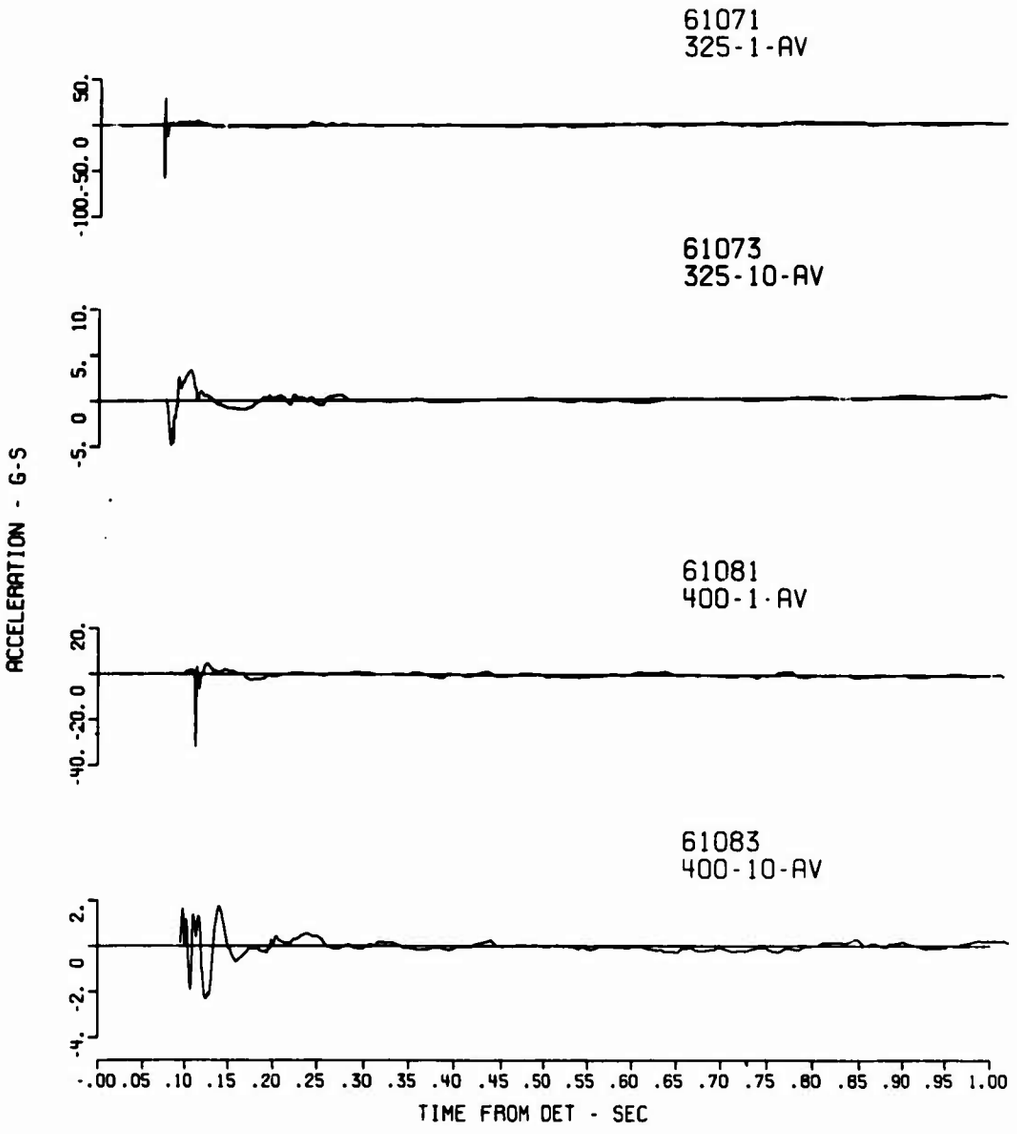
61071
325-1-AV
50.
0
-50.
-100.
61073
325-10-AV
10.
5.
0
-5.
61081
400-1-AV
20.
0
-20.
-40.
61083
400-10-AV
2.
0
-2.
-4.
ACCELERATION - G-S
.00 .05 .10 .15 .20 .25 .30 .35 .40 .45 .50 .55 .60 .65 .70 .75 .80 .85 .90 .95 1.00
TIME FROM DET - SEC

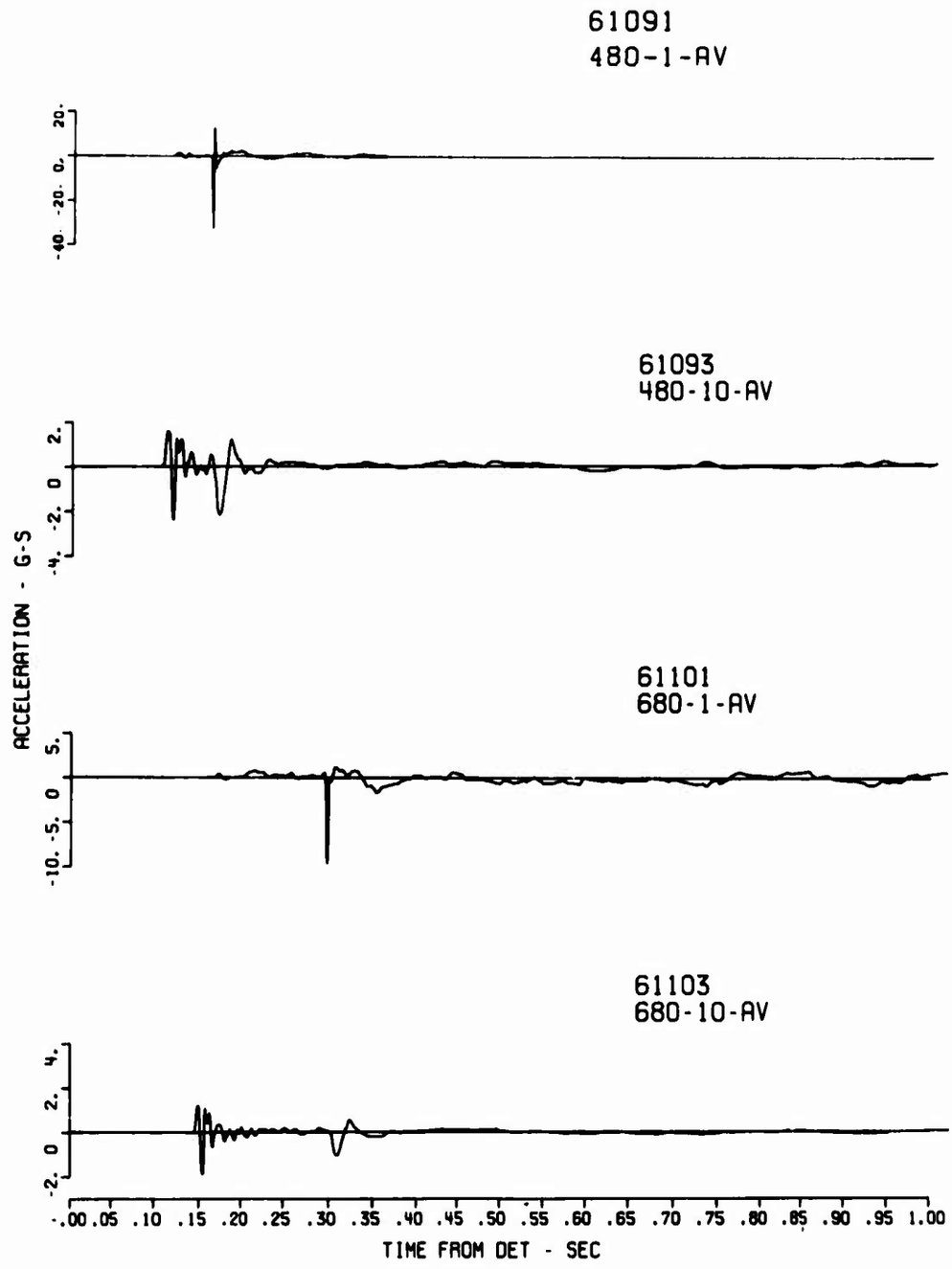
61091
480-1-AV
20.
0.
-20.
-40.
61093
480-10-AV
2.
0
-2.
-4.
ACCELERATION - G-S
61101
680-1-AV
5.
0
-5.
-10.
61103
680-10-AV
4.
2.
0
-2.
.00 .05 .10 .15 .20 .25 .30 .35 .40 .45 .50 .55 .60 .65 .70 .75 .80 .85 .90 .95 1.00
TIME FROM DET - SEC

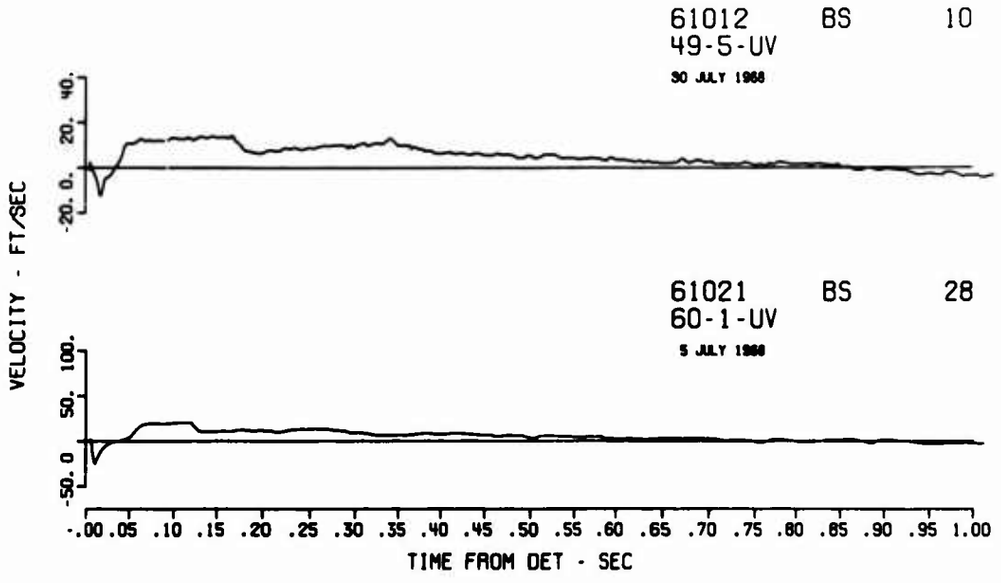
61012 BS 10
49-5-UV
30 JULY 1968
61021 BS 28
60-1-UV
5 JULY 1968
VELOCITY - FT/SEC
40.
20.
0.
-20.
100.
50.
0
-50.
-.00 .05 .10 .15 .20 .25 .30 .35 .40 .45 .50 .55 .60 .65 .70 .75 .80 .85 .90 .95 1.00
TIME FROM DET - SEC

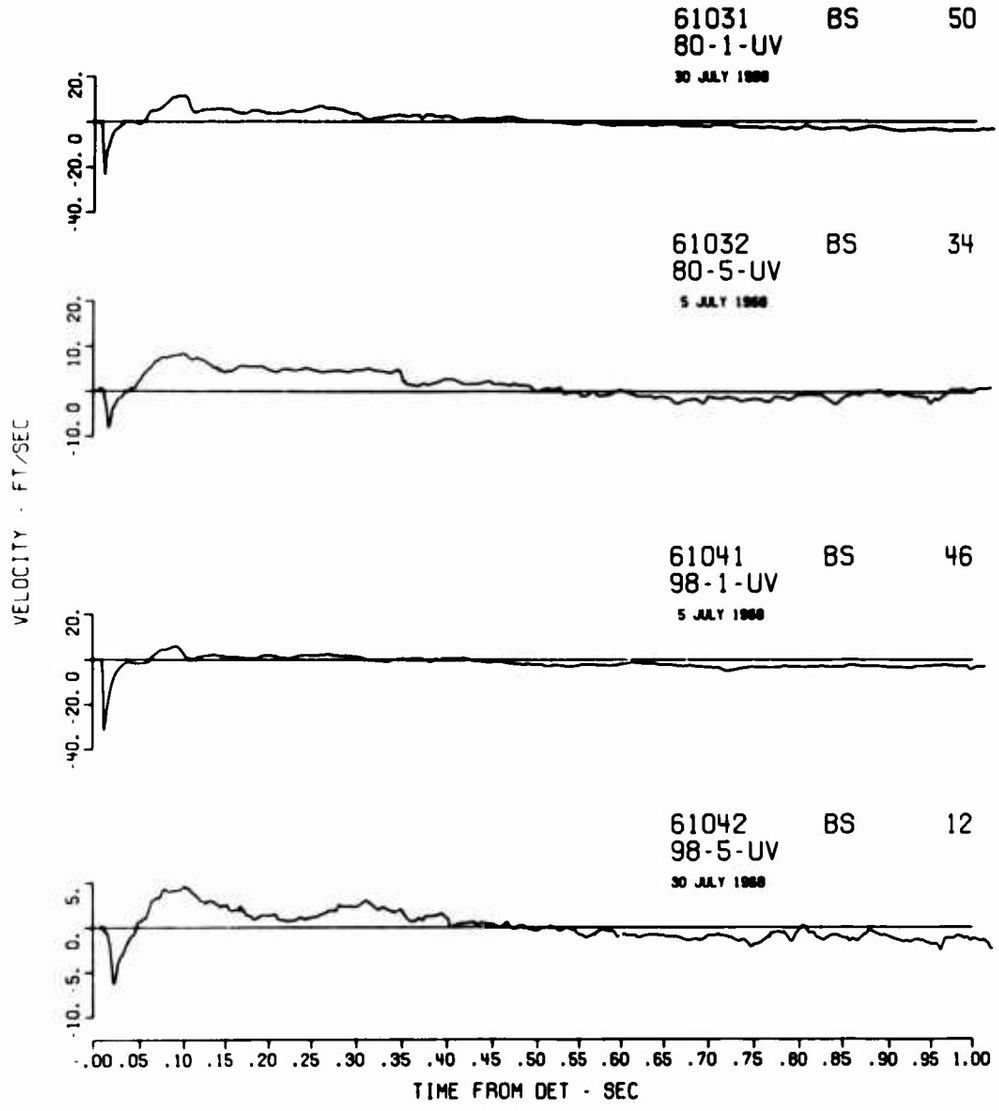
61031 BS 50
80-1-UV
30 JULY 1968
20.
0
-20.
-40.
61032 BS 34
80-5-UV
5 JULY 1968
20.
10.
0
-10.
61041 BS 46
98-1-UV
5 JULY 1968
20.
0
-20.
-40.
61042 BS 12
98-5-UV
30 JULY 1968
5.
0.
-5.
-10.
VELOCITY - FT/SEC
.00 .05 .10 .15 .20 .25 .30 .35 .40 .45 .50 .55 .60 .65 .70 .75 .80 .85 .90 .95 1.00
TIME FROM DET - SEC

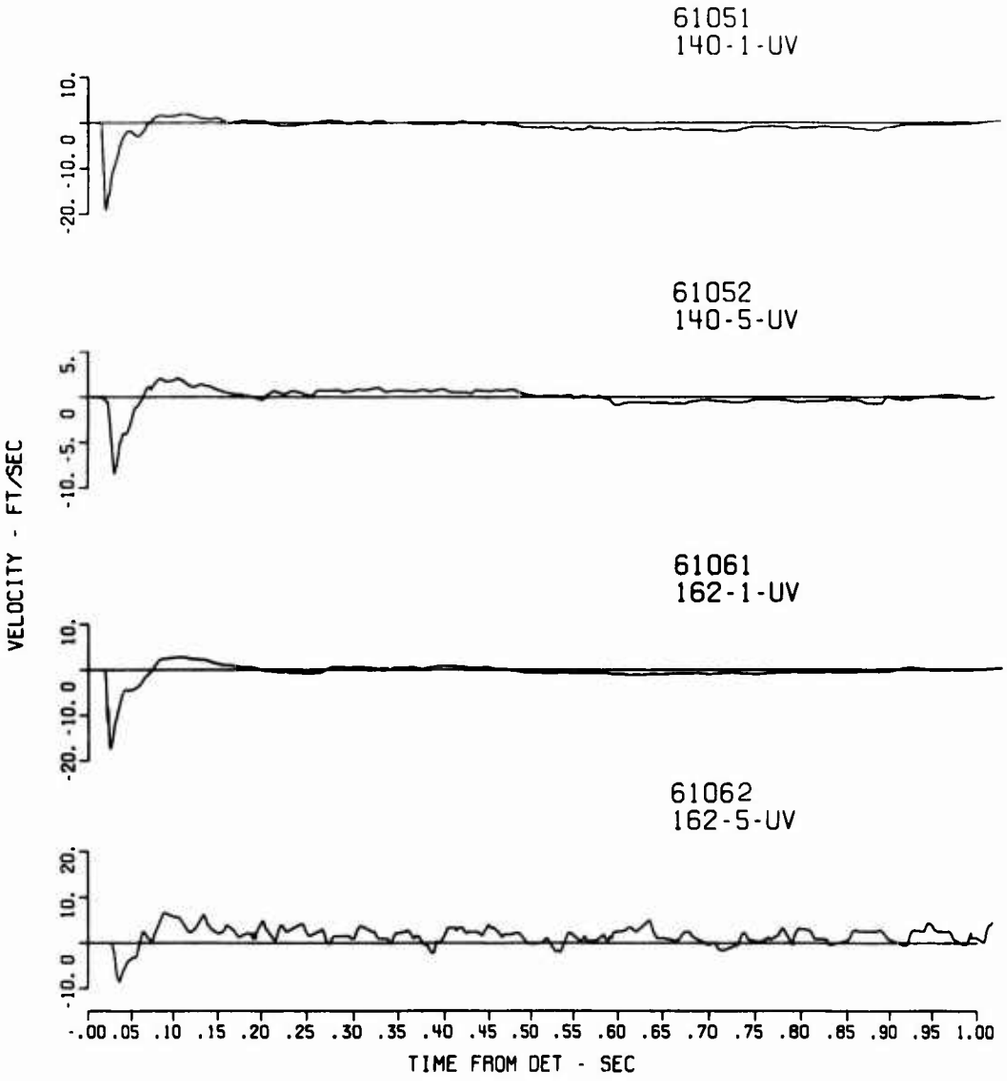
61051
140-1-UV
61052
140-5-UV
61061
162-1-UV
61062
162-5-UV
VELOCITY - FT/SEC
TIME FROM DET - SEC
-.00 .05 .10 .15 .20 .25 .30 .35 .40 .45 .50 .55 .60 .65 .70 .75 .80 .85 .90 .95 1.00

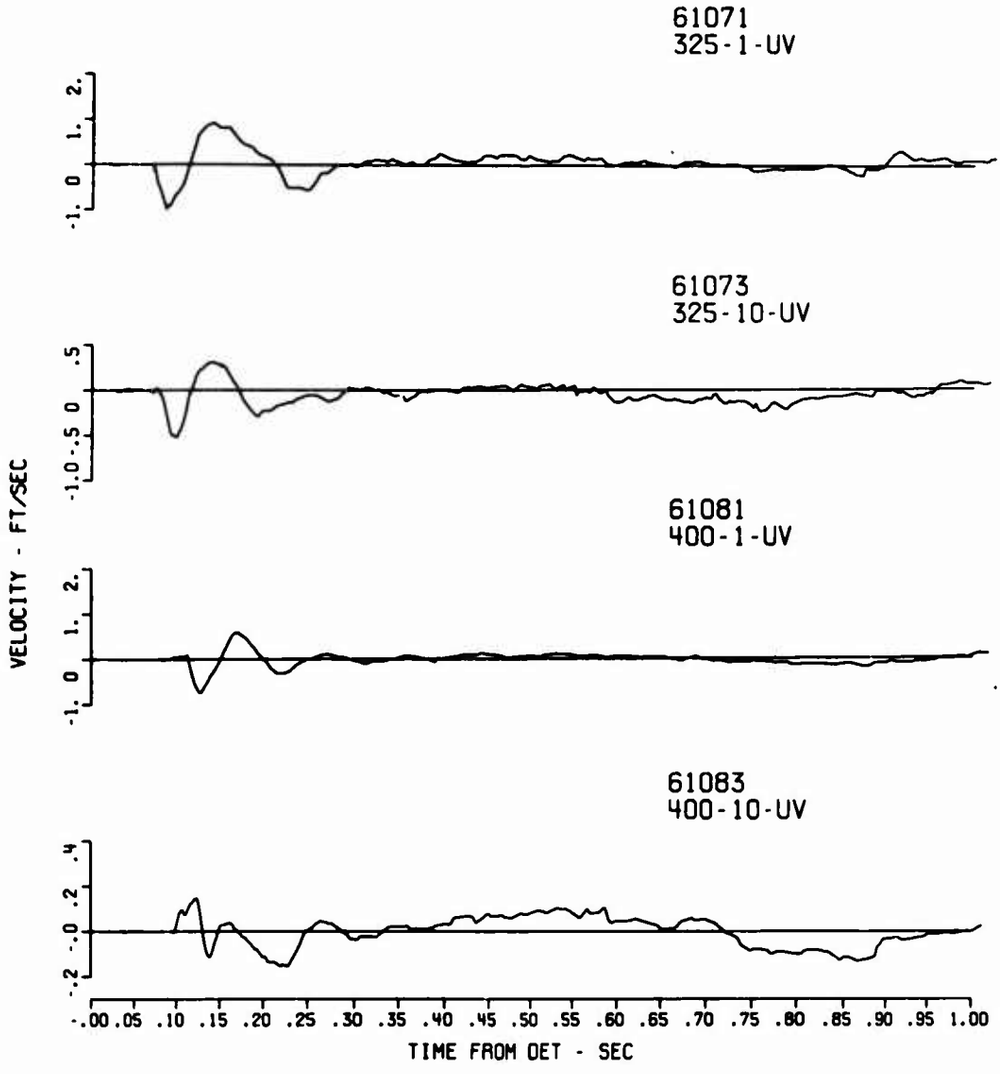
61071
325-1-UV
61073
325-10-UV
61081
400-1-UV
61083
400-10-UV
VELOCITY - FT/SEC
TIME FROM OET - SEC

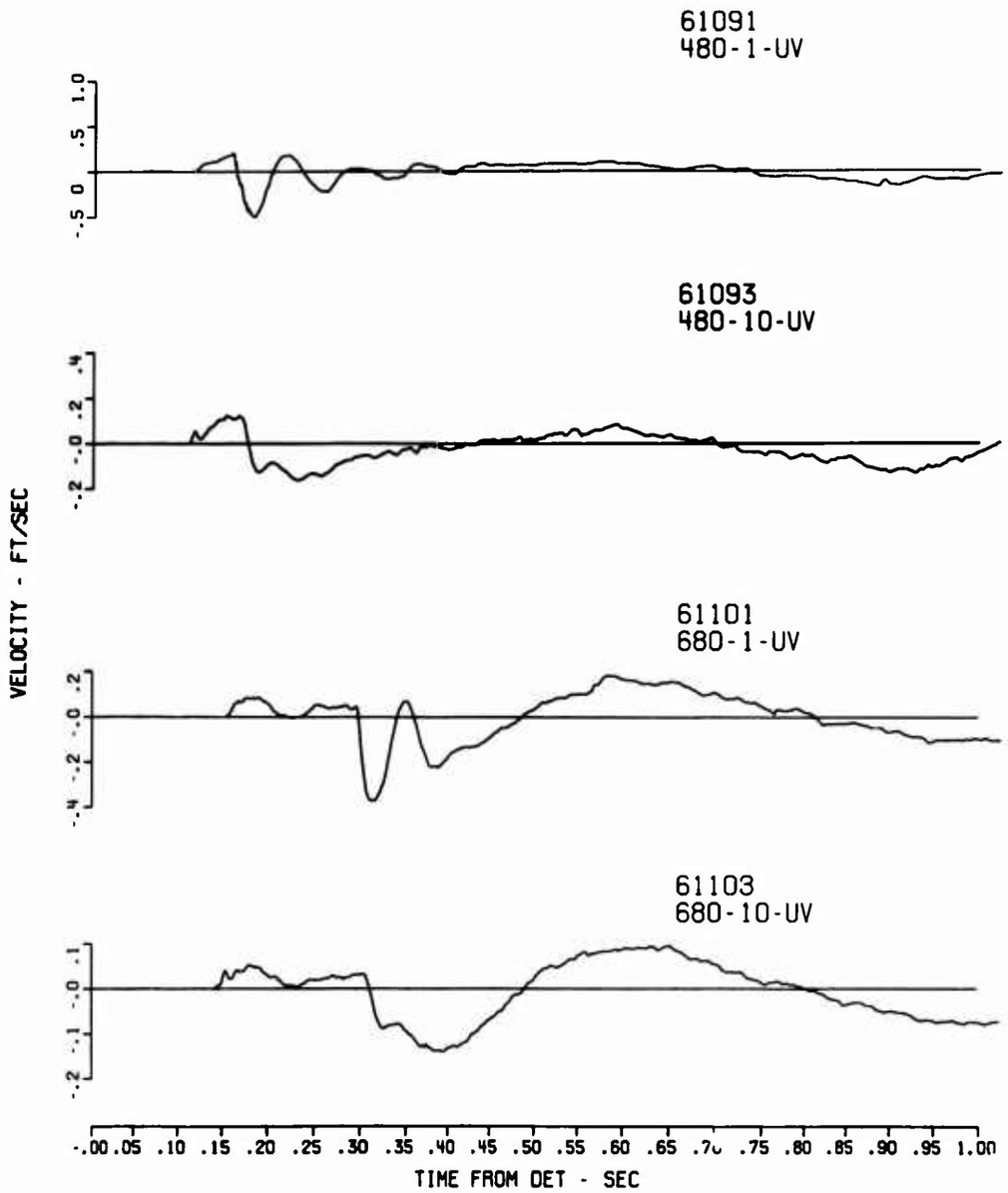
61091
480-1-UV
61093
480-10-UV
61101
680-1-UV
61103
680-10-UV
VELOCITY - FT/SEC
TIME FROM DET - SEC

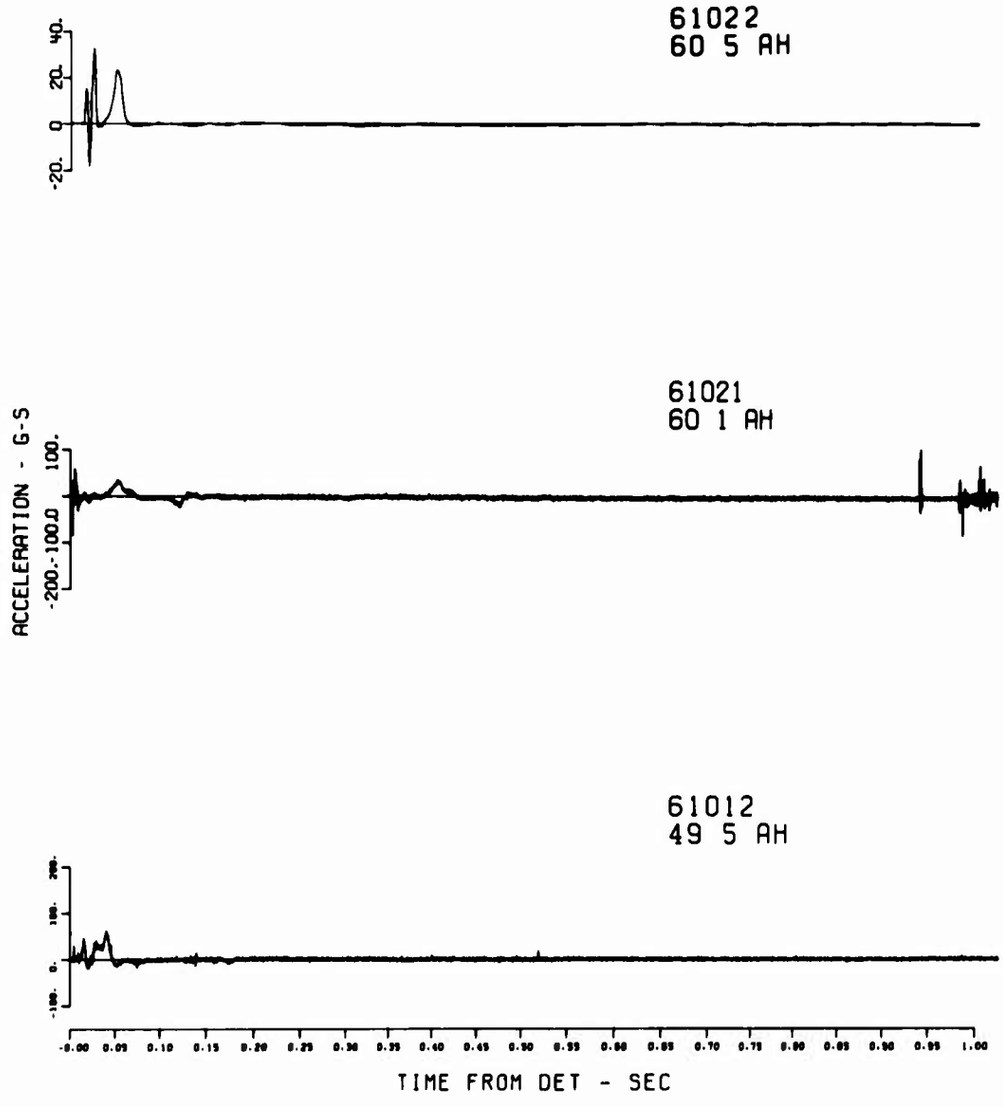
61022
60 5 AH
61021
60 1 AH
61012
49 5 AH
ACCELERATION - G-S
TIME FROM DET - SEC

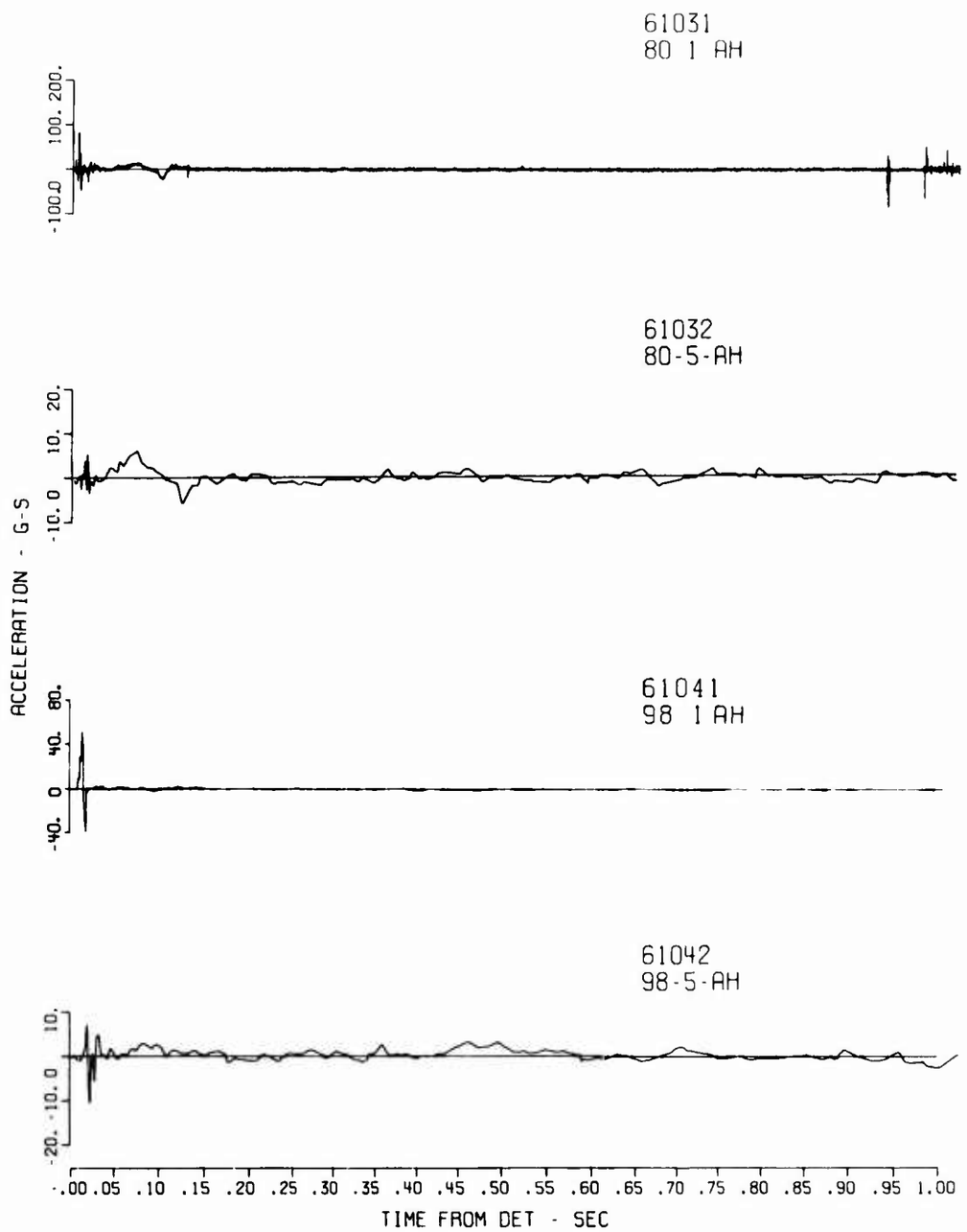
61031
80 1 AH
100. 200.
-100.0
61032
80-5-AH
10. 20.
-10. 0
ACCELERATION - G-S
61041
98 1 AH
80.
40.
0
-40.
61042
98-5-AH
10.
-20. -10. 0
.00 .05 .10 .15 .20 .25 .30 .35 .40 .45 .50 .55 .60 .65 .70 .75 .80 .85 .90 .95 1.00
TIME FROM DET - SEC

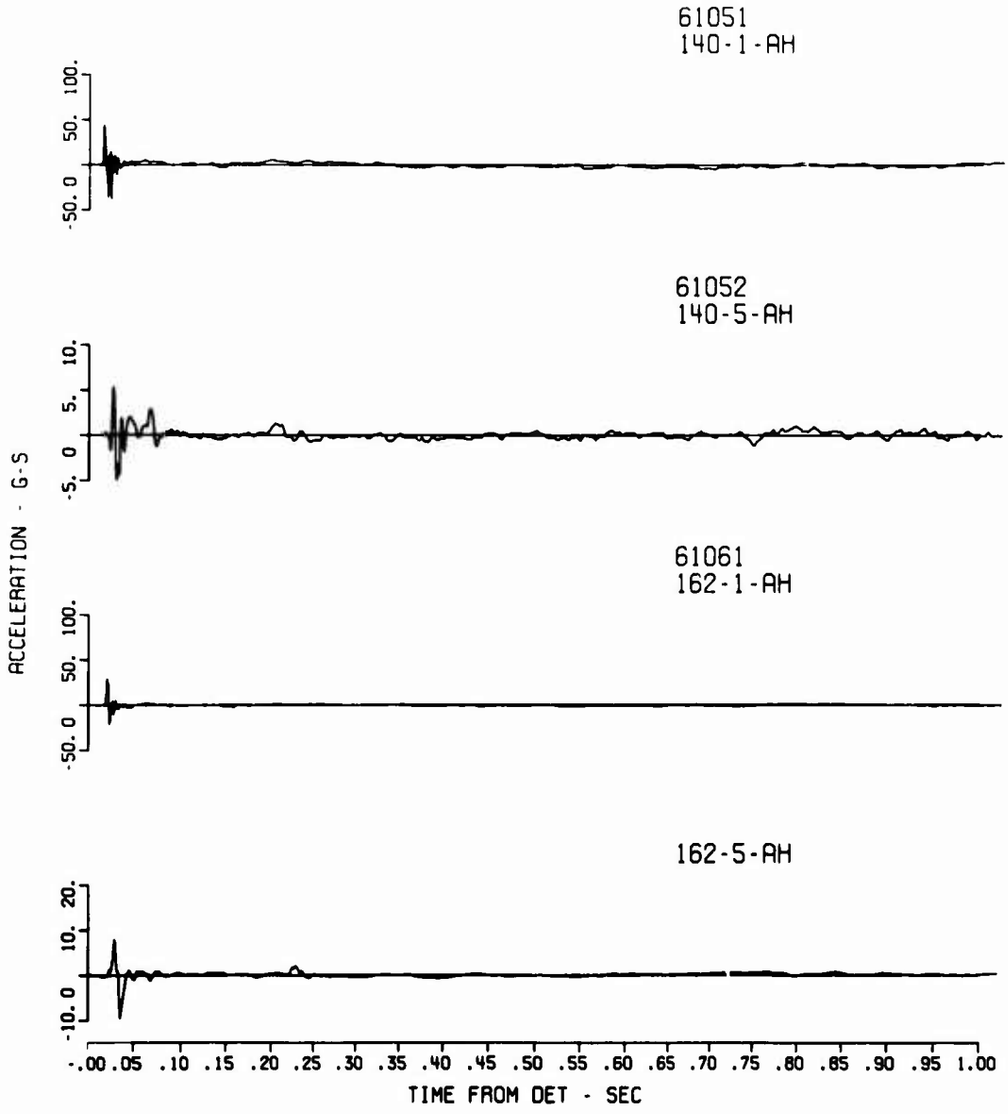
61051
140-1-AH
100.
50.
0
-50.
61052
140-5-AH
10.
5.
0
-5.
61061
162-1-AH
100.
50.
0
-50.
162-5-AH
20.
10.
0
-10.
ACCELERATION - G-S
-.00 .05 .10 .15 .20 .25 .30 .35 .40 .45 .50 .55 .60 .65 .70 .75 .80 .85 .90 .95 1.00
TIME FROM DET - SEC

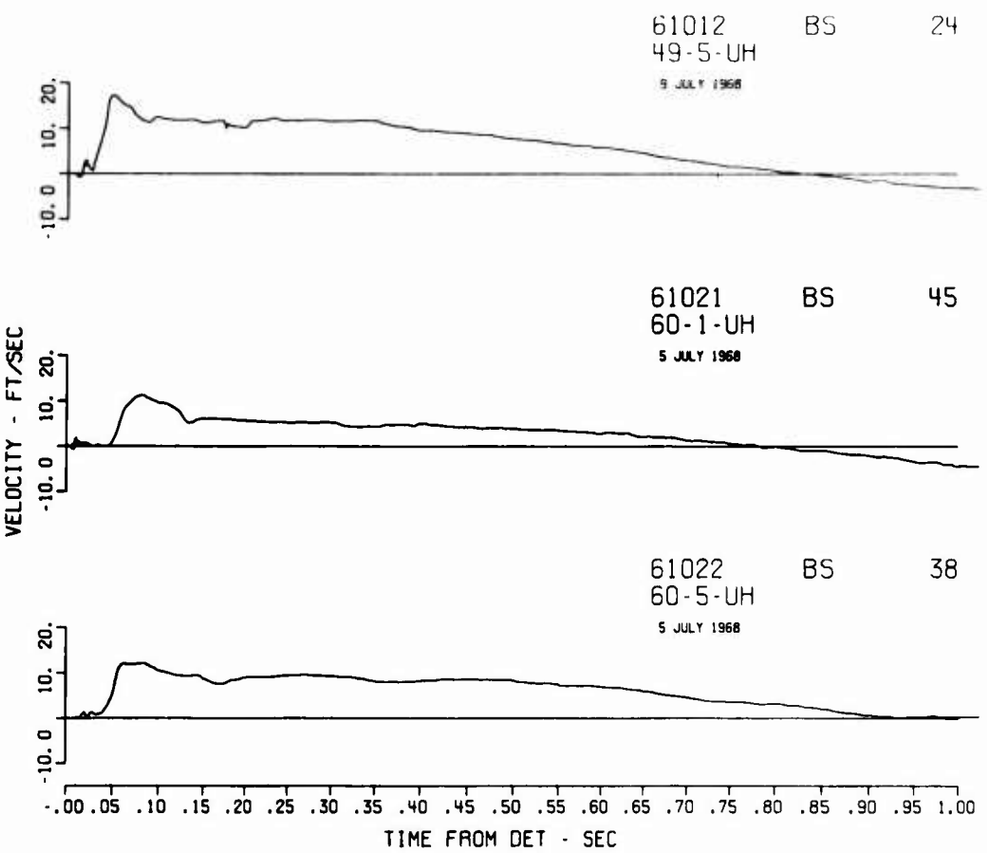
61012 BS 24
49-5-UH
9 JULY 1968
61021 BS 45
60-1-UH
5 JULY 1968
61022 BS 38
60-5-UH
5 JULY 1968
VELOCITY - FT/SEC
20.
10.
-10.0
-.00 .05 .10 .15 .20 .25 .30 .35 .40 .45 .50 .55 .60 .65 .70 .75 .80 .85 .90 .95 1.00
TIME FROM DET - SEC

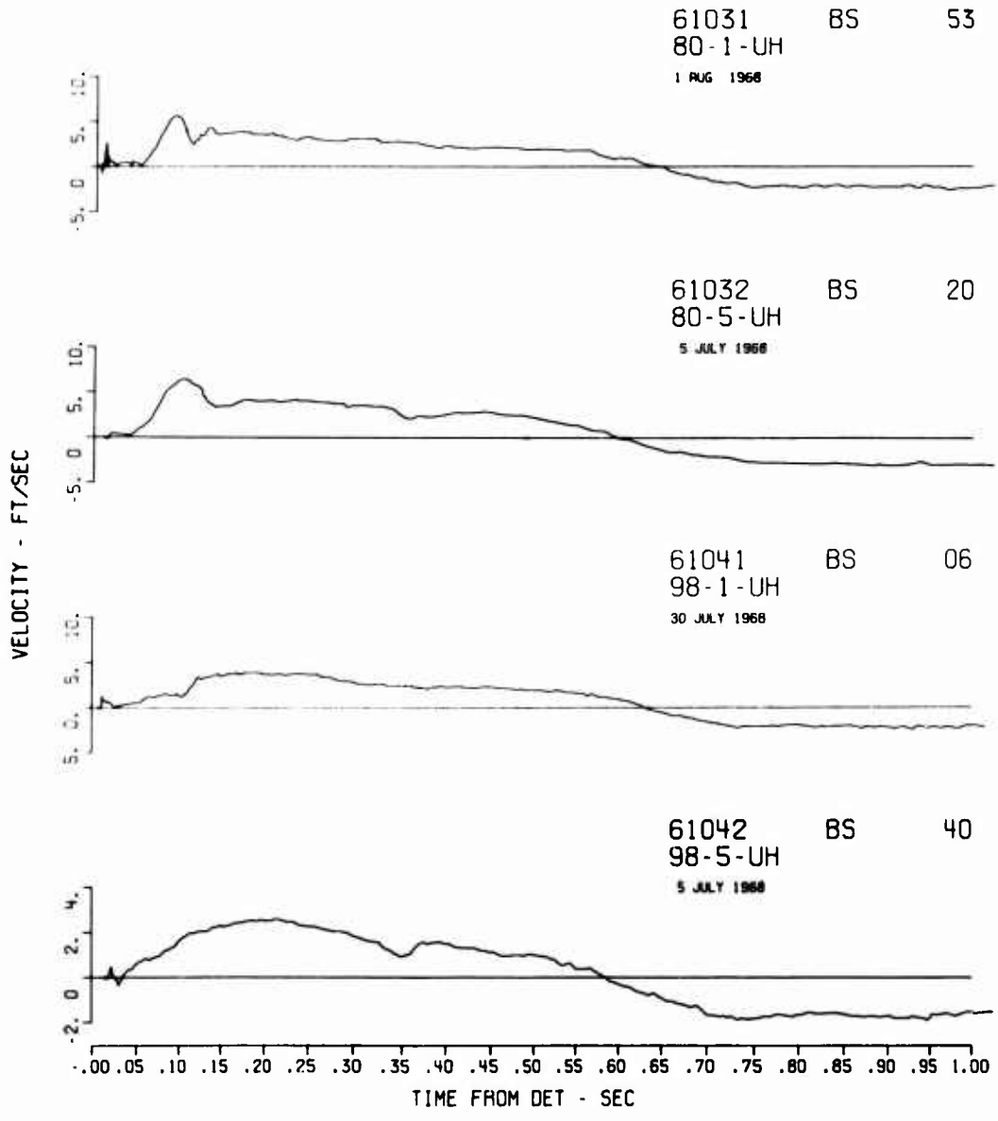
61031 BS 53
80-1-UH
1 AUG 1968
61032 BS 20
80-5-UH
5 JULY 1968
61041 BS 06
98-1-UH
30 JULY 1968
61042 BS 40
98-5-UH
5 JULY 1968
VELOCITY - FT/SEC
TIME FROM DET - SEC

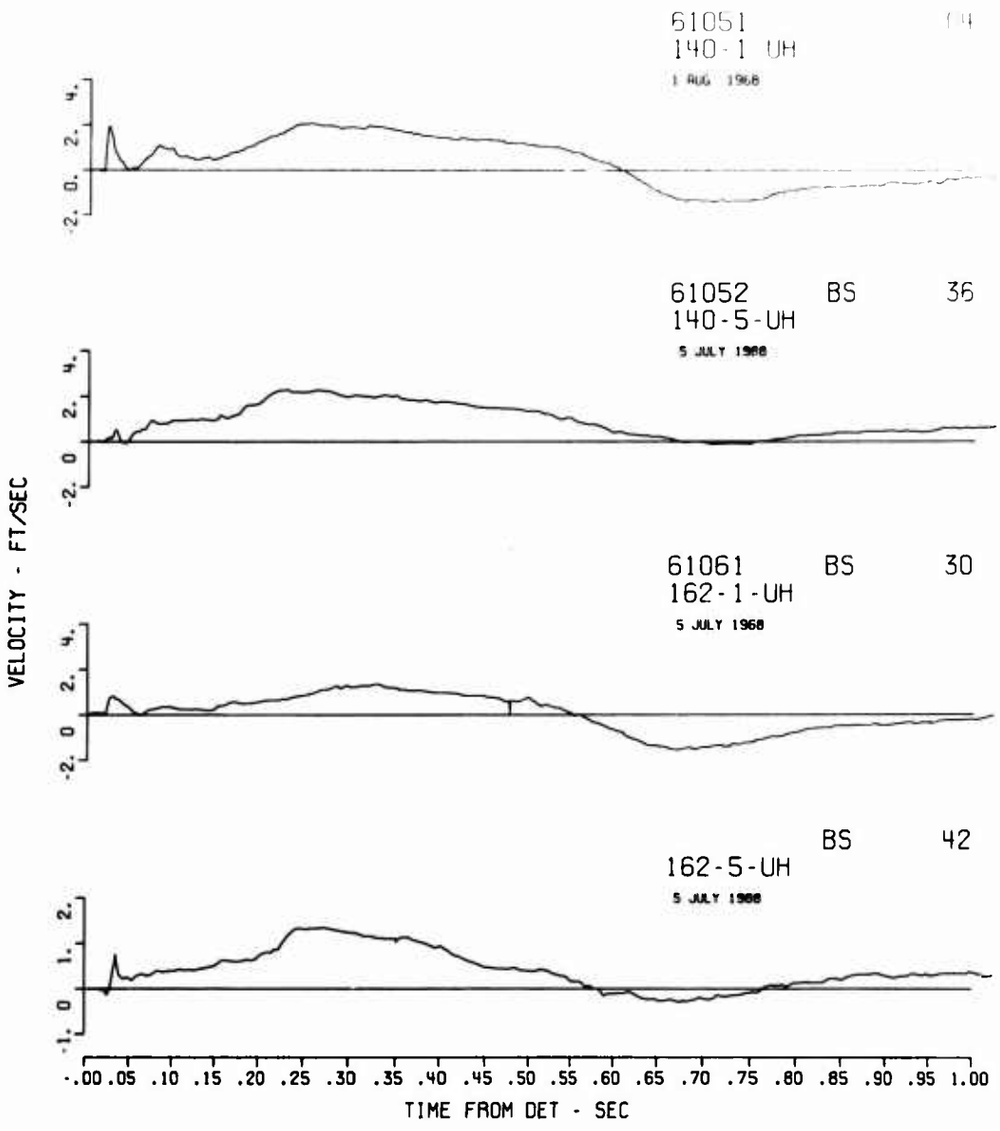
61051
140-1 UH
1 AUG 1968
61052 BS 36
140-5-UH
5 JULY 1968
61061 BS 30
162-1-UH
5 JULY 1968
BS 42
162-5-UH
5 JULY 1968
VELOCITY - FT/SEC
TIME FROM DET - SEC
-.00 .05 .10 .15 .20 .25 .30 .35 .40 .45 .50 .55 .60 .65 .70 .75 .80 .85 .90 .95 1.00

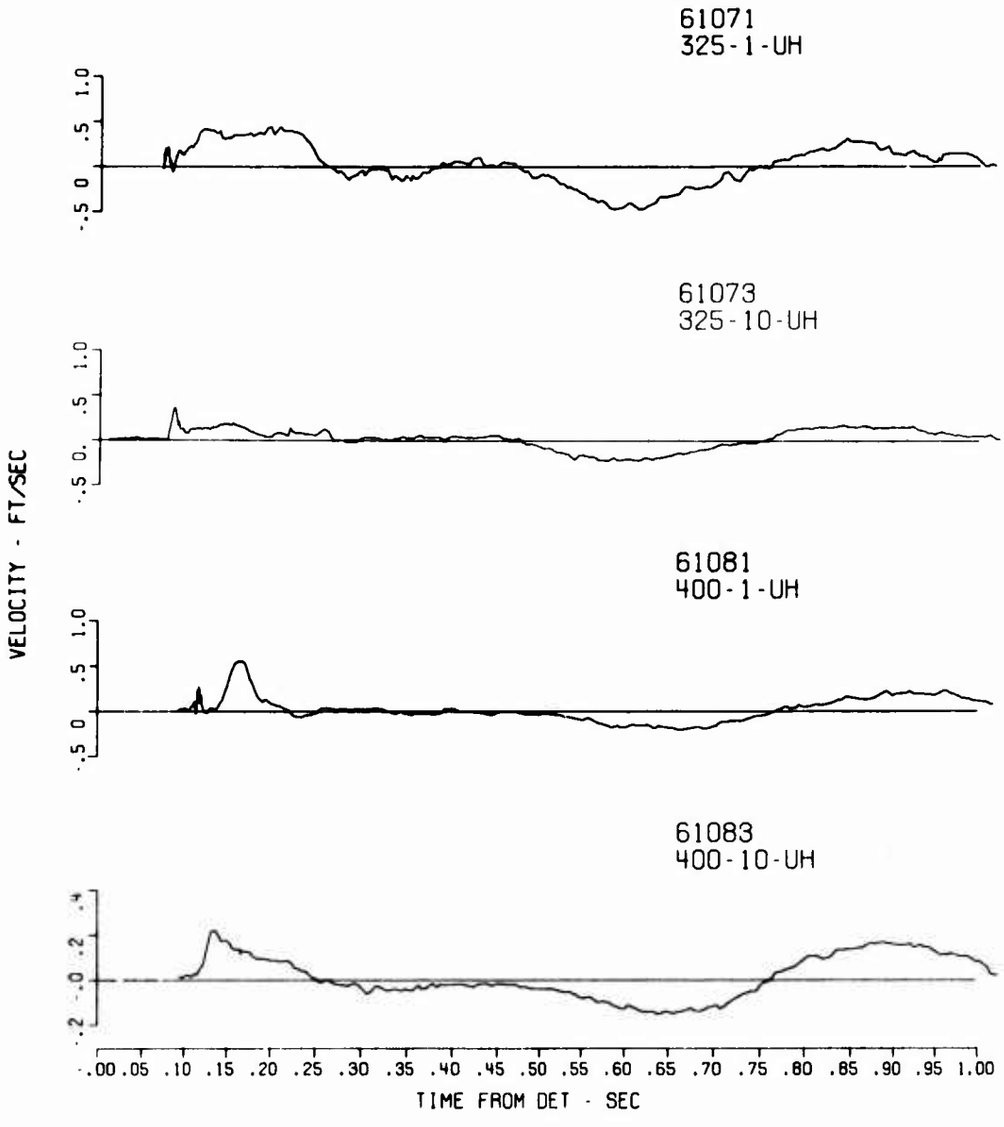
61071
325-1-UH
61073
325-10-UH
61081
400-1-UH
61083
400-10-UH
VELOCITY - FT/SEC
-.5 0 .5 1.0
-.5 0. .5 1.0
-.5 0 .5 1.0
-.2 .0 .2 .4
.00 .05 .10 .15 .20 .25 .30 .35 .40 .45 .50 .55 .60 .65 .70 .75 .80 .85 .90 .95 1.00
TIME FROM DET - SEC

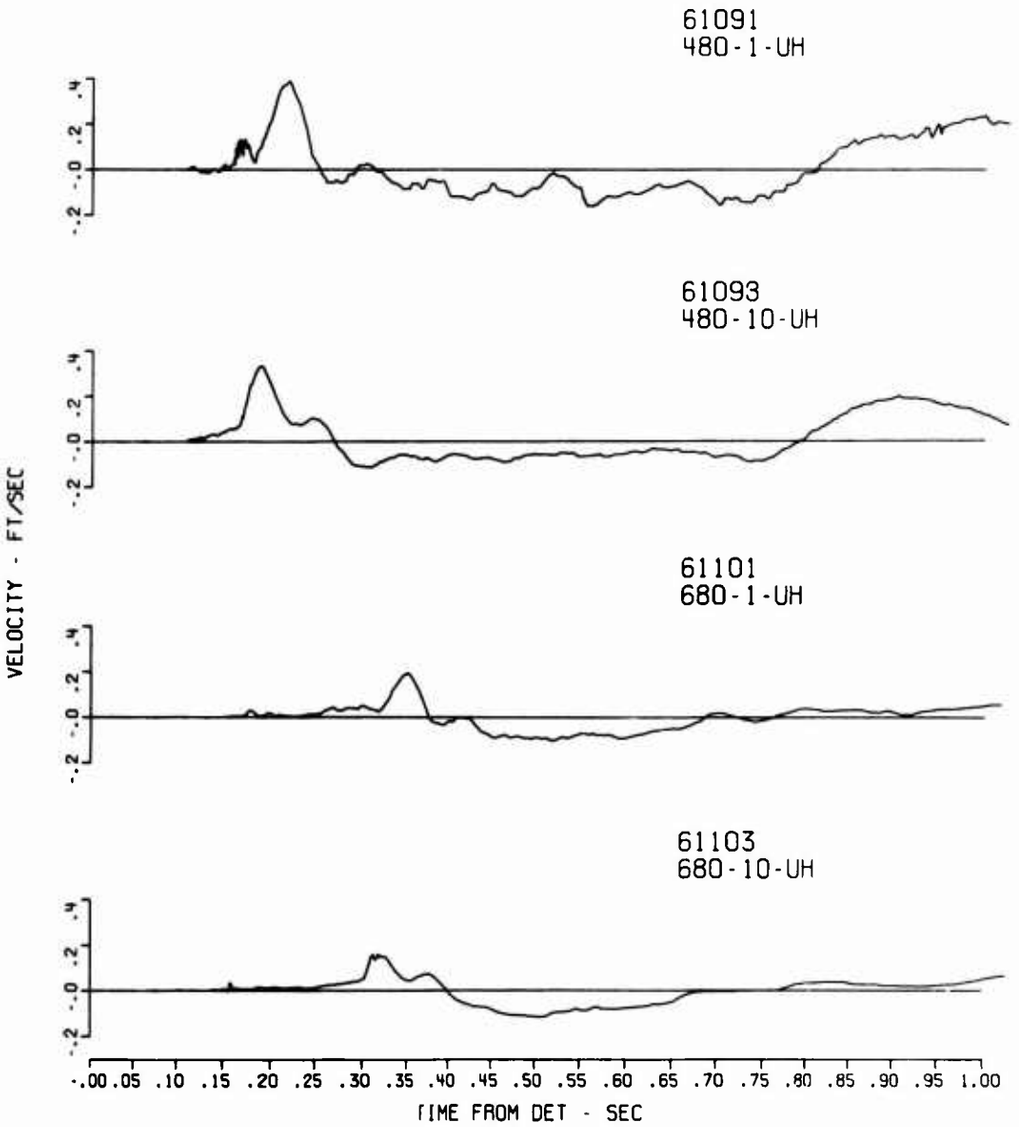
61091
480-1-UH
61093
480-10-UH
61101
680-1-UH
61103
680-10-UH
VELOCITY - FT/SEC
-.2 -.0 .2 .4
.00 .05 .10 .15 .20 .25 .30 .35 .40 .45 .50 .55 .60 .65 .70 .75 .80 .85 .90 .95 1.00
TIME FROM DET - SEC

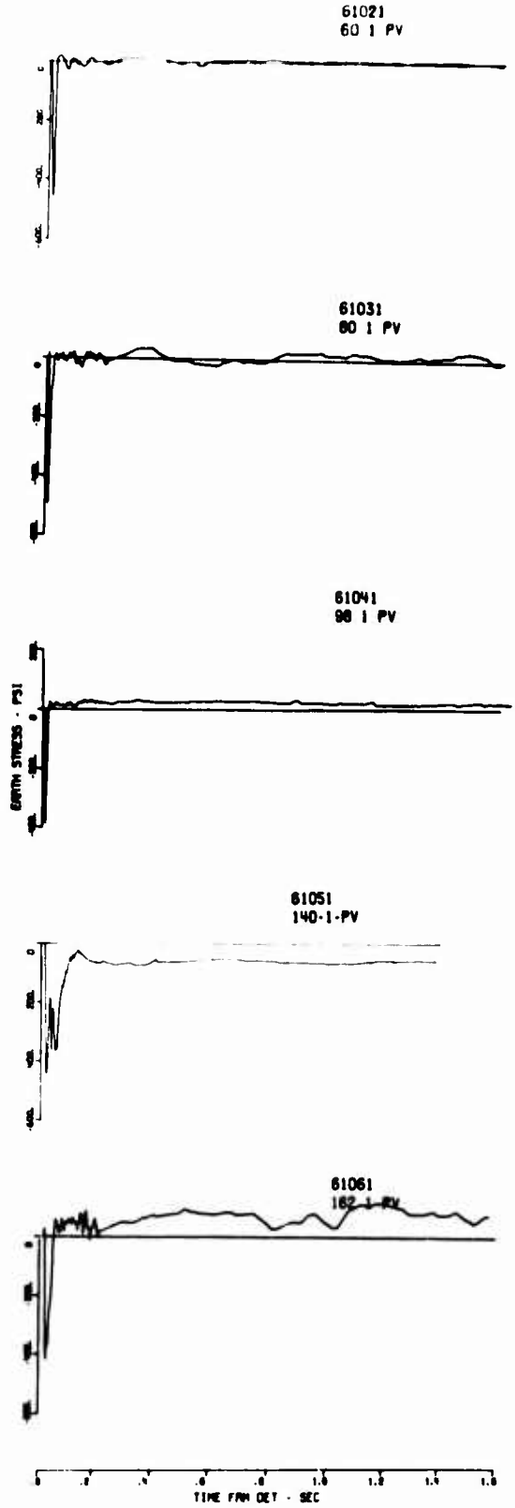
61021
60 1 PV
61031
80 1 PV
61041
98 1 PV
EARTH STRESS - PSI
61051
140-1-PV
61061
162-1-PV
TIME FRM DET - SEC

61014
49-17-PV

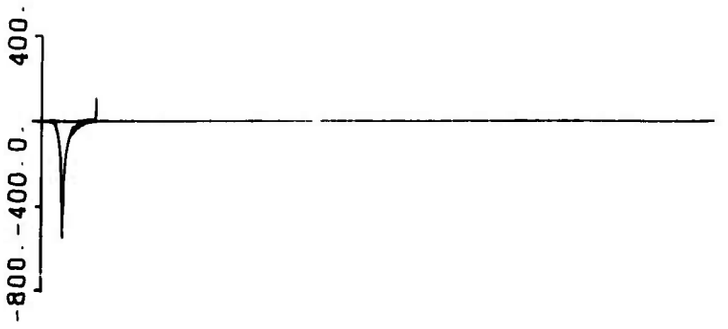

61064
162 17 PV

61064
162 17 PH

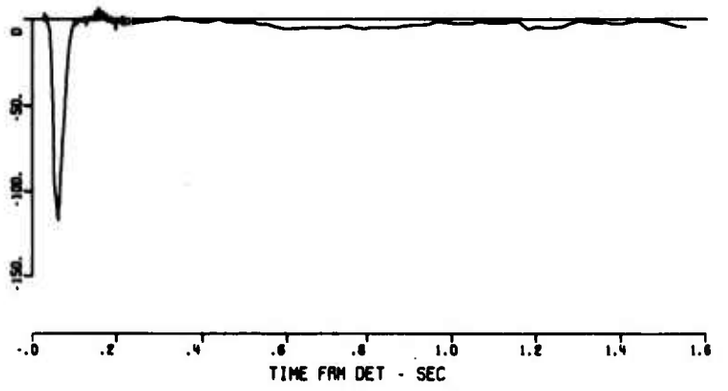

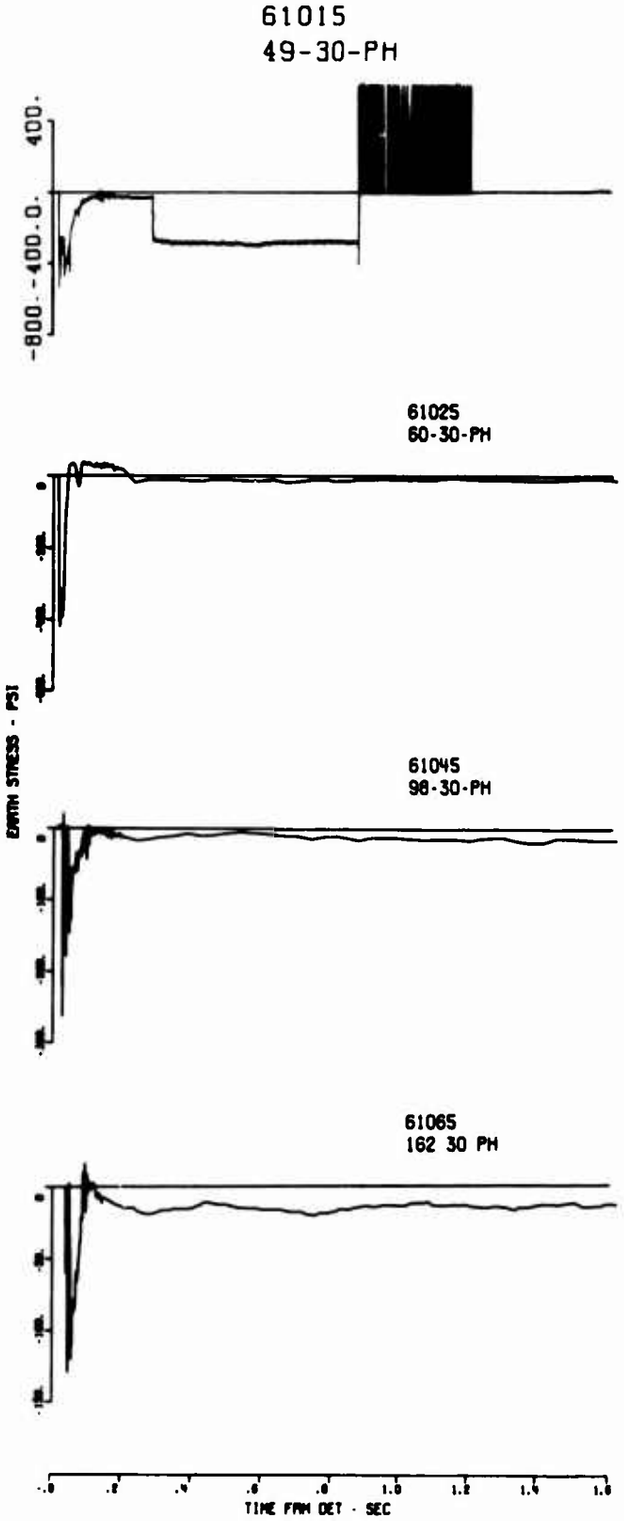
61015
49-30-PH
400.
-800.
-400.
0.
61025
60-30-PH
61045
98-30-PH
61065
162 30 PH
EAWN STRESS - PSI
TIME FRM DET - SEC

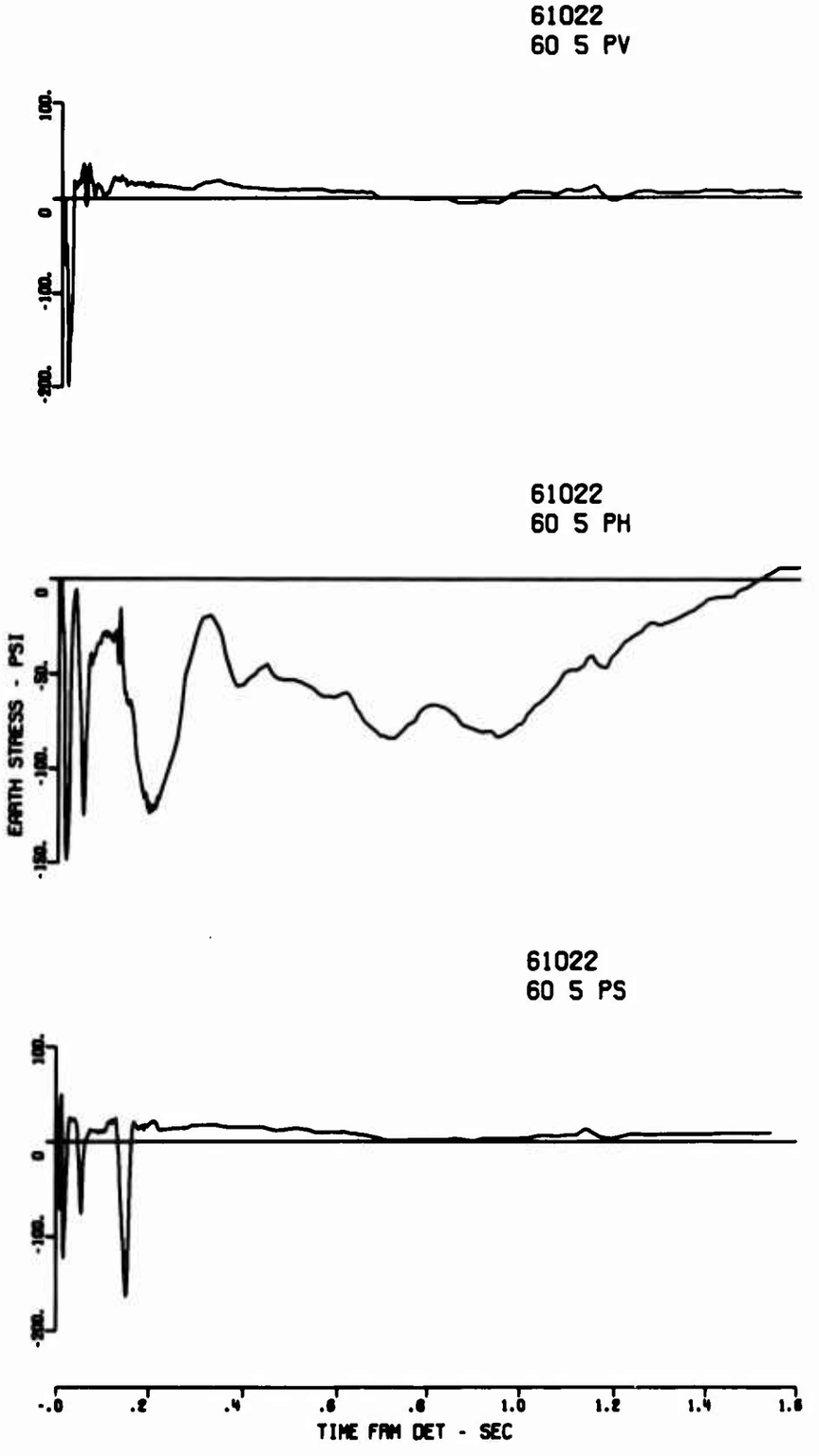
61022
60 5 PV
100.
0
-100.
-200.
61022
60 5 PH
EARTH STRESS - PSI
0
-50.
-100.
-150.
61022
60 5 PS
100.
0
-100.
-200.
-.0
.2
.4
.6
.8
1.0
1.2
1.4
1.6
TIME FRM DET - SEC

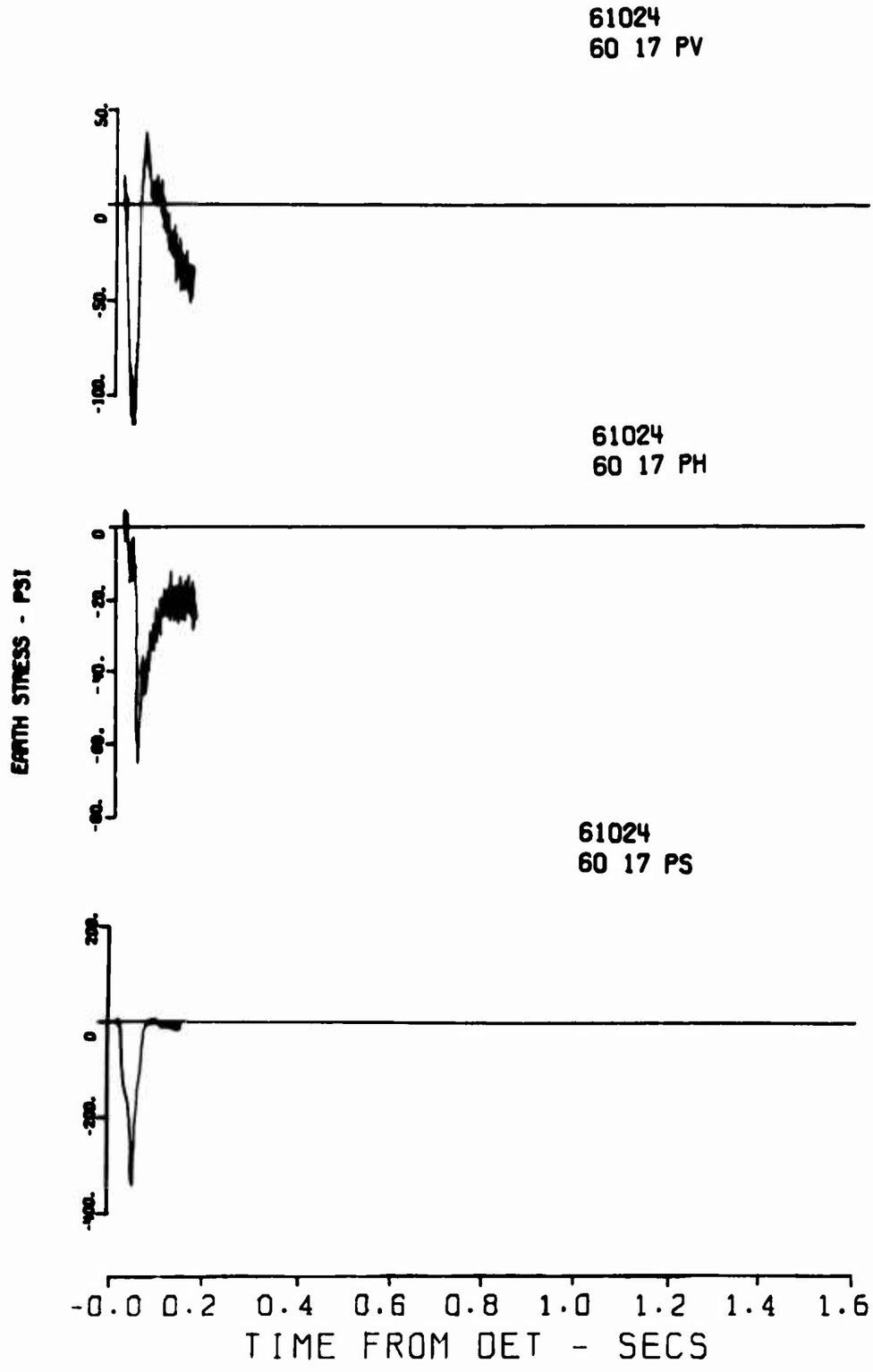
61024
60 17 PV
50.
0
-50.
-100.
61024
60 17 PH
0
-30.
-60.
-90.
-120.
EARTH STRESS - PSI
61024
60 17 PS
200.
0
-200.
-400.
-0.0 0.2 0.4 0.6 0.8 1.0 1.2 1.4 1.6
TIME FROM DET - SECS

61032
80-5-PV

61032
80-5-PH

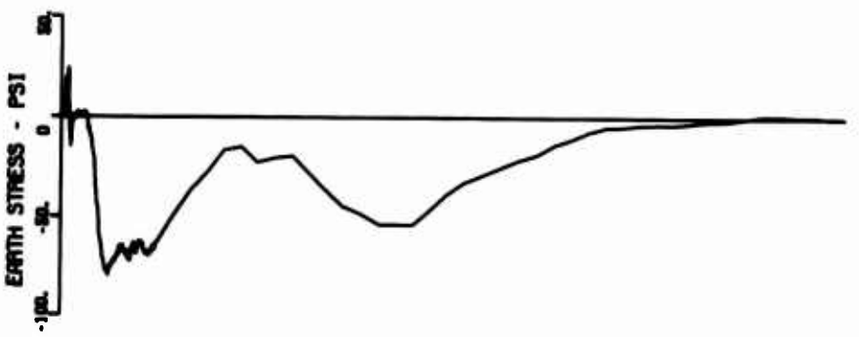

61032
80-5-PS

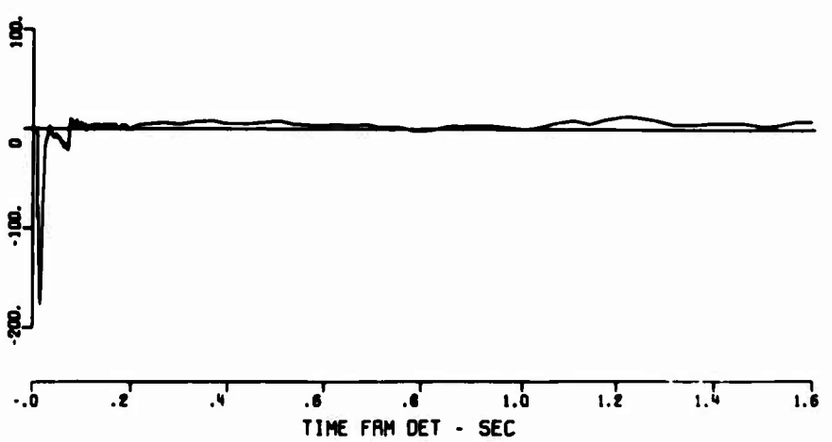

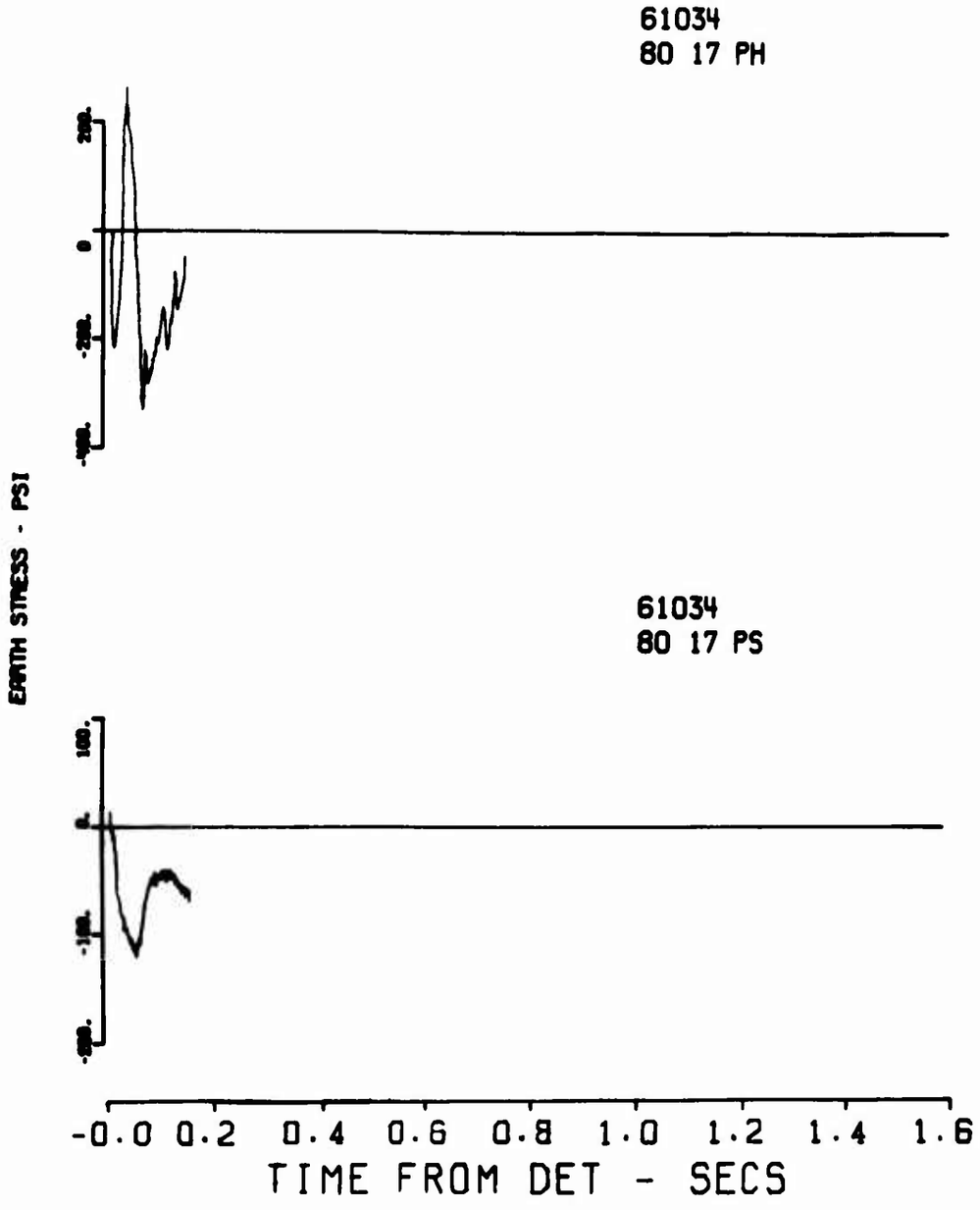
61034
80 17 PH
61034
80 17 PS
EARTH STRESS - PSI
-0.0 0.2 0.4 0.6 0.8 1.0 1.2 1.4 1.6
TIME FROM DET - SECS

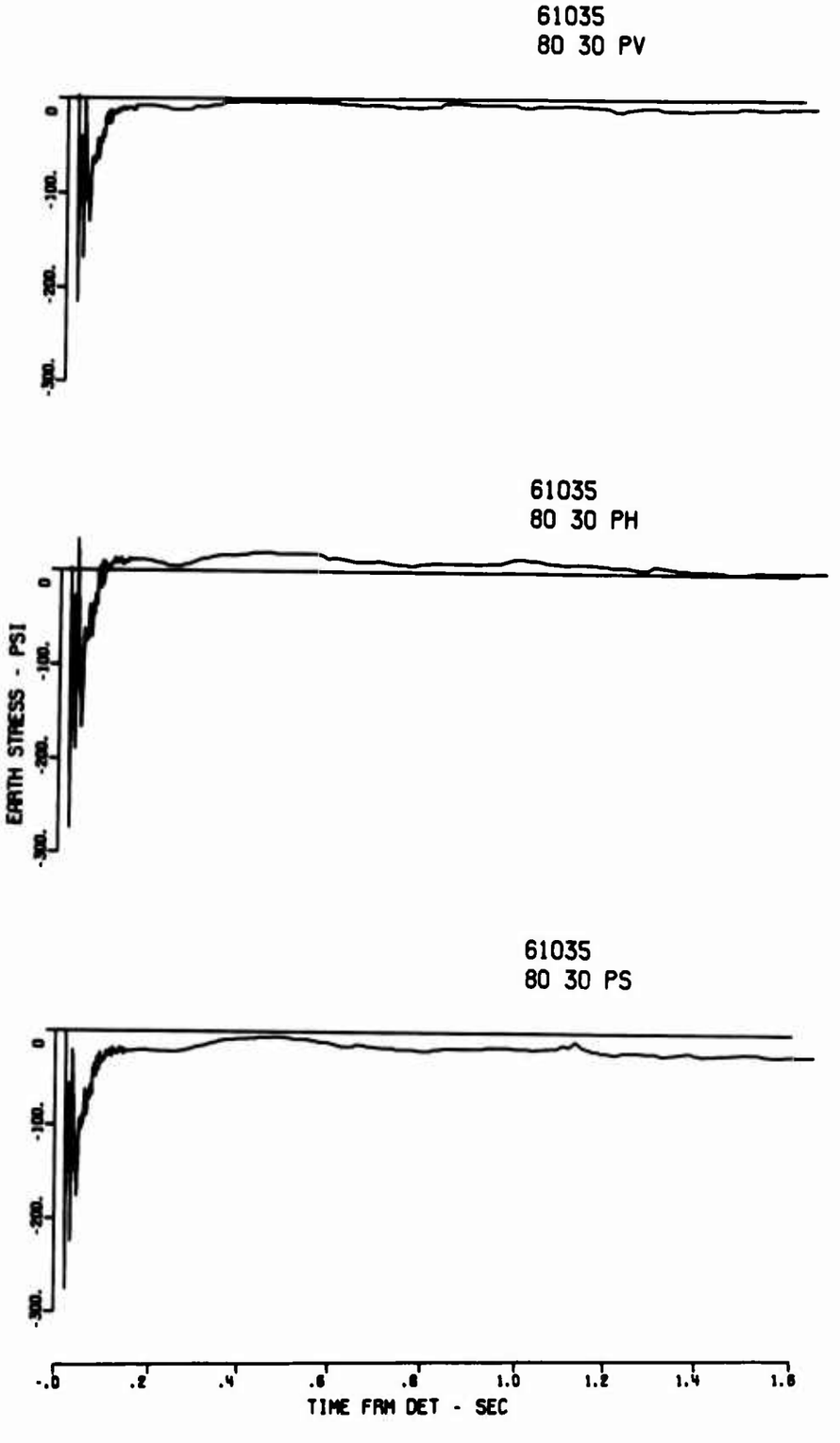
61035
80 30 PV
61035
80 30 PH
61035
80 30 PS
EARTH STRESS - PSI
0
-100.
-200.
-300.
-.0
.2
.4
.6
.8
1.0
1.2
1.4
1.6
TIME FRM DET - SEC

61042
98-5-PV

61042
98-5-PH

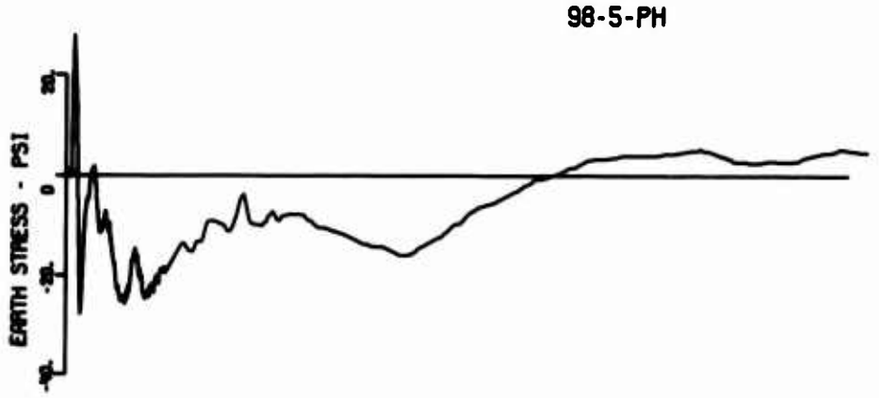

61042
98-5-PS

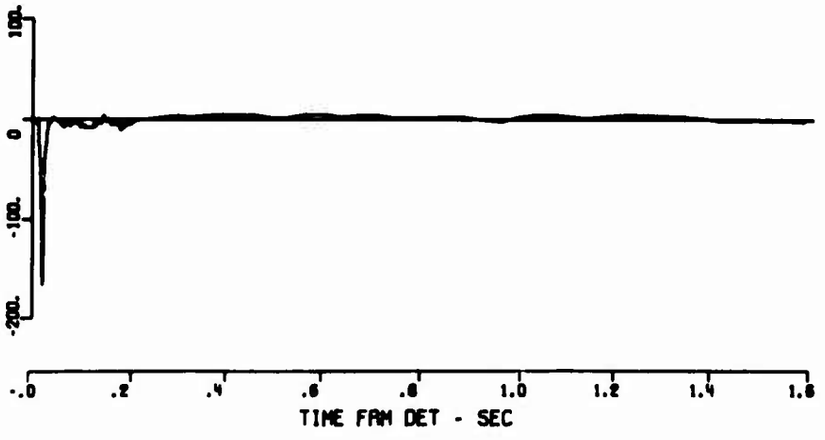

61044
98 17 PV

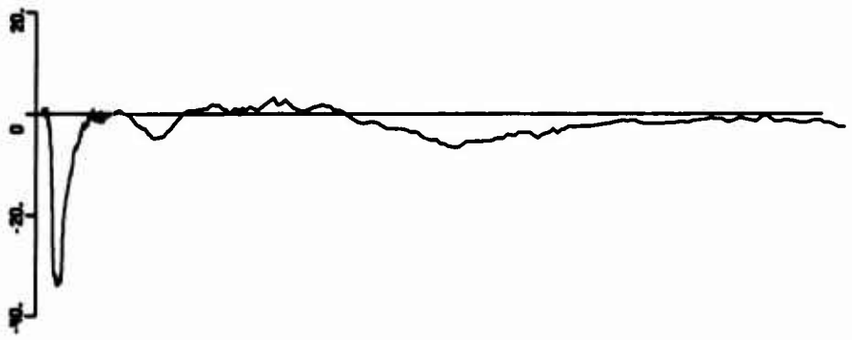

61044
98 17 PH

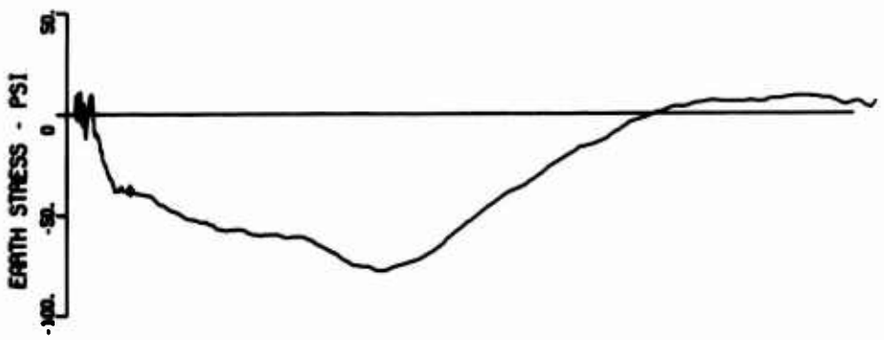

61044
98 17 PS

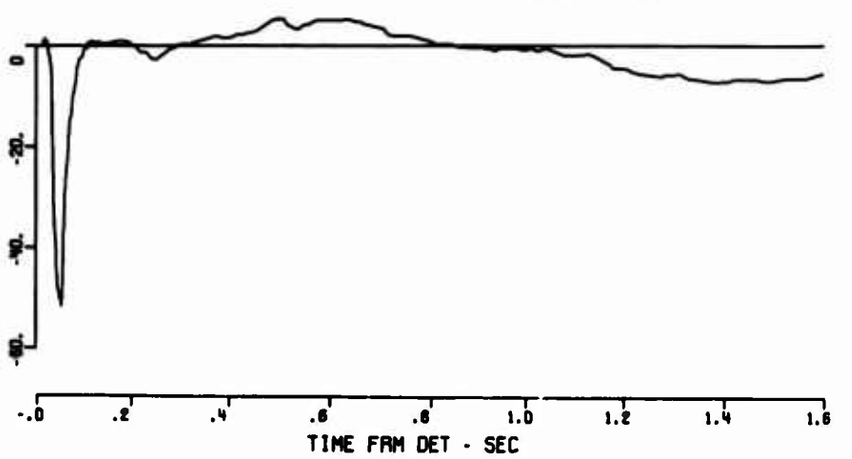

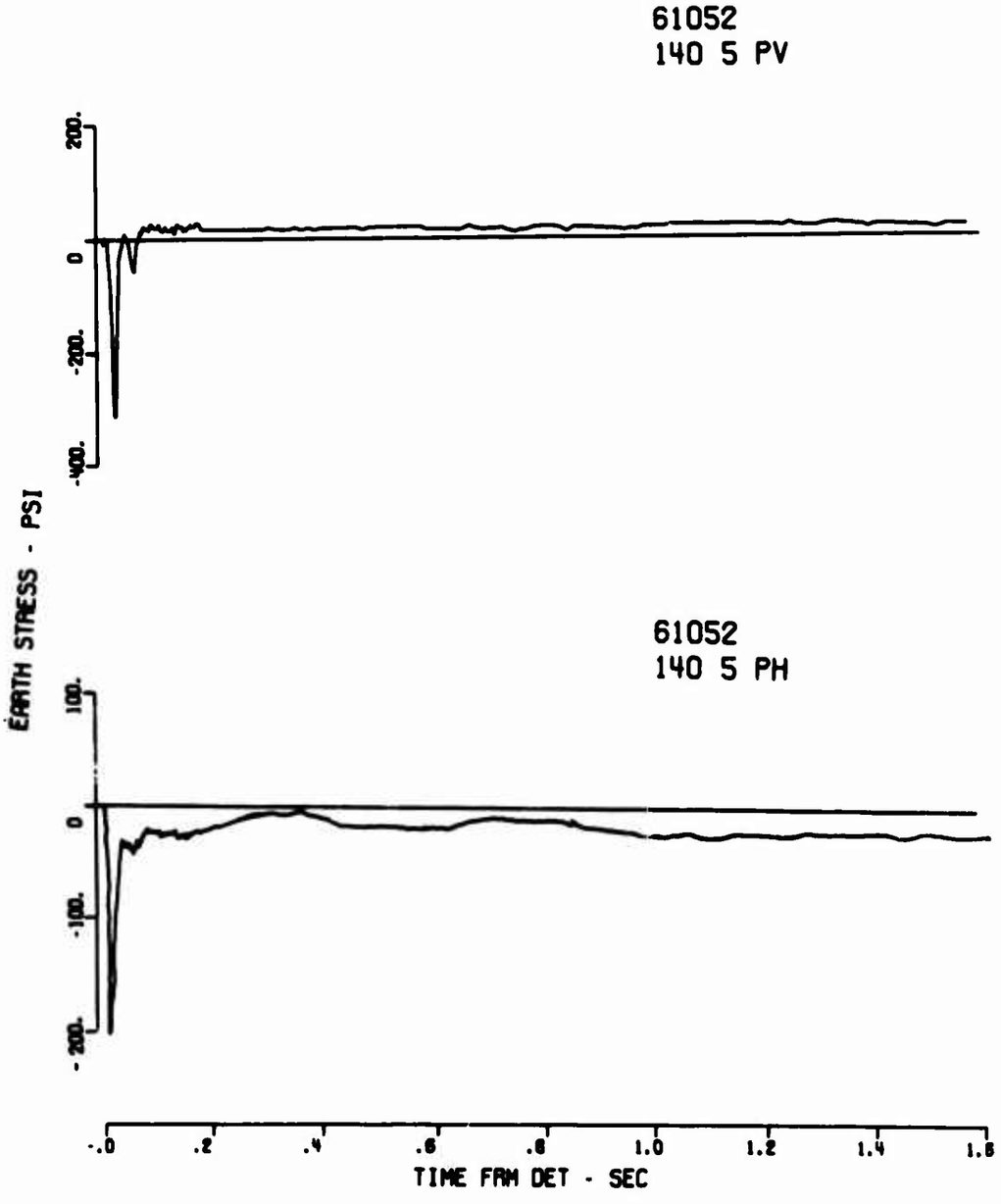
61052
140 5 PV
200.
0
-200.
-400.
61052
140 5 PH
100.
0
-100.
-200.
EARTH STRESS - PSI
.0
.2
.4
.6
.8
1.0
1.2
1.4
1.6
TIME FRM DET - SEC

61054
140 17 PV

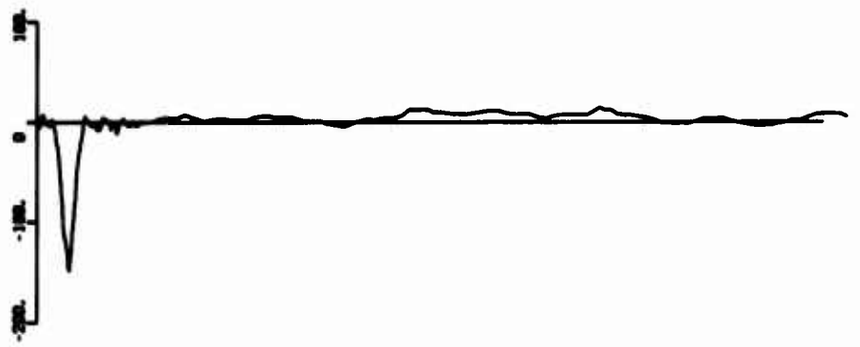

61054
140 17 PH

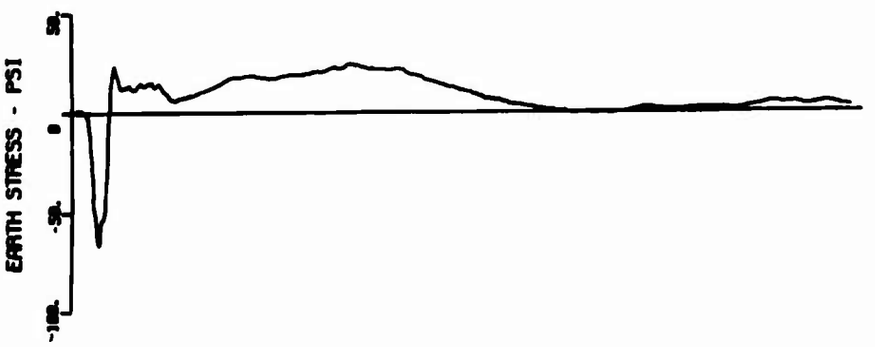

61054
140 17 PS

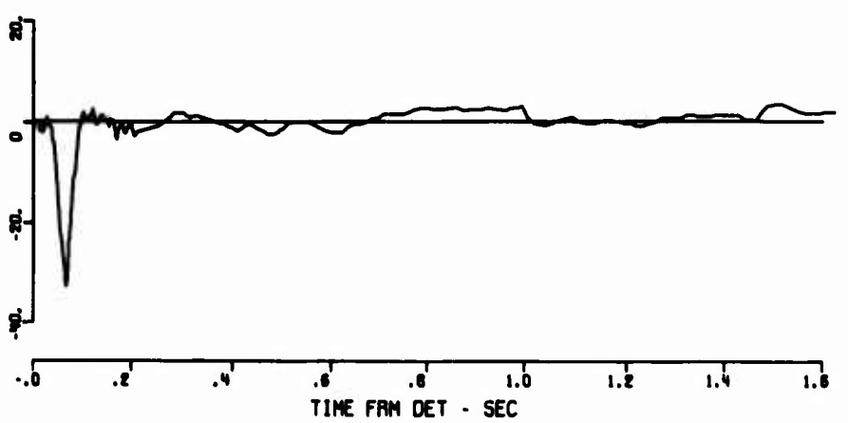

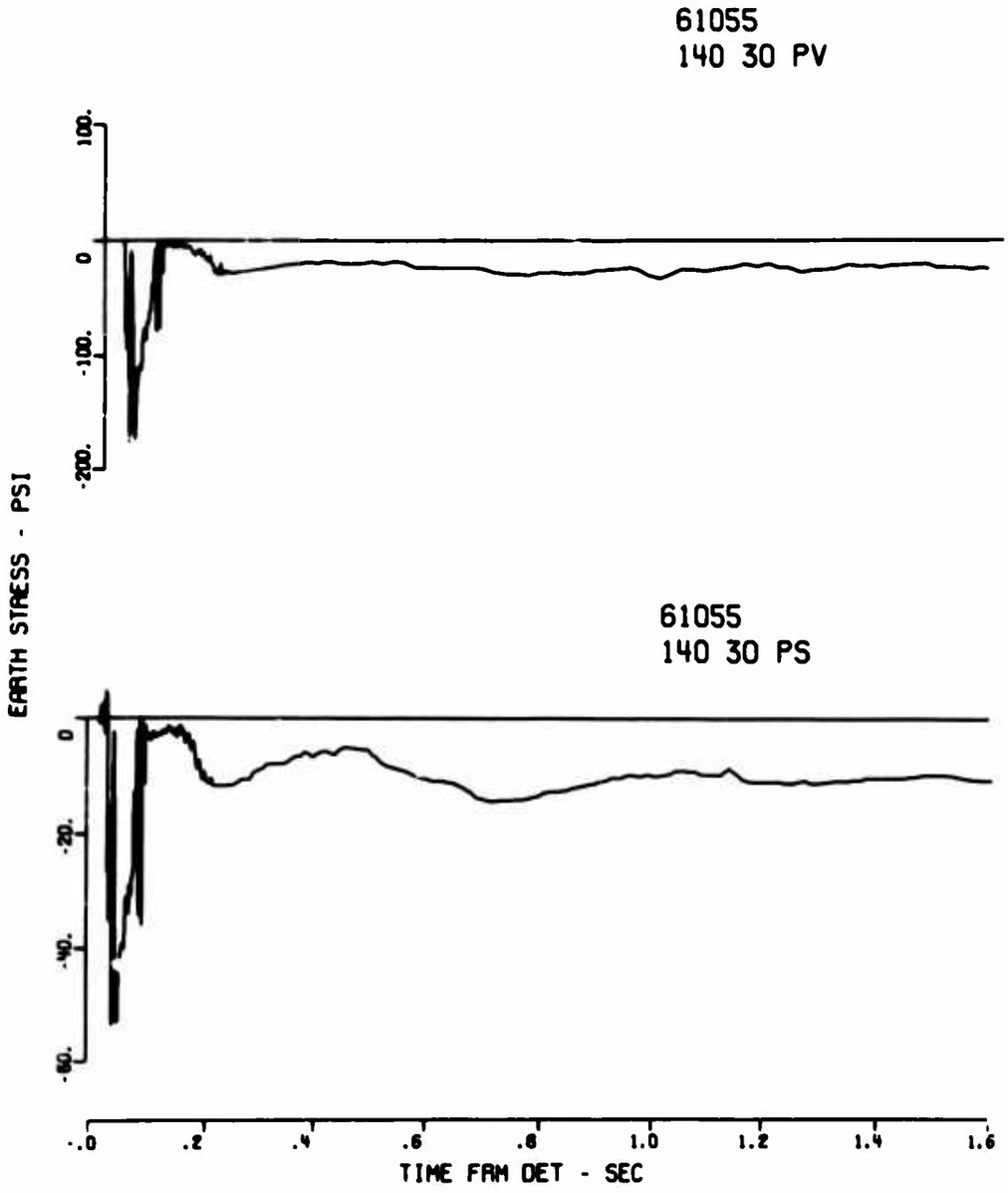
61055
140 30 PV
100.
0
-100.
-200.
61055
140 30 PS
0
-20.
-40.
-60.
EARTH STRESS - PSI
.0
.2
.4
.6
.8
1.0
1.2
1.4
1.6
TIME FRM DET - SEC

61062
162 5 PV

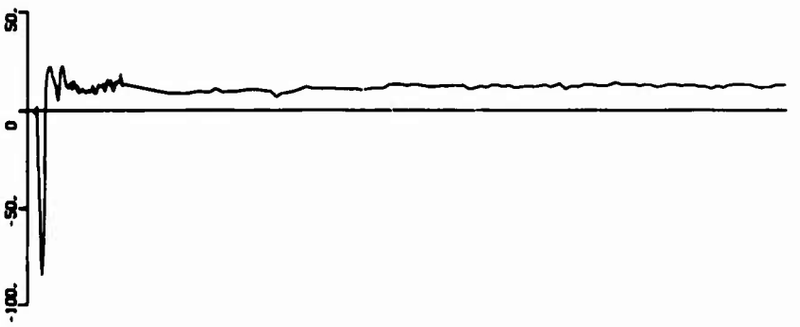

61062
162 5 PH

61062
162 5 PS

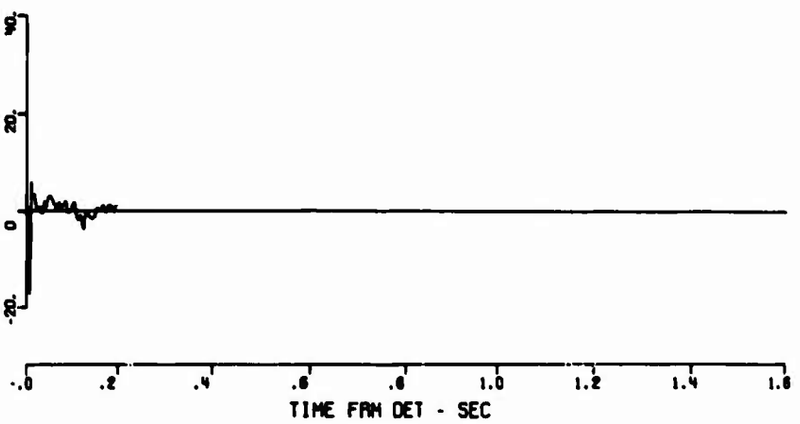

BLANK PAGE

APPENDIX B

EVENT 1A TIME HISTORIES

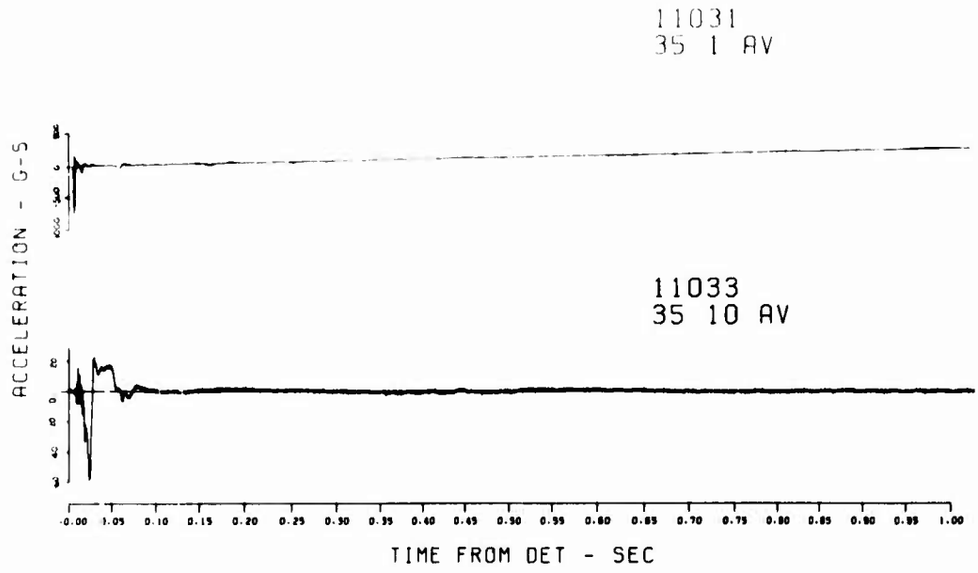
11031
35 1 AV
11033
35 10 AV
ACCELERATION - G-S
TIME FROM DET - SEC

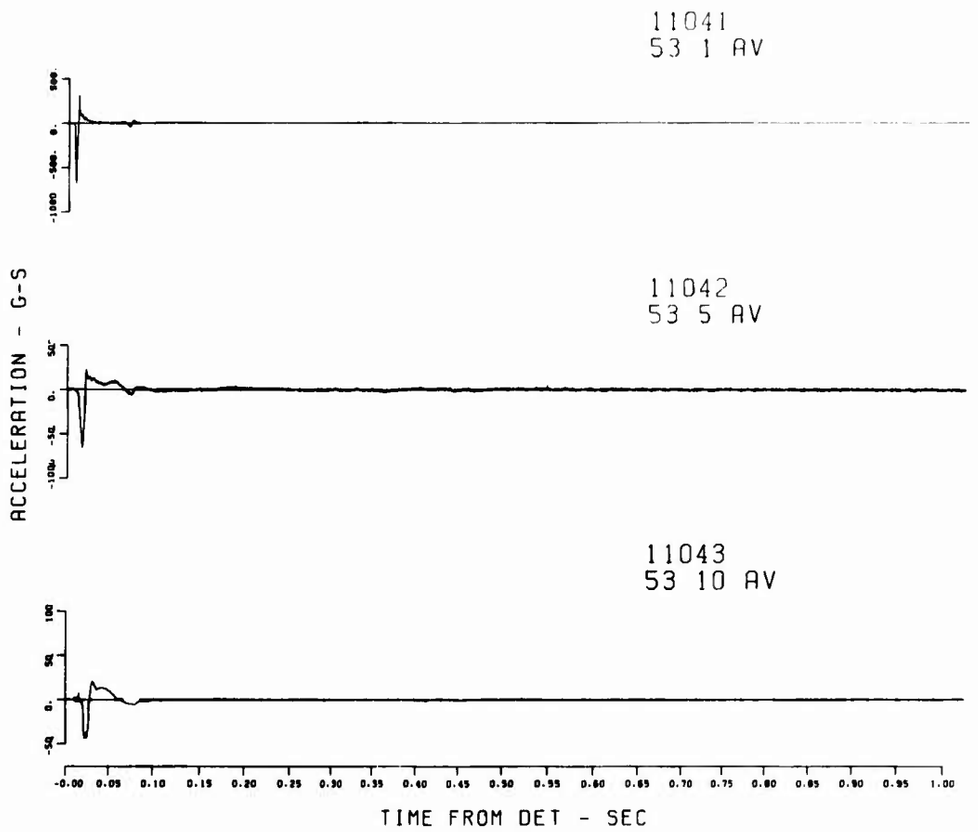
11041
53 1 AV
11042
53 5 AV
11043
53 10 AV
ACCELERATION - G-S
-0.00 0.05 0.10 0.15 0.20 0.25 0.30 0.35 0.40 0.45 0.50 0.55 0.60 0.65 0.70 0.75 0.80 0.85 0.90 0.95 1.00
TIME FROM DET - SEC

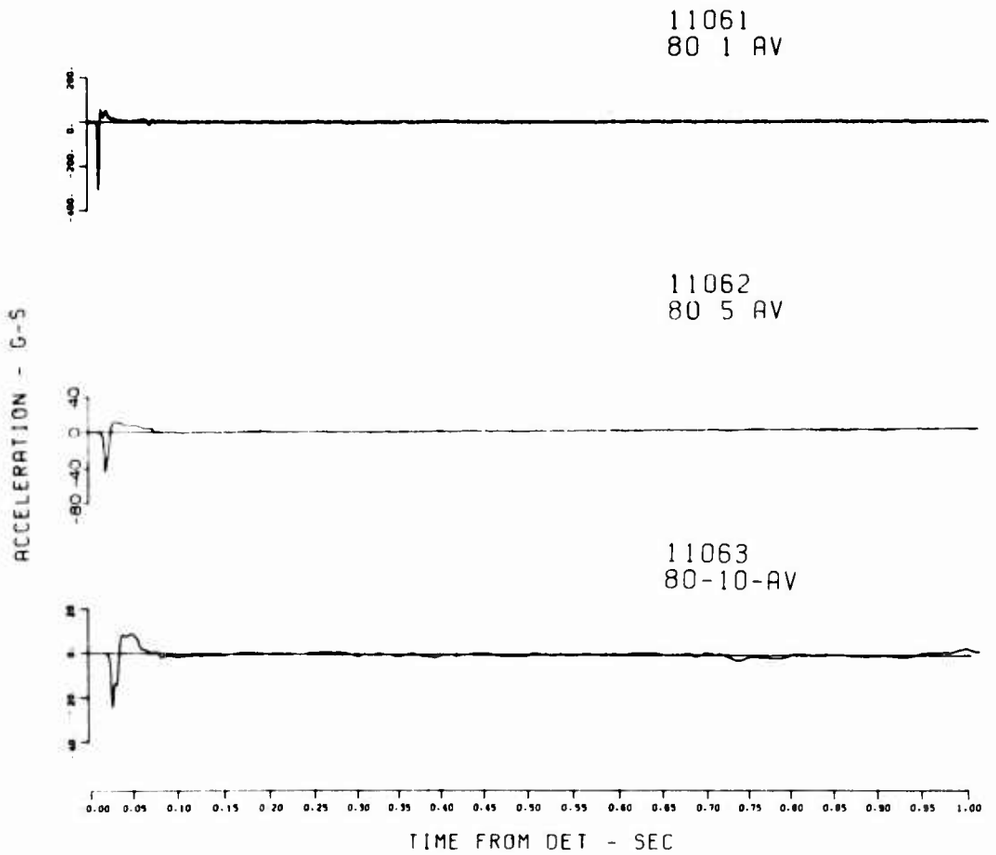
11061
80 1 AV
11062
80 5 AV
11063
80-10-AV
ACCELERATION - G-S
-80 -40 0 40
0.00 0.05 0.10 0.15 0.20 0.25 0.30 0.35 0.40 0.45 0.50 0.55 0.60 0.65 0.70 0.75 0.80 0.85 0.90 0.95 1.00
TIME FROM DET - SEC

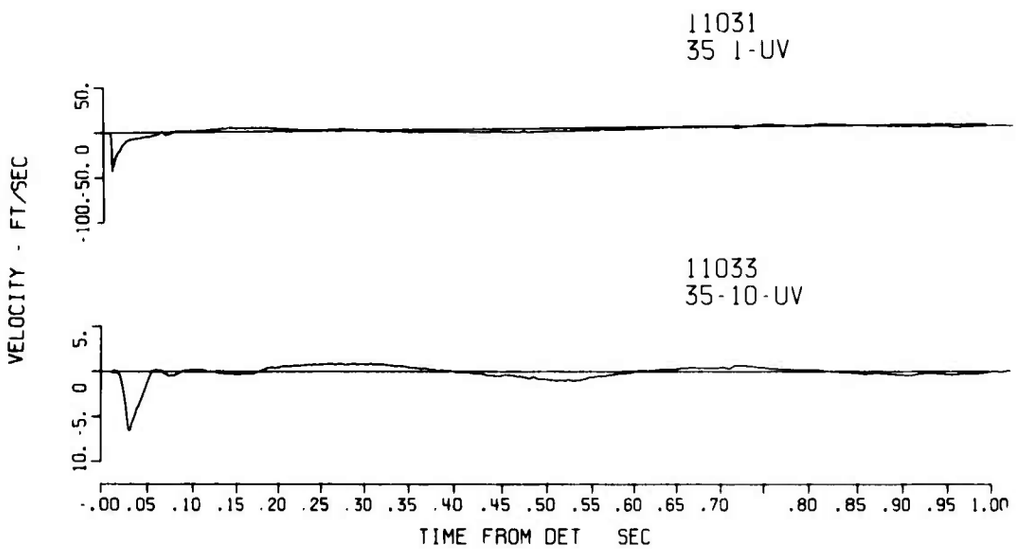
11031
35 1-UV
50.
0
-50.
-100.
11033
35-10-UV
5.
0
-5.
-10.
VELOCITY - FT/SEC
-.00 .05 .10 .15 .20 .25 .30 .35 .40 .45 .50 .55 .60 .65 .70 .80 .85 .90 .95 1.00
TIME FROM DET SEC

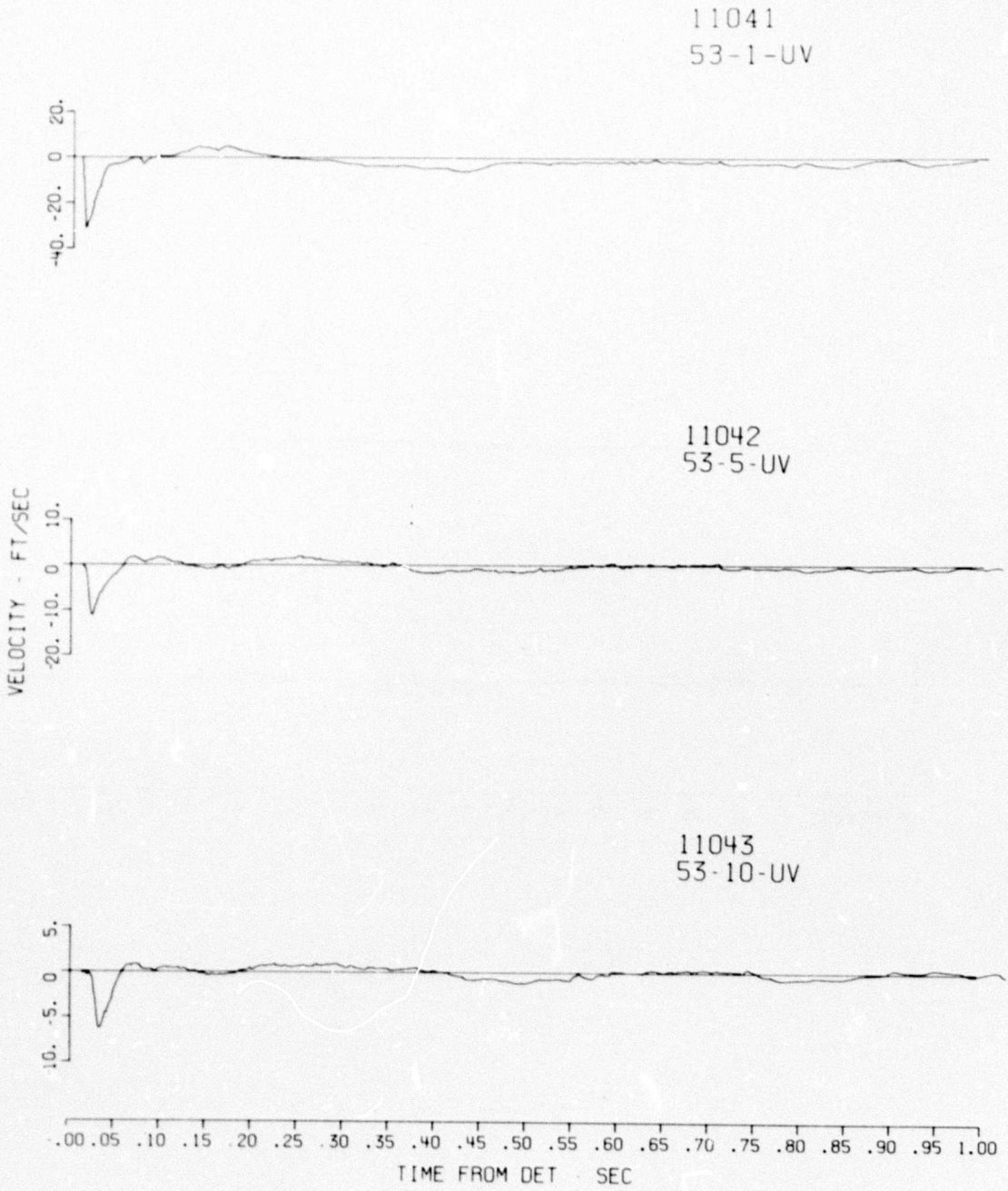
11041
53-1-UV
20.
0
-20.
-40.
11042
53-5-UV
VELOCITY - FT/SEC
10.
0
-10.
-20.
11043
53-10-UV
5.
0
-5.
-10.
.00 .05 .10 .15 .20 .25 .30 .35 .40 .45 .50 .55 .60 .65 .70 .75 .80 .85 .90 .95 1.00
TIME FROM DET - SEC

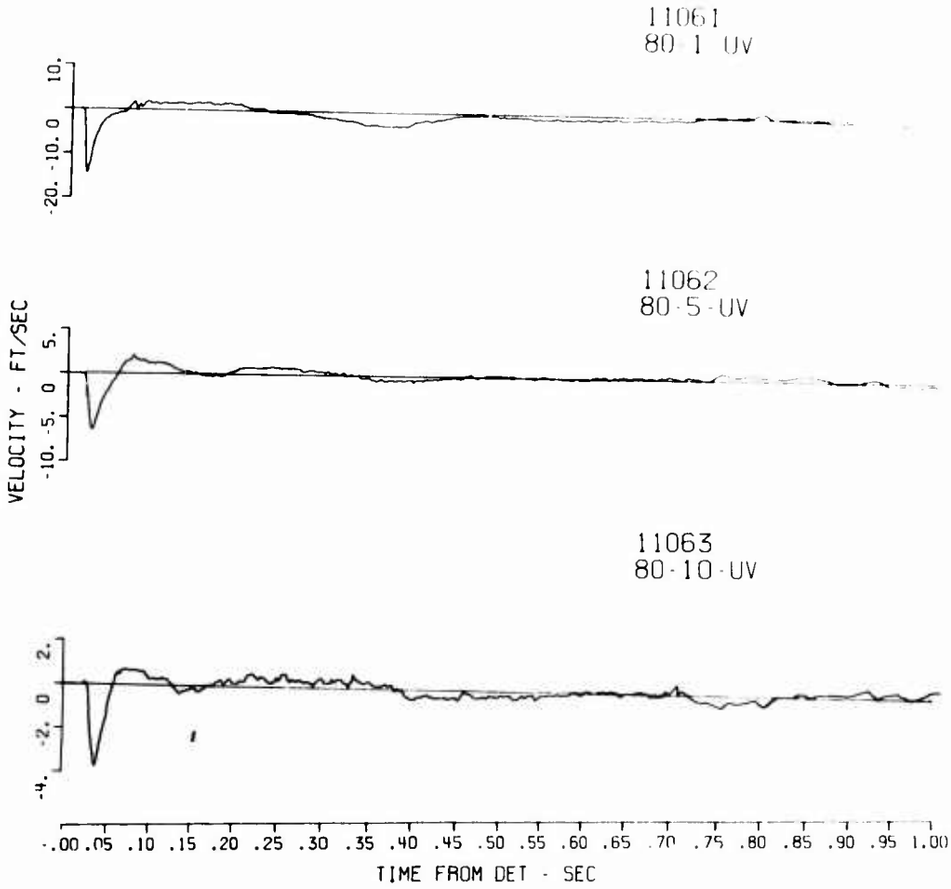
11061
80-1-UV
10.
0
-10.
-20.
11062
80-5-UV
5.
0
-5.
-10.
VELOCITY - FT/SEC
11063
80-10-UV
2.
0
-2.
-4.
.00 .05 .10 .15 .20 .25 .30 .35 .40 .45 .50 .55 .60 .65 .70 .75 .80 .85 .90 .95 1.00
TIME FROM DET - SEC

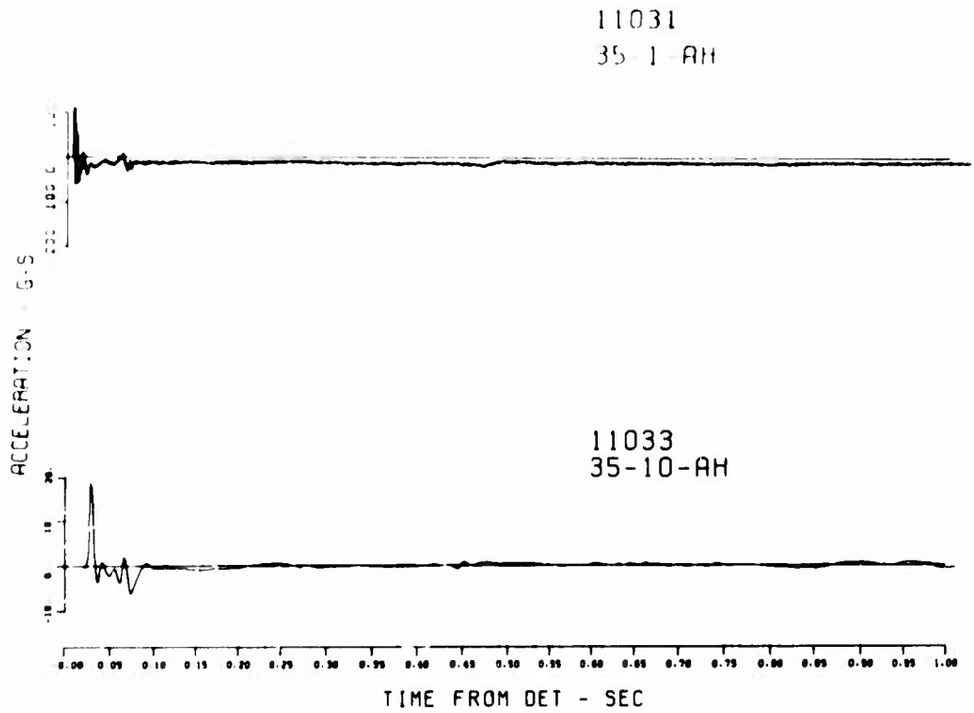
11031
35 1 AH
ACCELERATION - G-S
11033
35-10-AH
TIME FROM DET - SEC

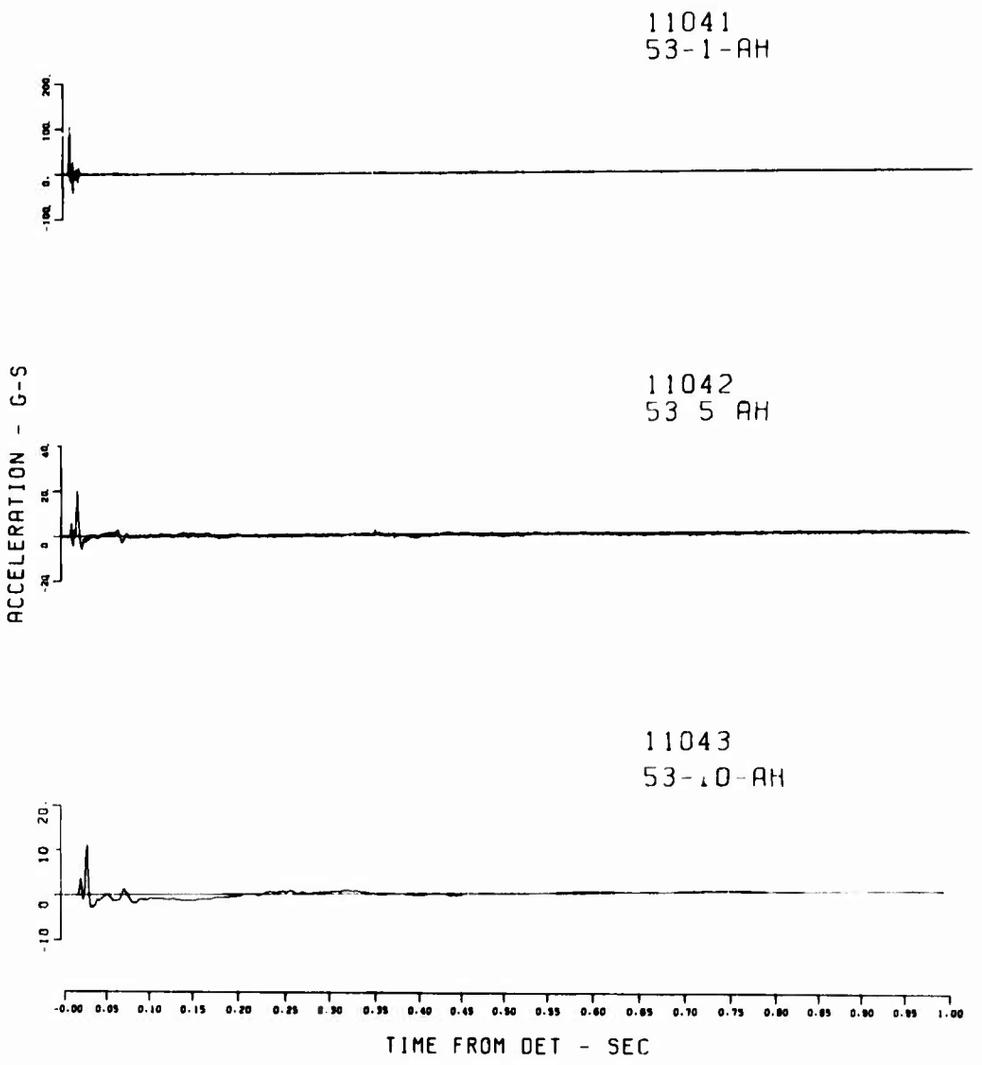
11041
53-1-AH
11042
53 5 AH
11043
53-10-AH
ACCELERATION - G-S
TIME FROM DET - SEC

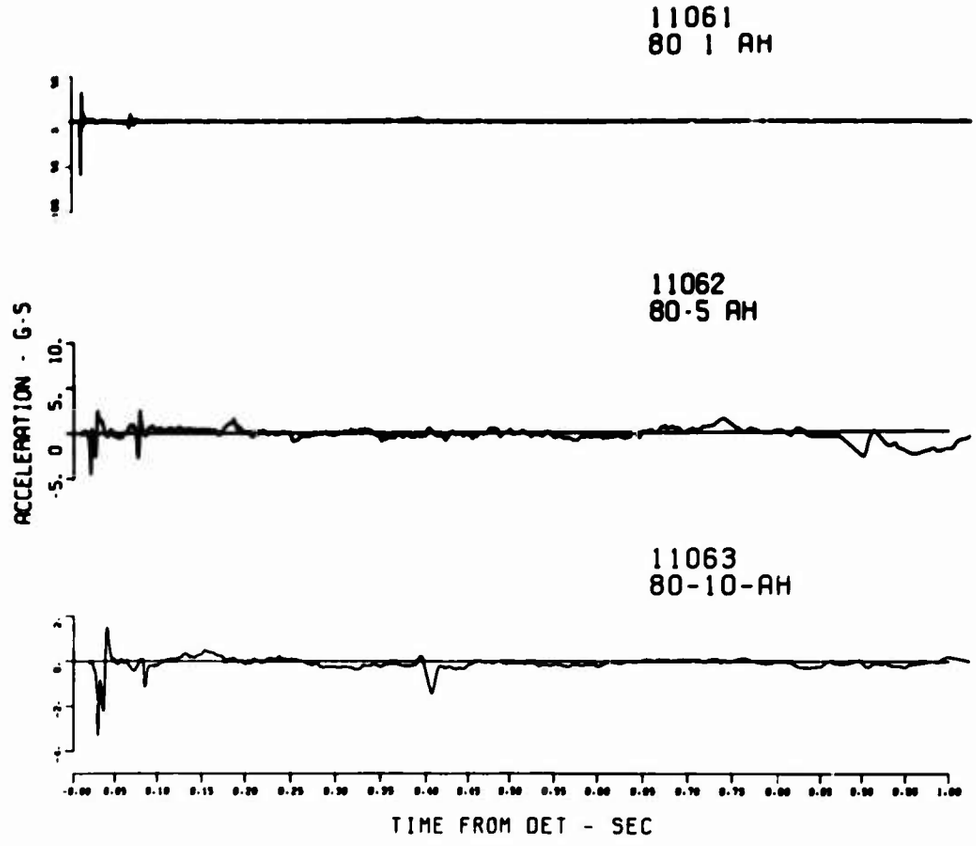
11061
80 1 AH
11062
80-5 AH
ACCELERATION - G-S
10.
5.
0
-5.
11063
80-10-AH
TIME FROM DET - SEC

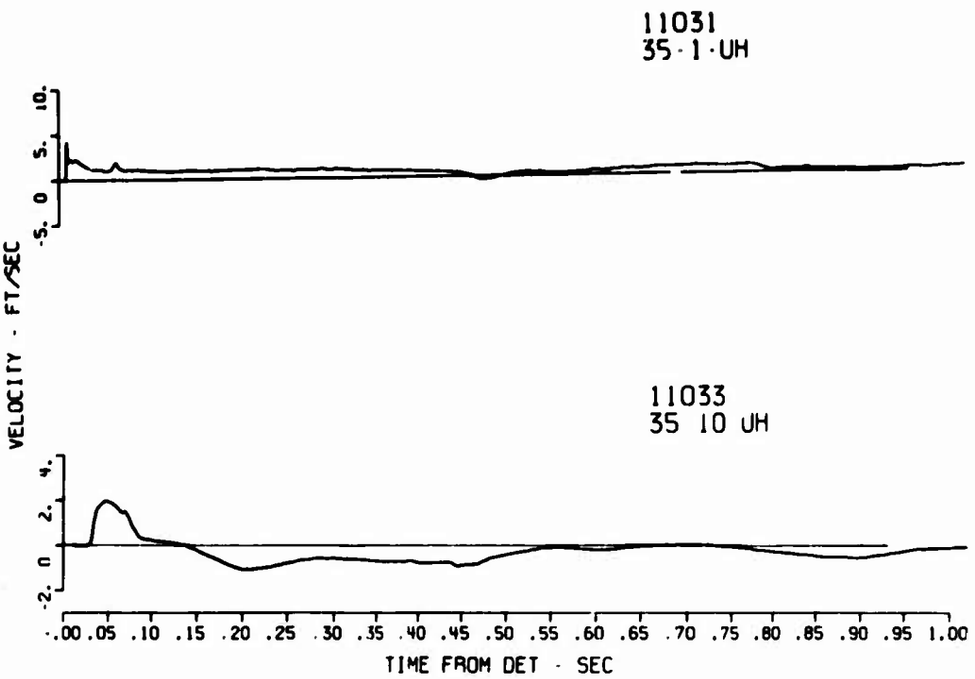
11031
35-1-UH
10.
5.
0
-5.
11033
35 10 UH
4.
2.
0
-2.
VELOCITY - FT/SEC
.00 .05 .10 .15 .20 .25 .30 .35 .40 .45 .50 .55 .60 .65 .70 .75 .80 .85 .90 .95 1.00
TIME FROM DET - SEC

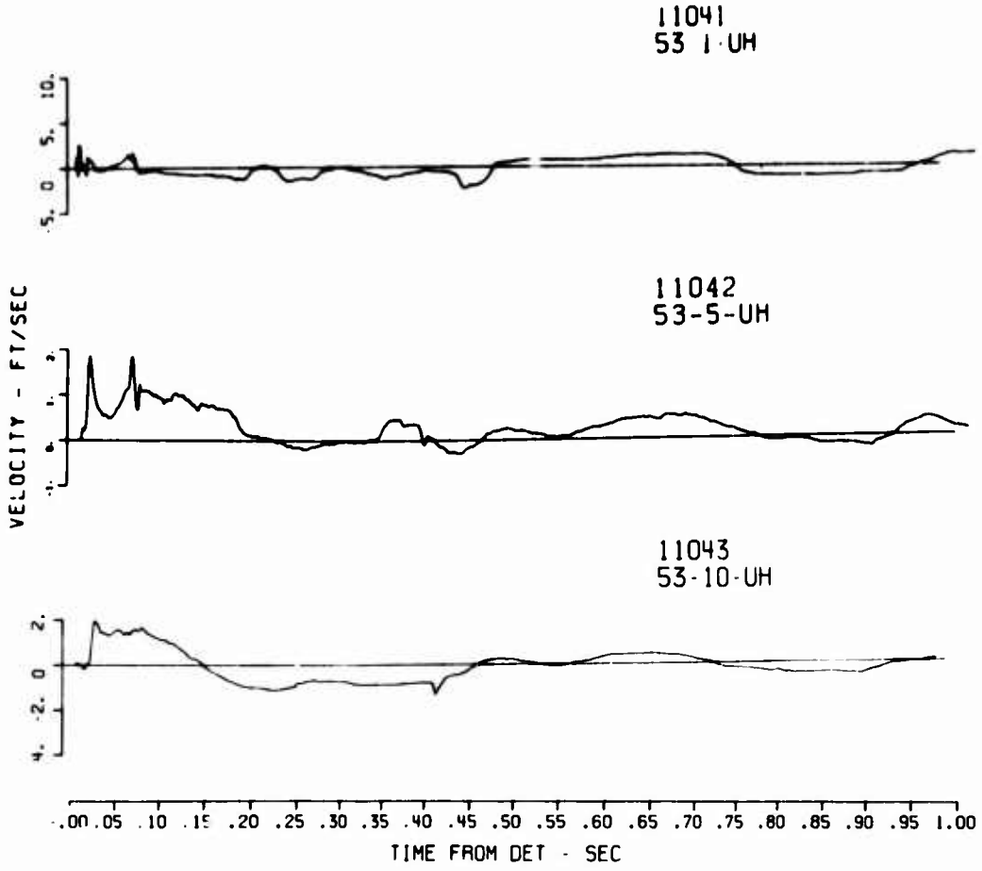
11041
53 1-UH
11042
53-5-UH
11043
53-10-UH
VELOCITY - FT/SEC
TIME FROM DET - SEC

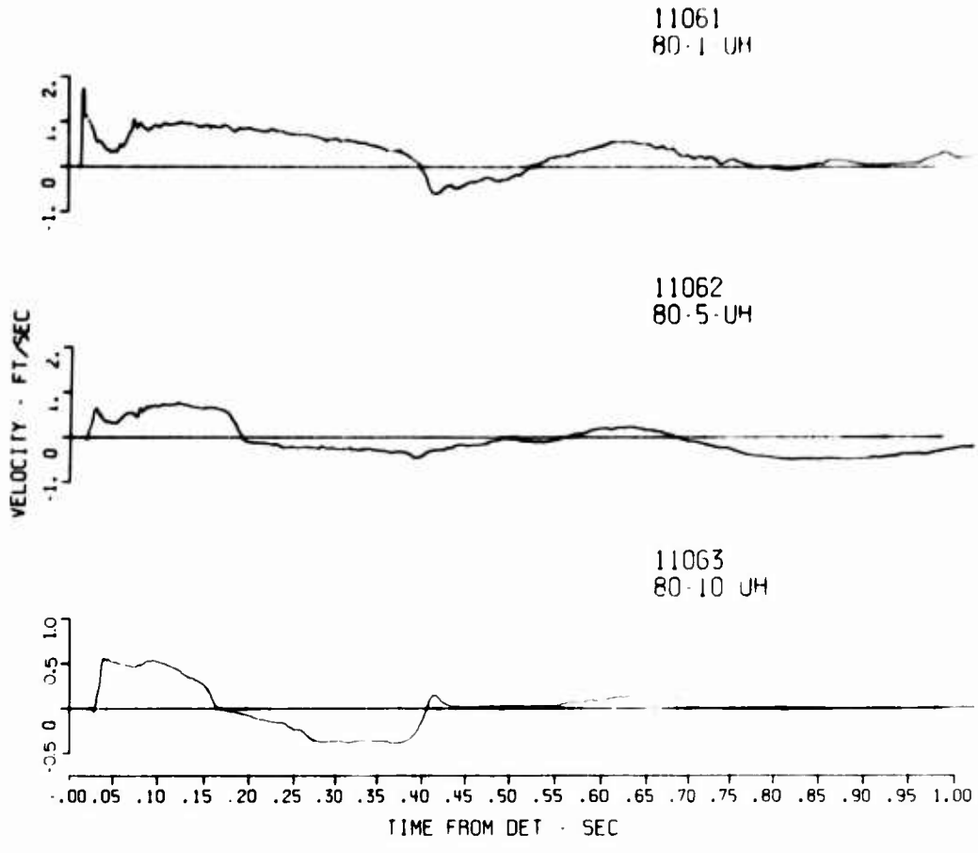
11061
80·1 UH
11062
80·5·UH
11063
80·10 UH
VELOCITY - FT/SEC
-1. 0
1.
2.
-.5 0
.5
1.0
.00 .05 .10 .15 .20 .25 .30 .35 .40 .45 .50 .55 .60 .65 .70 .75 .80 .85 .90 .95 1.00
TIME FROM DET · SEC

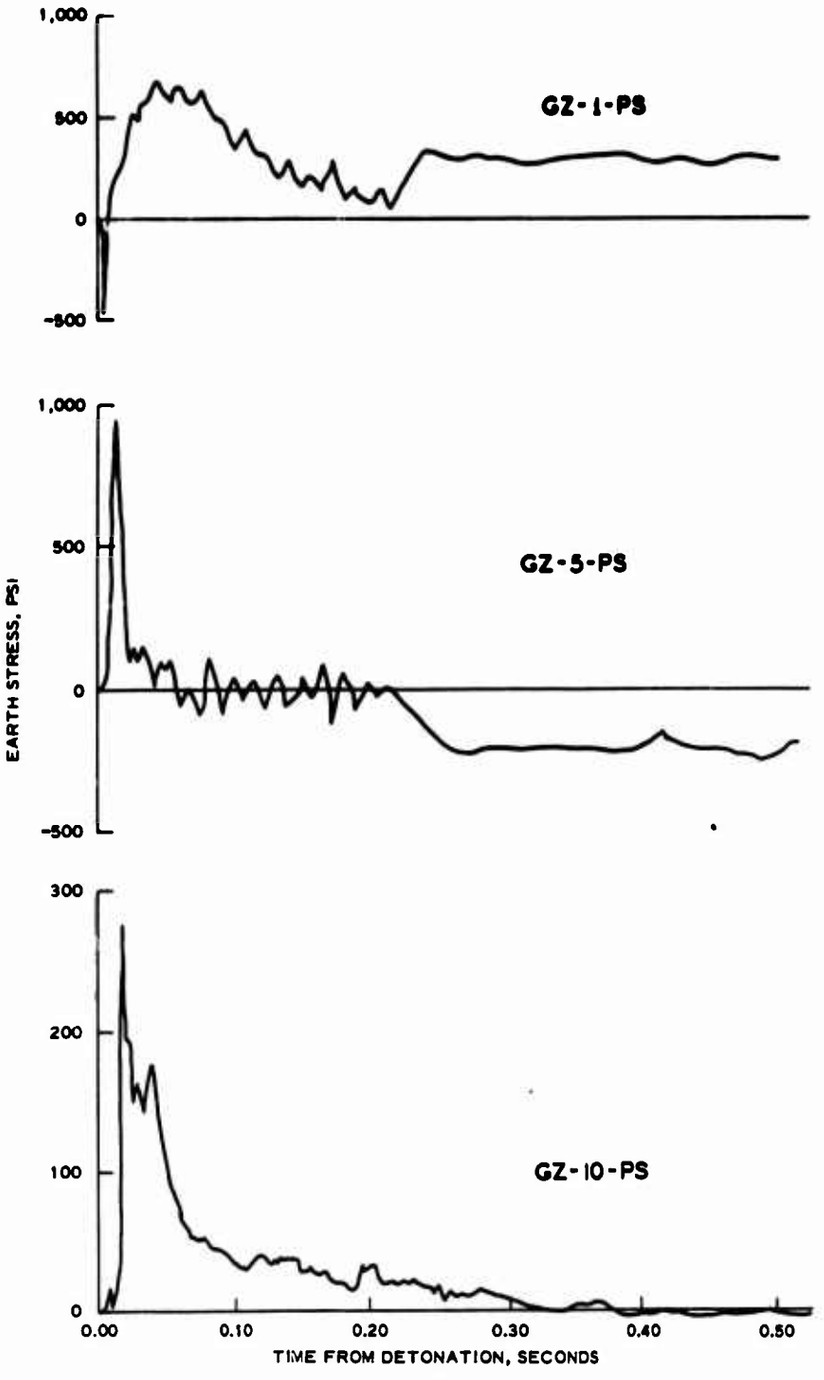
1,000
500
0
-500
GZ-1-PS
1,000
500
0
-500
GZ-5-PS
EARTH STRESS, PSI
300
200
100
0
GZ-10-PS
0.00
0.10
0.20
0.30
0.40
0.50
TIME FROM DETONATION, SECONDS

11042

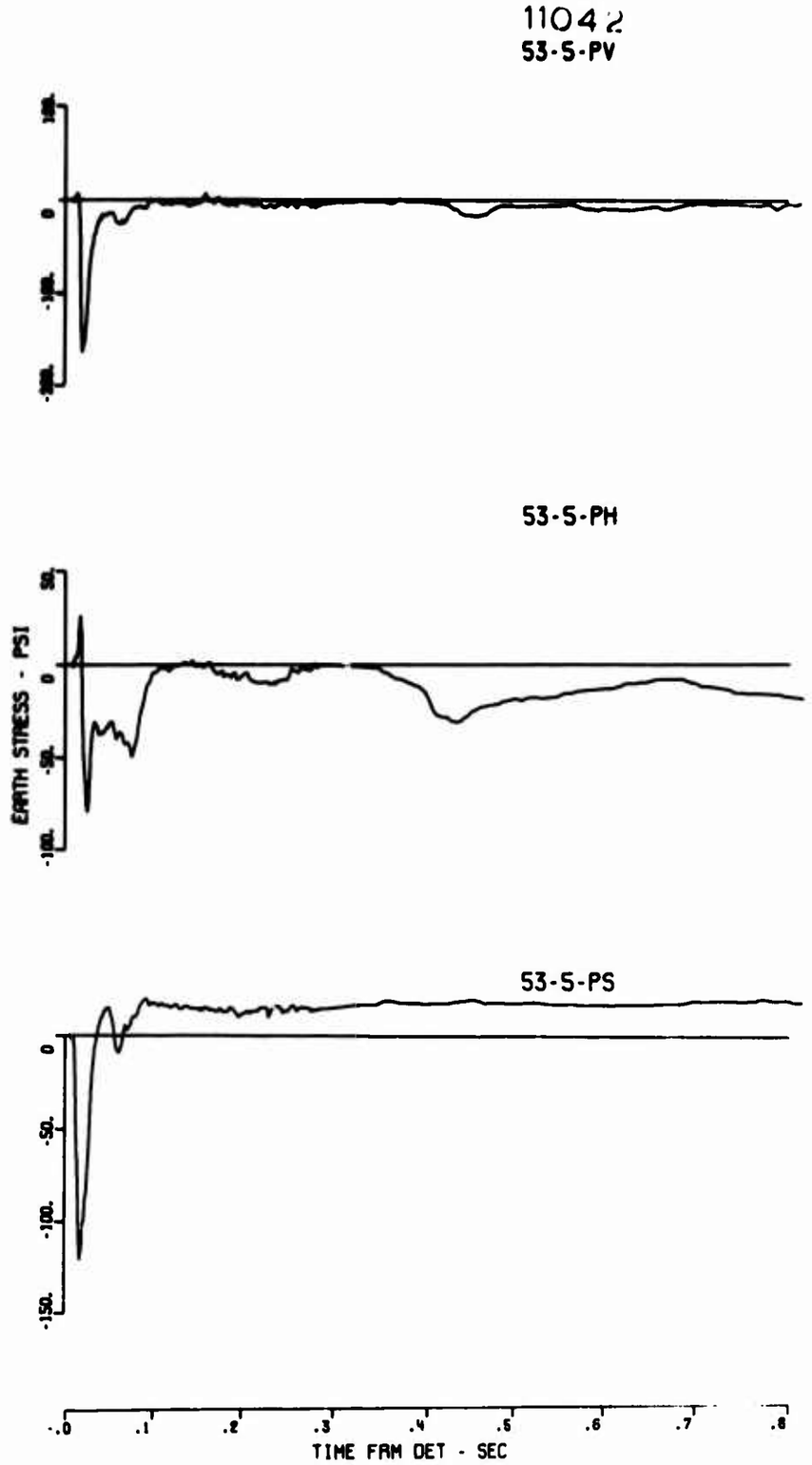
53-5-PV
53-5-PH
EARTH STRESS - PSI
50.
0
-50.
-100.
53-5-PS
0
-50.
-100.
-150.
.0
.1
.2
.3
.4
.5
.6
.7
.8
TIME FRM DET - SEC

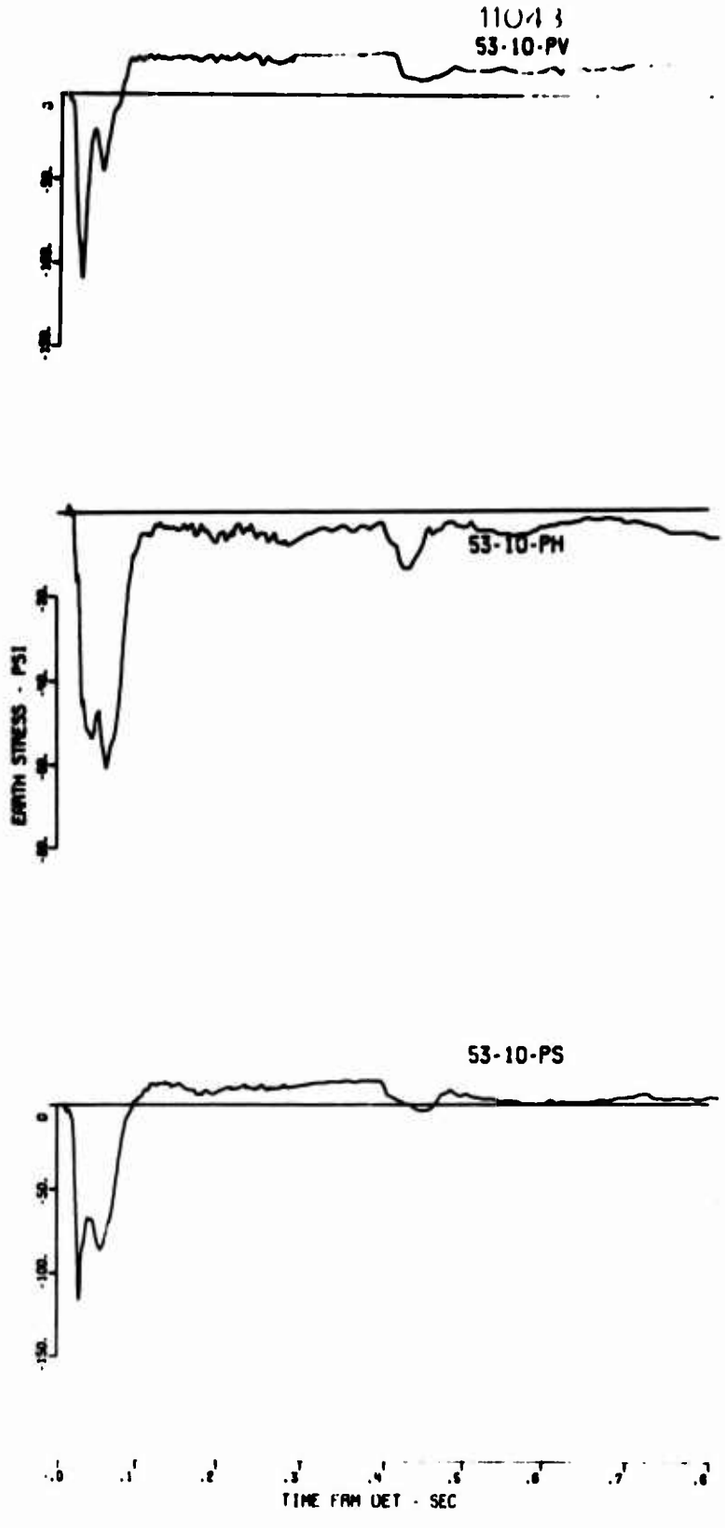
11043
53-10-PV
53-10-PH
EARTH STRESS - PSI
53-10-PS
TIME FRM LIFT - SEC

11062

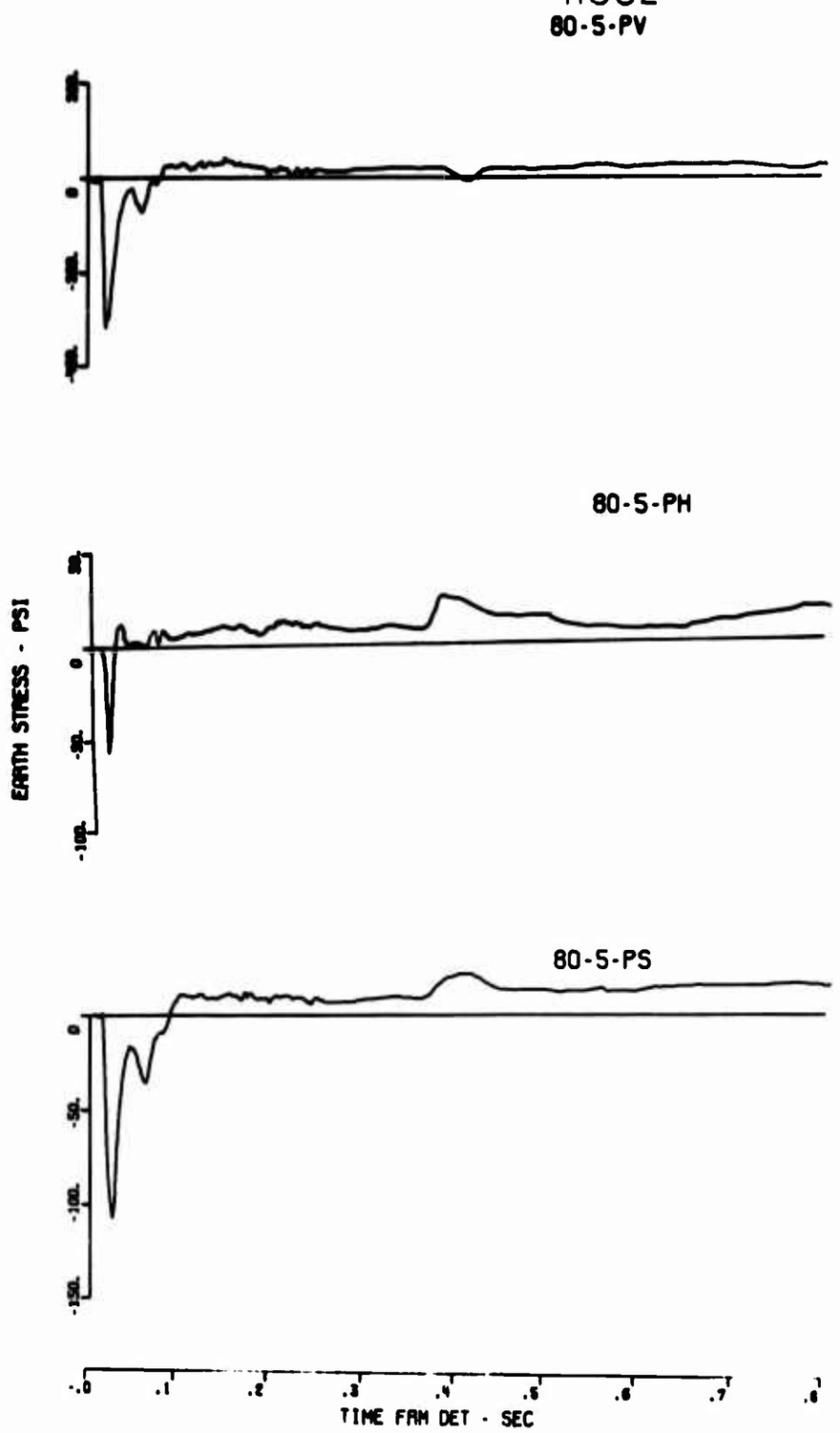
80-5-PV
80-5-PH
80-5-PS
EARTH STRESS - PSI
0
-50.
-100.
-150.
.0
.1
.2
.3
.4
.5
.6
.7
.8
TIME FRM DET - SEC

11063

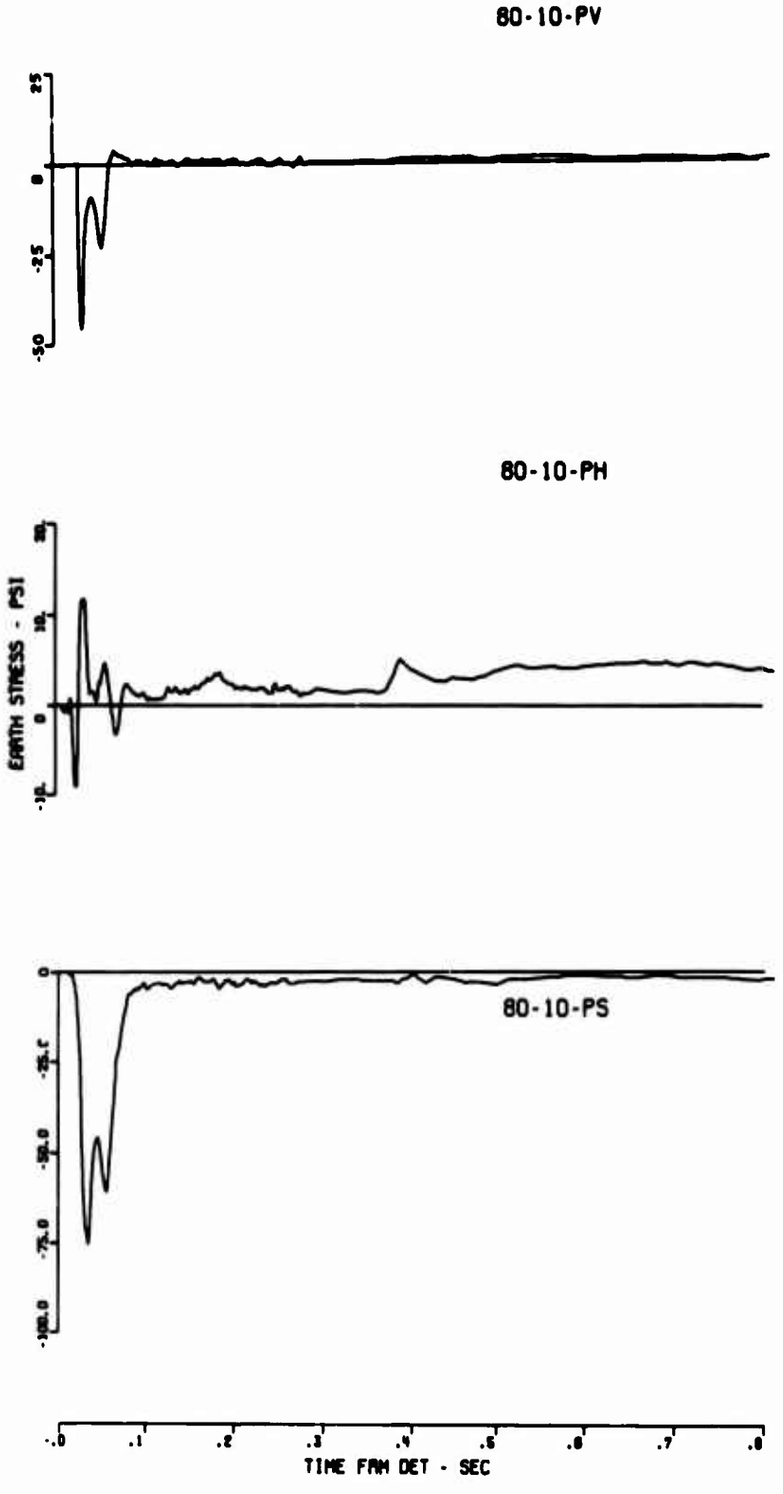

REFERENCES

1. W. R. Perret and V. L. Gentry; "Operation Upshot-Knothole, Project 1.4, Free-field Measurements of Earth Stress, Strain, and Ground Motion"; WT-716, February 1955; Atomic Energy Commission, Oak Ridge, Tenn.; Unclassified.

2. N. M. Newmark and J. D. Haltiwanger; "Air Force Design Manual; Principles and Practices for Design of Hardened Structures"; Technical Documentary Report No. AFSWC-TDR-62-138, December 1962; Air Force Special Weapons Center, Kirtland Air Force Base, New Mexico; Prepared by University of Illinois, Urbana, Ill.; Unclassified.

3. D. W. Murrell; "Operation Snowball, Project 3.6--Earth Motion Measurements"; Technical Report No. 1-759, March 1967; U. S. Army Engineer Waterways Experiment Station, CE, Vicksburg, Miss.; Unclassified.

4. J. K. Ingram; "Project Officer's Final Report, Operation Distant Plain, Events 1, 2A, 3, 4, and 5, Project 3.02a, Earth Motion and Stress Measurements"; (in preparation); U. S. Army Engineer Waterways Experiment Station, CE, Vicksburg, Miss.; Unclassified.

5. F. M. Sauer; "Distant Plain, Events 6 and 1A, Report of Special Assistant to Test Director"; October 1967; Stanford Research

Institute, Menlo Park, Calif.; Unclassified.

6. A. J. Hendron, Jr.; "Correlation of Operation Snowball Ground Motions with Dynamic Properties of Test Site Soils"; Miscellaneous Paper No. 1-745, October 1965; U. S. Army Engineer Waterways Experiment Station, CE, Vicksburg, Miss.; Unclassified.

7. J. L. Gatz; "Soil Survey and Support Activities, Operation Distant Plain Event 6"; Miscellaneous Paper No. 3-990, April 1968; U. S. Army Engineer Waterways Experiment Station, CE, Vicksburg, Miss.; Unclassified.

8. J. G. Jackson, Jr., and J. E. Windham; "Preliminary Report, Operation Distant Plain, Event 6, Soil Property Investigation for Project 3.10, Soil Sampling and Testing"; December 1967; Defense Atomic Support Agency, Washington, D. C.; Prepared by U. S. Army Engineer Waterways Experiment Station, CE, Vicksburg, Miss.; Unclassified.

9. J. K. Ingram; "Development of a Free-Field Soil Stress Gage for Static and Dynamic Measurements"; Technical Report No. 1-814, February 1968; U. S. Army Engineer Waterways Experiment Station, CE, Vicksburg, Miss.; Unclassified.

10. R. E. Reisler; "Events 5, 6A, and 6, Project 1.01, Air Blast Measurements"; Operation Distant Plain Symposium II, M. J. Dudash,

editor, DASA 2207, DASIAC SR-83, May 1968, Pages 70-106; DASA Information and Analysis Center, General Electric, TEMPO, Santa Barbara, Calif.; For Offical Use Only.

11. F. M. Sauer and C. T. Vincent; "Ferris Wheel Series, Flat Top Event; Project Officers Report--Project 1.2/1.3a, Earth Motion and Pressure Histories (U)"; POP 3002 (WT-3002) April 1967; Defense Atomic Support Agency, Washington, D. C.; Unclassified.

12. R. E. Reisler; "Air Blast Measurements, Operation Distant Plain, Event 1A"; Operation Distant Plain Symposium II, M. J. Dudash, editor, DASA 2207, DASIAC SR-83, May 1968, Pages 44-69; DASA Information and Analysis Center, General Electric, TEMPO, Santa Barbara, Calif.; For Official Use Only.

DISTRIBUTION LIST FOR TR N-70-14

Address	No. of Copies
Department of Defense	
Director, Defense Atomic Support Agency, Washington, D. C. 20301	
ATTN: Technical Library (APTL)	2
STSP	1
OAOP	1
OPQR	1
Commander, Field Command, Defense Atomic Support Agency, Sandia Base, Albuquerque, N. Mex. 87115	1
ATTN: Technical Library	1
FCTG-5	1
FCDV-1	
Commander, Test Command, Defense Atomic Support Agency, Sandia Base, Albuquerque, N. Mex. 87115	2
ATTN: Document Control	
Administrator, Defense Documentation Center, Cameron Station, Bldg. 5, Alexandria, Va. 22314	20
ATTN: Document Control	
Director, Defense Intelligence Agency, Washington, D. C. 20301	
ATTN: DIAAP-IK2	1
DIA-AP8B-1	1
Assistant to the Secretary of Defense (Atomic Energy), Washington, D. C. 20301	1
ATTN: Class Rec. Library	
Director of Defense Research and Engineering, Washington, D. C. 20301	
ATTN: Asst. Director (Strategic Weapons)	1
Asst. Director (Nuclear Programs)	1
Director, Weapons Systems Evaluation Group, Washington, D. C. 20305	1
ATTN: Document Control	
Joint Strategic Target Planning Staff, Offutt AFB, Nebr. 68113	1
Department of the Army	
Chief of Engineers, Department of the Army, Washington, D. C. 20314	
ATTN: ENGMC-E	1
Director of Military Construction	1
Chief of Research and Development, Department of the Army, Washington, D. C. 20310	1
ATTN: Nuclear, Chemical-Biological Division	
Commanding General, U. S. Army Engineer Center, Ft. Belvoir, Va. 22060	1
ATTN: Asst. Commandant Engineer School	
Commanding Officer, U. S. Army Combat Developments Command, Institute of Nuclear Studies, Ft. Bliss, Tex. 79916	1
ATTN: Document Control	

Unclassified

Security Classification

DOCUMENT CONTROL DATA - R & D

(Security classification of title, body of abstract and indexing annotation must be entered when the overall report is classified)

1. ORIGINATING ACTIVITY (Corporate author) U. S. Army Engineer Waterways Experiment Station Vicksburg, Mississippi	2a. REPORT SECURITY CLASSIFICATION Unclassified 2b. GROUP

3. REPORT TITLE

DISTANT PLAIN EVENTS 6 AND 1A, PROJECT 3.02a, EARTH MOTION AND STRESS MEASUREMENTS

4. DESCRIPTIVE NOTES (Type of report and inclusive dates)

Final report

5. AUTHOR(S) (First name, middle initial, last name)

Donald W. Murrell

6. REPORT DATE	7a. TOTAL NO. OF PAGES	7b. NO. OF REFS
September 1970	145	12

8a. CONTRACT OR GRANT NO. b. PROJECT NO. c. d.	9a. ORIGINATOR'S REPORT NUMBER(S) Technical Report N-70-14 9b. OTHER REPORT NO(S) (Any other numbers that may be assigned this report)

10. DISTRIBUTION STATEMENT

This document has been approved for public release and sale; its distribution is unlimited.

11. SUPPLEMENTARY NOTES	12. SPONSORING MILITARY ACTIVITY
	Defense Atomic Support Agency Washington, D. C.

13. ABSTRACT

The objectives of this study were to measure and analyze earth motions produced by Events 6 and 1A of Operation Distant Plain. Event 6 was a 100-ton TNT surface-tangent sphere, and Event 1A a 20-ton TNT sphere detonated at a height of burst of 29.5 feet. Acceleration, particle velocity, and soil stress gages were installed for both events to measure ground motion. Time histories obtained by this instrumentation are included in Appendixes A and B. For Event 6, ground shock arrival times indicated development of outrunning ground motion at about the 30-psi level. Shock propagation velocities were calculated to be 1,100 ft/sec above the water table and 5,500 ft/sec below it. The ratio of acceleration to overpressure for the 1.5-foot depth for both events was about 0.4 g/psi at the 1,000-psi level, and increased to 1.0 g/psi at the 20-psi level. At depths of 5 and 10 feet, accelerations averaged 20 and 7.5 percent of the shallow data, respectively. At the 1.5-foot depth the ratio of velocity to overpressure varied from 0.03 ft/sec/psi at 1,600 psi to 0.08 ft/sec/psi at 10 psi. Velocities attenuated less sharply with depth than did accelerations. Velocities at the 5-foot depth were about 40 percent of those at 1.5 feet, while those from the 10-foot depth were about 30 percent of those at 1.5 feet. Horizontal velocities were dominated by the cratering-induced motion. These motions attenuated as the -2.7 power of distance. Vertical stresses attenuated more rapidly than did the velocities, with stresses at the 5-foot depth averaging 25 percent of those at the 1.5-foot depth. Horizontal stresses measured below the water table behaved similar to free-water measurements, attenuating as the -1.15 power of distance, versus -1.13 power for water. Calculations of shear stress were made for three locations on each shot. Peak values ranged from 40 to 70 psi.

DD FORM 1 NOV 68 1473 REPLACES DD FORM 1473, 1 JAN 64, WHICH IS OBSOLETE FOR ARMY USE.

Unclassified

Security Classification

14. KEY WORDS	LINK A		LINK B		LINK C	
	ROLE	WT	ROLE	WT	ROLE	WT
Distant Plain (Operation)						
Earth movements						
Explosion effects						
Ground motion						
Stress gages (soils)						